PHASE RELATIONS IN THE Au-Ag-Te SYSTEM

by

Louis J. Cabri

A thesis submitted to the Faculty of Graduate Studies and Research of McGill University in partial fulfillment of the requirements for the degree of Doctor of Philosophy.

Department of Geological Sciences

McGill University

September, 1964

Table of Contents

Table of Contents (cont'd.)

Tables

Tables (cont'd.)

Appendix

Figures

Appendix

Introduction

In recent years our knowledge of ore deposits, and of the conditions under which they were deposited, has been augmented by experimental investigations of sulphide, and to a lesser extent, arsenide, oxide, selenide, and telluride systems. The physical conditions of formation for the gold-silver tellurides were examined in detail in the present study. These minerals have a wide geographic distribution and occur in several geological environments. The spectacular ores at the gold and silver mining camps of Cripple Creek, Colorado, Kalgoorlie, Western Australia, and Sacarambu and Offenbanya in Transylvania consisted of telluride mineralization. Gold-silver tellurides are also present as minor constituents in some sulphide ore deposits and quartz-vein-type gold deposits. There are as many as 26 such occurrences in the Canadian shield alone (Thompson, 1949).

In crystal-chemical terms tellurides form a link between sulphide minerals having metallic and co-valent bonding and synthetic alloys having metallic bonding. Thus, experimental determination of phase relations in the Au-Ag-Te system may be of considerable interest to students of atomic bonding in several scientific disciplines.

Numerous inconsistencies exist in the literature with regard to the phase relations in the ternary system and additional confusion has been caused by misidentifications of natural gold-silver tellurides which have similar physical properties. This confusion is compounded by the presence of several synthetic phases which have not been reported as naturally occurring minerals and also by several of the phases occurring in two or more polymorphic forms. The compositional relations of the minerals reported in the Au-Ag-Te ternary system are shown in Figure 1.

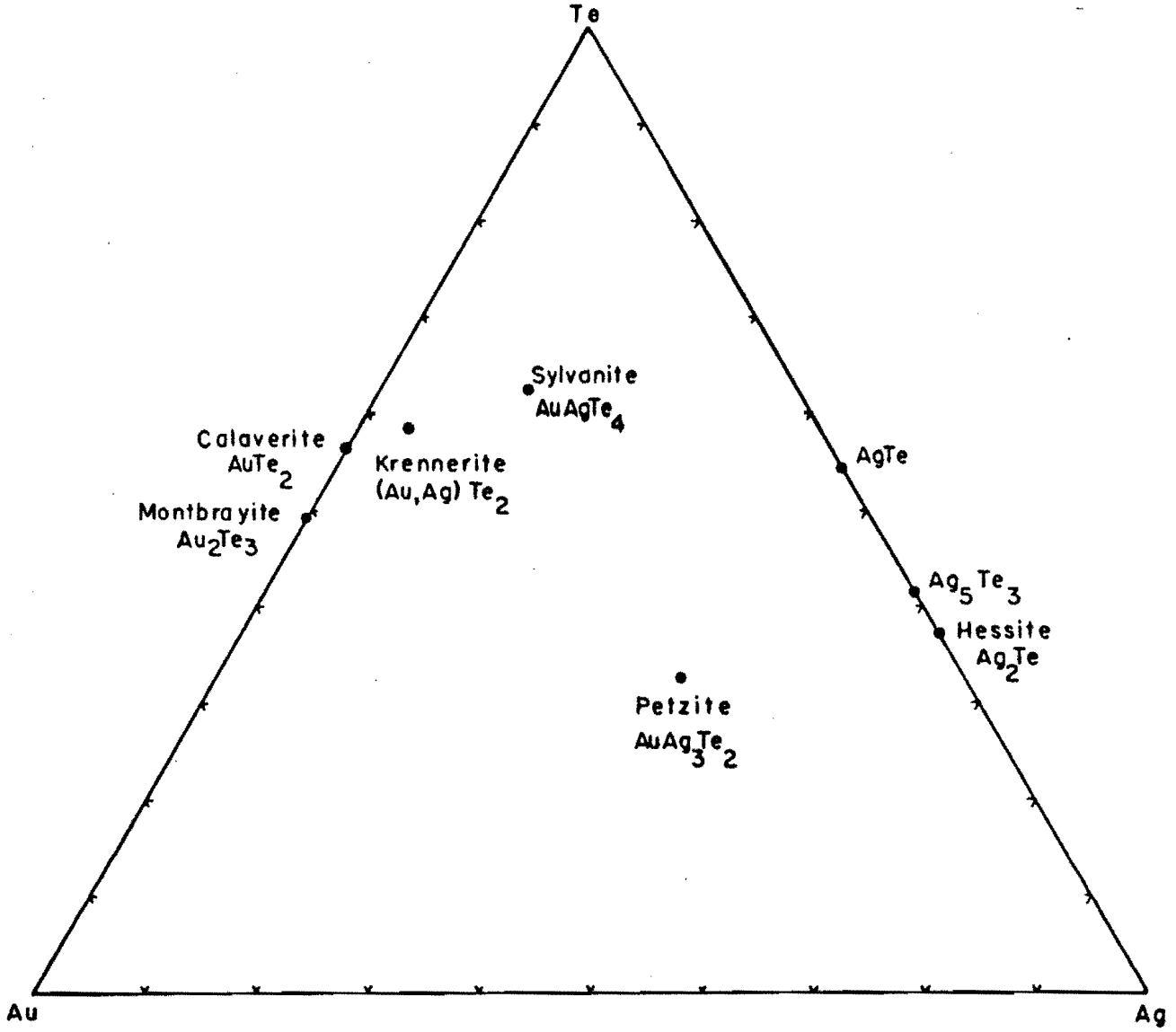

Figure 1. Compositional relations of minerals reported in the Au-Ag-Te system shown in weight per cent. The term empressite has been applied to a mineral having the composition AgTe by Bradley (1914) and Honea (1964). However, Thompson et al (1951) applied the term empressite to a mineral of approximate composition Ag_5Te_3, recently renamed stuetzite by Honea (1964).

The immediate purpose of this investigation was to re-examine the phase relations employing more modern equipment and techniques with the hope of solving some of the problems reported by earlier workers. Secondly, it was hoped to apply this knowledge to the interpretation of the physical-chemical environments of deposits containing gold-silver tellurides.

In brief, the present investigation comprises a series of isothermal sections at 356°, 335°, and 290°C within the mineralogically most important area of the ternary system which are determined in greater detail than previously. Phase relations at 170°C were also partly clarified. In addition, the phase relations along the $AuTe_2$-"$AgTe_2$" and $AuAg_3Te_2$-Ag_2Te joins, and the Ag-Te binary were determined over the temperature ranges 270°-440°C, 20°-810°C, and 50°-810°C respectively. The x-ray powder diffraction patterns of all phases encountered in this investigation were studied and where possible compared to natural minerals.

Previous work in the Au-Ag-Te system

The binary systems

Gold-Silver. The phase relations for the Au-Ag system were compiled by Hansen and Anderko (1958) from the work of Jäneck (1911) and Raydt (1912). There is complete solid solution with no eutectic, gold melting at 1063°C and silver at 960.5°C (see appendix, figure A2).

Gold-Tellurium. Rose (1908), Pelabon (1909), and Pellini and Quercigh (1910) studied the gold-tellurium system, and the data from the latter are taken as most reliable as they gave the best melting points of tellurium and $AuTe_2$. The $AuTe_2$-Te part of the diagram has a simple eutectic at 416°C and 88 at. % Te with $AuTe_2$ melting at 464°C and Te (Kracek, 1941, 1963) at 449.8° ± 0.2°C. The Au-$AuTe_2$ portion has a eutectic at 447°C and 53 at. % Te (see appendix, figure A2).

No binary solid solutions were observed by the above investigators; nor were any observed by Markham (1960, p. 1157).

Besides gold and tellurium, the only other compound in the binary represented by a mineral species is calaverite, $AuTe_2$, Thompson (1948). The mineral montbrayite Au_2Te_3, has not been synthesized. Markham (1957), Peacock and Thompson (1946).

Silver-Tellurium. The silver-tellurium system has been investigated by several workers; notably Pelabon (1906), Pellini and Quercigh (1910a), Chikashige and Saito (1916), Koern (1940), Kracek and Ksanda (1940), Thompson et al (1951), Kracek and Rowland (1955), Kiukkola and Wagner (1957), and Kracek and Ksanda (unpublished).

Only two binary phases were found by all these investigators except for Kiukkola and Wagner. There was general agreement on the

existence of the phase Ag_2Te which corresponds to the mineral hessite, but the other phase was given various formulae such as AgTe (Pellini and Quercigh), Ag_7Te_4 (Chikashigi and Saito), $Ag_{12}Te_7$ (Koern), Ag_5Te_3 and $Ag_{2-x}Te_{1+x}$ (Thompson et al), $Ag_{5-x}Te_{3.00}$ (Donnay et al, 1956), $Ag_{12}Te_7$ (Sharma, 1963), and Ag_5Te_3 (Kracek and Ksanda, unpublished).

Kiukkola and Wagner show, by means of solid-state titrations at 250°C and 300°C, that there is evidence for the existence of a third phase. The phases were indicated by curves on a plot of the EMF of a cell Ag/AgI/(Ag, Te) vs. Ag/Te ratio. The curves were separated by horizontal lines representing two phase fields. They designated these phases α, γ and ϵ corresponding to decreasing Ag content. Regarding compositions they say (p. 386), "At 300°C the Ag/Te ratio ranges from 1.99 to 2.00 for the α phase, from 1.88 to 1.91 for the γ phase, and from 1.63 to 1.66 for the ϵ phase." This would correspond to Ag_2Te for α, $Ag_{1.9}Te$ for γ, and $Ag_{5-x}Te_3$ for ϵ with x less than 0.11.

The first two analyses of empressite, Bradley (1914), were in agreement with the formula AgTe. Subsequent work on material from the type locality by Thompson et al (1951) gave a formula closer to Ag_5Te_3 and this material gave the same x-ray diffraction pattern as synthetic Ag_5Te_3. This lead Thompson et al to recommend that Ag_5Te_3 be called empressite and that the name stuetzite be dropped. (Stuetzite was the name given by Shrauf [1878] for material thought to be Ag_4Te and determined by Thompson et al to be Ag_5Te_3). This was the usage current until 1964, even though Thompson et al (1951) obtained a totally different x-ray diffraction picture, which was not indexed, from one unanalyzed sample, from the type locality. Honea (1964) reports that a chemical

analysis made on material from the type locality gives the formula AgTe, thus substantiating Bradley's early analyses. He further made x-ray single crystal and differential thermal analysis examinations of this material and proposes calling the phase AgTe empressite and the phase $Ag_{5-x}Te_3$ stuetzite. The Debeye-Scherrer pattern of Honea is similar to the pattern of Thompson et al (1951) which was not indexed. In view of the confusion in applying any name to $Ag_{5-x}Te_3$ at the time of writing, the chemical composition will be used throughout.

The phase relations in the Ag-Te binary are derived essentially from data provided by Kracek and Rowland (1955) with a few additions from Kracek and Ksanda (unpublished). The Te-Ag_2Te section of the diagram has a eutectic at 33.3 at. % Ag and 353 $\pm$ 0.5°C. Ag_2Te melts at 960°C. Ag_2Te was reported as having two transitions, the lower one is at 105 $\pm$ 25°C on the Te-rich side and 145 $\pm$ 3° on the Ag-rich side. The second transition is at 689 $\pm$ 5° on the Te-rich side and 802 $\pm$ 3° on the Ag-rich side. Ag_5Te_3 melts incongruently at 460 $\pm$ 5° to form Ag_2Te + liquid. It has a transition at 419 $\pm$ 5° on the Te-rich side and at 417 $\pm$ 2°C on the Ag-rich side. At 295 $\pm$ 10°C Ag_5Te_3 shows a "distributed heat effect".

On the Ag_2Te-Ag side of the binary, a two liquid field exists from 69.6 to 87.5 at. % Ag above 881 $\pm$ 3°C. The liquidus extends from the melting point of Ag to 869 $\pm$ 3°C where it forms a eutectic with Ag_2Te at 87.5 at. % Ag (see appendix, figure A3).

The room temperature polymorph of hessite is monoclinic (Frueh, 1959a). Sharma (1963) prepared thin films of Ag_2Te by different methods of evaporation and investigated by electron diffraction the structural

changes vs. temperature. He reports the transition temperature as 157°C with the structure changing from orthorhombic to face centered cubic. Ag_5Te_3 is hexagonal at room temperature (Thompson et al, 1951). AgTe is orthorhombic at room temperature and decomposes to Ag_5Te_3 + Te at 210°C (Honea, 1964).

The ternary system Au-Ag-Te

This section briefly summarizes all the known reports of previous work in the ternary system as well as those relating to some chemical, crystallographic, and physical properties of ternary phases and calaverite with Ag in solid solution, as well as some of the reported assemblages in the ternary.

The early work on the liquidus by Pellini (1915) has been superseded by the findings of Kracek and Ksanda (1940). They determined the position of the ternary eutectic at 330°C where the solid phases tellurium, Ag_5Te_3 and sylvanite coexisted with a liquid of approximate composition $Au_4Ag_{35}Te_{61}$ atomic per cent. Figure 2 is an unpublished liquidus diagram from Kracek.

Markham (1957, 1960) studied the subsolidus phase relations in the ternary system. He determined an isothermal section at 300°C based on the appearance or disappearance of phases as deduced from Debeye-Scherrer x-ray diffraction photographs. At 300°C he found the following three phase fields to be stable: calaverite-petzite-gold; petzite-hessite-AuAg; petzite-hessite-sylvanite; hessite-$Ag_{5-x}Te_3$-sylvanite; $Ag_{5-x}Te_3$-sylvanite-tellurium; and sylvanite-calaverite-tellurium. The isothermal section at 300°C shows limited solid solution between the phases. On the basis of runs in the petzite-hessite-sylvanite field at 330°C, Markham determined

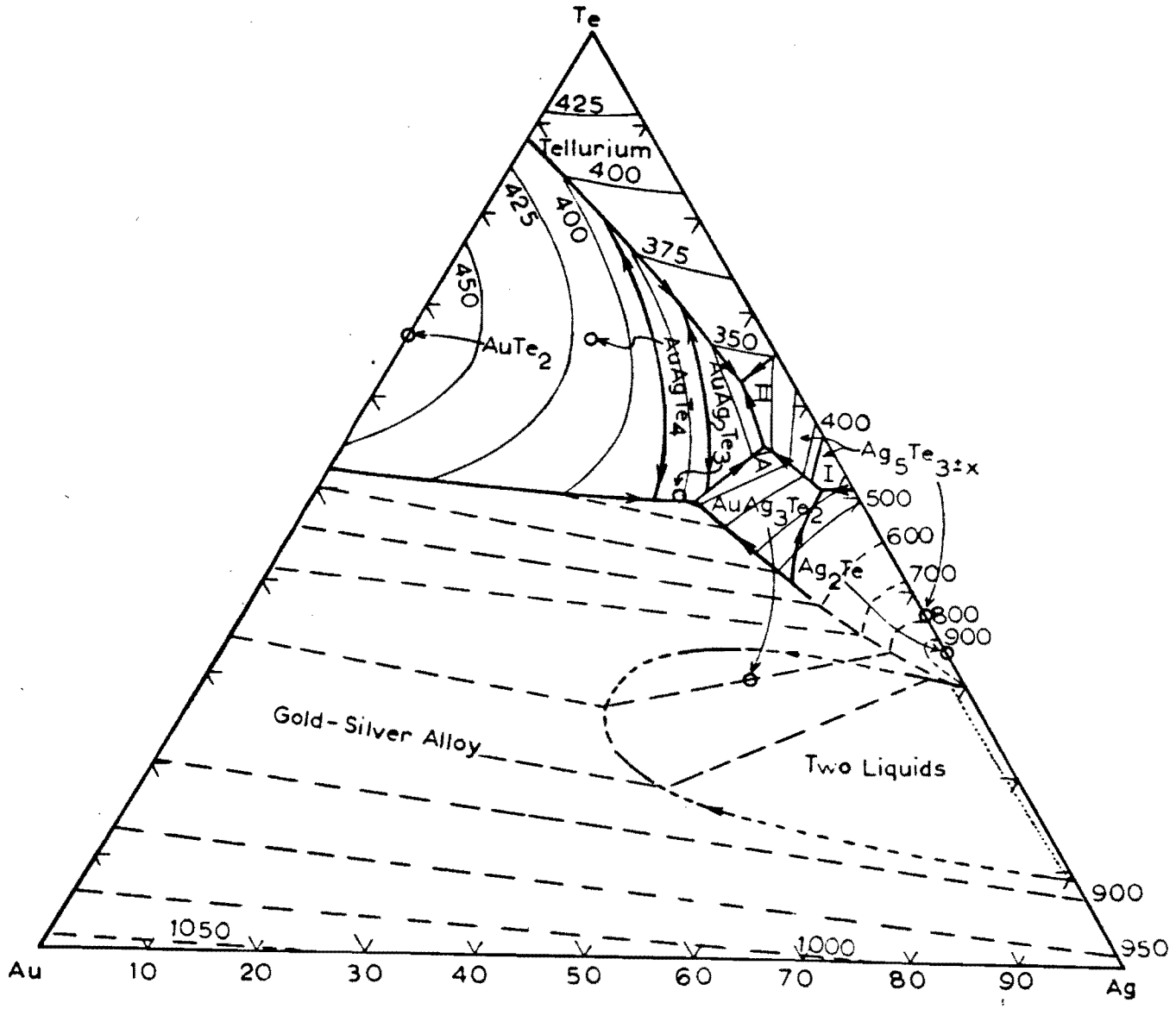

Figure 2. Liquidus surface of the Au-Ag-Te system after Kracek (unpublished) shown in atomic per cent. Note that the point for $AuAg_3Te_2$ (petzite) is misplaced, and that the present investigation has shown no indication of the phase $AuAg_2Te_3$.

that the tie-line joining hessite and sylvanite at 300°C changed to an $Ag_{5-x}Te_3$-petzite join at 315 ± 10°C. He was unable to synthesize krennerite, (Au, Ag)Te_2 and speculated that it was the low-temperature, low-pressure polymorph of $AuTe_2$.

Phase relations along the join $AuTe_2$-"$AgTe_2$"

Previous studies by Borchert (1935), Tunell and Ksanda (1936), and Markham (1957, 1960) indicated that the stability fields of the naturally occurring phases on this join were far from completely understood. Further confusion was added by the unreliability of many reported analyses and identifications of these phases because of their great similarity in polished sections. This is especially true when no x-ray diffraction study was made.

It is appropriate to outline in tabular form some of the crystallographic, physical, and chemical properties of the three minerals known to occur on the $AuTe_2$-"$AgTe_2$" join.

TABLE 1

Crystallographic data for calaverite, krennerite, and sylvanite (taken from Tunell, 1954, p. 3 and 44).

Mineral	Space group	a Å	b Å	c Å	B	Å^3	Cell content	Source
Calaverite	C^3_{2h}-C^2/m	7.19	4.40	5.07	90° 13'	160.4	2(Au,Ag)Te_2	Tunell (unpublished
Krennerite	C^4_{2v}-P_{ma}	16.54	8.82	4.46		162.6	8(Au,Ag)Te_2	Tunell & Murata (1950)
Sylvanite	C^4_{2h}-P^2/c	8.86	4.49	14.62	145° 26'	166.9	2$AuAgTe_4$	Tunell (1941)

"The structures of calaverite, krennerite, and sylvanite are basically similar, although they have three different space-group symmetries. In all three minerals each gold and silver atom is surrounded by six tellurium atoms, which are not at the same distance, however. In calaverite and sylvanite each tellurium atom is surrounded by three gold or silver atoms and three tellurium atoms. In krennerite, part of the tellurium atoms are surrounded by one gold or silver atom and five tellurium atoms, part by five gold or silver atoms and one tellurium atom." (Tunell, 1954, p. 4)

TABLE 2

Some physical and chemical data for calaverite, krennerite, and sylvanite.

Mineral	Calc. density	Measured density	wt. % silver (1)	
Calaverite	9.26 (2)	9.29 (2)	0.25,0.33	Kirkland Lake area, Ontario (3)
		9.10-9.40 (4)	0.40,1.74	Cripple Creek, Colorado (5)
		9.155 (6)	0.77,0.79	Colorado (6)
			0.58-2.3	Kalgoorlie, Aust. (7)
			2.24,2.56	Red Cloud Mine, Colorado (8)
Krennerite	8.86 (9)	8.63 (9)	4.87,5.4	Cripple Creek, Colorado (9)
		8.62,8.18 (10)	5.87	Sacarambu, Nagy-Ag (10)
			2.0-6.64	Kalgoorlie, Aust. (11)
Sylvanite	8.11 or 8.17 (12)	8.16 (13)	12.49	Cripple Creek, Colorado (13)
		8.24 (4)	9.18-11.77	Kalgoorlie, Aust. (7)
			11.74	Vatukoula, Fiji (7)
		7.943 (8)	11.52, 11.92, 13.05	Red Cloud Mine, Colorado (8)

TABLE 2 (cont'd.)

(1) Most of the reported calaverite analyses with more than 3% Ag are by Hillebrand (1895) p. 129 and Genth (1868) p. 314 and (1877) p. 118 giving 3.23, 3.52, 3.08, 3.03, and 3.08% respectively. Besides containing many impurities, none of these analyses were performed on crystallographically examined samples and so cannot be considered too significant as it is quite likely that the calaverite examined contained small amounts of krennerite or other silver-rich tellurides.

(2) Tunell (1954) p. 5; measured density determined pycnometrically.

(3) Todd (1928) p. 77, 78; these analyses contained over 5% altaite and have been recalculated on the assumption that all the silver was contained in the calaverite.

(4) Thompson (1949) p. 347, 353.

(5) Penfield and Ford (1901) p. 246.

(6) Smith (1902) p. 149 - density is the mean of three specimens.

(7) Markham (1960) p. 1166, 1170, 1469.

(8) Genth (1874) p. 228, 229 - sylvanite analyses contained also quartz, Cu, Pb, Zn, Fe, Se, and S.

(9) Tunell and Murata (1950) p. 962, 964 - density pycnometrically determined, average of five single crystals.

(10) Sipöcz (1885) p. 176 - this material contained 2.29% quartz, 0.33% Cu, 0.58% Fe, 0.64% Sb.

(11) Markham (1960) p. 1169 - most of these values are taken from Simpson (1948, 1951, 1952) and had been originally given as analyses for sylvanite, but thought by Markham to be krennerite based on the amount of silver.

(12) Tunell (1941) p. 459.

(13) Palache (1900) p. 419, 422 - the density was determined with a hydrostatic balance on three specimens.

One can make the following observations from the above data:

(1) The silver content as well as the molar volume increase from calaverite through krennerite to sylvanite.

(2) Calaverite generally contains silver, but less than about 3 wt. %.

(3) Krennerite generally contains about 4-6 wt. % Ag silver.

(4) Sylvanite has not been analysed with its theoretical Au:Ag ratio of 1:1 which would amount to 13.23 wt. % Ag; but the analyses indicate a range from about 9-13 wt. % Ag.

Much of the uncertainty of the stability fields of these three minerals has centered around krennerite. Borchert (1935), on the basis of heating experiments on natural krennerite, concluded that above 184°C krennerite was transformed to calaverite and furthermore that all natural calaverite has passed through this inversion. Tunell and Ksanda (1936) have shown, however, that the apparently single crystals of calaverite that they studied have undergone no polymorphic inversion and are not paramorphic.

There remain crystallographic problems connected with calaverite in that some of the complex faces present have been found to be related to certain adventive diffraction spots on the Weissenberg photographs (Tunell and Ksanda, 1936, Tunell, 1954). A complete explanation has not yet been found for the complex faces or the adventive diffraction spots. Markham (1957, 1960) could not synthesize krennerite and made some heating experiments with natural krennerite, calaverite, and runs of krennerite composition (2.0 to 8.0 wt. % Ag) at 430°, 400°, 300°, 250° and 150°C. On the basis of his results he concluded that krennerite is the low-temperature, low-pressure polymorph of calaverite and that "krennerite is always metastable with respect to calaverite." (Markham, 1960, p. 1160)

Natural occurrences of calaverite, krennerite, and sylvanite

It is instructive to look at natural assemblages of these minerals in order to correlate and understand experimental work done in the synthetic system. It will become apparent as reported occurrences are cited that misidentification is an ever present danger.

Thompson (1949) lists over eighty Canadian telluride localities. He makes the correct distinction of reporting separately those occurrences which had been confirmed by x-ray diffraction. In summarized form, his findings related to the minerals being discussed are given below.

17 localities reported calaverite of which 12 were confirmed.

3 localities reported calaverite plus sylvanite but these are unconfirmed.

2 localities reported krennerite but these are unconfirmed.

3 localities reported sylvanite but these are unconfirmed.

1 locality reported calaverite plus krennerite plus sylvanite but only the calaverite is confirmed.

Price (1933) describes one specimen with the assemblage calaverite-sylvanite-tetradymite-unknown telluride and shows a drawing of calaverite in contact with sylvanite (plate 80). His identifications, however, are by means of optical properties, etch, and microchemical tests only, and he does state that the sylvanite does not show twinning in all areas.

There is thus no confirmed evidence of the assemblage calaverite-sylvanite in these Canadian localities and the presence of krennerite is likewise unconfirmed.

Lovering and Goddard (1950) p. 299, show in the following sentences

the reliability of some identifications at Cripple Creek, Colorado. "The most common telluride is calaverite, but considerable sylvanite and krennerite are also present. The term sylvanite is frequently applied by the miners to silvery calaverite and the term calaverite to yellowish or slightly tarnished crystals, fine aggregates of which may be confused with fine grained pale-yellow-pyrite."

Tunell (1954) p. 1, reports that "By detailed examination with the binocular microscope of all the specimens in the collections of Cripple Creek ores in the laboratories of the Geological Survey (U.S.) and in the National Museum (Washington) the author proved that, contrary to published statements, calaverite and krennerite were present in these ores in approximately equal abundance. Sylvanite, as had been stated in several publications, was found to be present in a much smaller quantity than calaverite or krennerite." No mention is made if calaverite and sylvanite were found together.

Kelly (1963), after his extensive examination of polished sections from Boulder County, Colorado, has observed that the assemblage calaverite-sylvanite is very rare (three out of 195 polished sections). In the very few sections where this occurred, identification of the sylvanite was by optical means, unconfirmed by x-rays. The identification of the calaverite was confirmed by x-ray, but the sylvanite was so fine-grained that pure phases could not be extracted for x-ray. The sylvanite in each case showed conspicuous polylamellar twinning and strong bireflectance and was identified only on the basis of these properties.

Markham (1960) reports that calaverite is the most abundant telluride at Kalgoorlie and out of the 110 telluride bearing specimens examined, he

found five specimens where calaverite was in contact with krennerite and only two occasions where the calaverite-sylvanite assemblage occurred. He based his identifications on x-ray diffraction. The earlier Australian workers, Simpson and Stillwell, realized that much of their "sylvanite" could be krennerite, and so less weight can be placed on their reports in this context. Baker (1956, p. 1) reports krennerite from Kalgoorlie associated with fringes of smaller grained sylvanite, and with sylvanite-hessite intergrowths. He also reports that calaverite and petzite could not be positively identified by the mineragraphic method employed.

Both krennerite and sylvanite have been identified at Vatukoula, Fiji Islands, by Markham (1960) and he noted that these are found together in several instances.

It can thus be said that confirmed reports of the assemblage calaverite-sylvanite are very rare, whereas the assemblages calaverite-krennerite and krennerite-sylvanite do occur.

Materials, methods of synthesis, and techniques

Materials

Two lots of gold of 99.9995+% purity were obtained from Johnson, Matthey, and Mallory Ltd., Montreal and Toronto. The first lot was in the form of irregular pellets and the second (unfluxed gold) was a powder of approximately 100 mesh grain size.

Tellurium (in bar form of 99.999+% purity, with Mg, Fe, Cu all < 0.0001%) was obtained from the American Smelting and Refining Company.

Silver rods (99.999+% purity) were obtained from the Consolidated Mining and Smelting Company (Cominco 59 grade, lot no. 2706). They contained the following impurities in parts per million: CaO - 0.1, Cu - 0.2, Fe - 4.0, Mg - 0.1, Si - 0.1.

All these materials, as well as bulk quantities of some synthesized minerals, were kept in an evacuated dessicator.

Methods of synthesis

Most of the runs were performed in simple, sealed tubes of transparent silica glass. The suitability of silica glass as well as the evacuation and sealing techniques are described by Clark (1959, p. 8-10). A loading technique by addition was evolved to nullify the adherence of reagents to the walls of the tubes by electrostatic charges; by using glass funnels of different lengths, a humidifier, and having a source of gamma radiation (a rich specimen of pitchblende) adjacent to the tube while loading.

The runs were cooled as rapidly as possible in cold water, or an ice-water mixture, and their charges were ground or reground in an agate mortar under acetone. Hessite, and hessite-rich charges, could not be

easily ground due to their malleability. Such charges were crushed in a steel mortar immersed in liquid air. Some of the runs performed at lower temperatures were pelletized in a 5 mm. internal diameter press under about 21,000 lbs/in^2. For similar periods of heating it was observed that runs which had been pelletized gave much sharper x-ray diffraction photographs. This was interpreted as a closer approach to equilibrium. Pelletized runs were also reground and annealed for a few days prior to being x-rayed.

A more detailed account of the loading, regrinding, and pelletizing techniques is described in the appendix.

Temperature control and measurement

Most of the runs were heated in horizontal, cylindrical, electric furnaces similar to those designed by Dr. G. Kullerud (with a bridge type control mechanism) [Clark, 1959, p. 11-12]. These furnaces maintain a constant temperature within $\pm$ 1°C over a 3.5 to 5 inch zone measured at 600°C. Temperatures were controlled to better than $\pm$ 2°C and were measured with chromel-alumel thermocouples. All temperatures were recorded continuously on a multi-channel recording potentiometer. Temperatures were checked once a week with a Rubicon potentiometer using a reference junction at 0°C and were never found to vary more than ½°C.

Identification of the products

(i) Reflecting microscope. Polished sections were made of those charges which were sufficiently solid; a portion being set in cold setting dental plastic and then fastened to a glass slide with vynilite. All polished sections were examined under the reflecting miscroscope using oil immersion objective lenses. Where phases had distinctive optical properties, less than one tenth of one per cent could be detected. Unfortunately,

many of the phases examined had very similar optical properties. Calaverite, krennerite, and sylvanite form one such group; and hessite, petzite, and $Ag_{5-x}Te_3$ form another.

A more detailed account of the polishing and identification techniques of some of these phases is described elsewhere (see appendix, p. A2).

(ii) X-ray diffraction. A portion of the original charge was examined by x-ray diffraction, and the remainder was stored in the original silica glass tube. Various x-ray powder diffraction techniques were experimented with as many of the Au-Ag tellurides have very similar x-ray diffraction patterns, and the d-spacings of selected reflections only varied in the fourth decimal place with increasing solid solution. Thus accuracy and reproducibility are very important factors.

Five different x-ray powder methods were used. The Phillips symmetrical back reflection focussing camera was found to be the most satisfactory instrument for studying the change in interplanar d-spacings of selected reflections.

The 114.6 mm. Debeye-Scherrer camera was used largely for qualitative work, and was superseded by the Guinier-de Wolfe forward reflection, focussing, multiple exposure powder camera because this camera was able to show the presence of very small amounts of some phases (less than ½ wt. % in some cases).

A Rigaku-Denki high-temperature x-ray powder diffraction camera was used to determine transition temperatures and to study the stability fields of those phases which could not be quenched.

Greater detail about each of the x-ray powder diffraction methods used is included in the appendix.

Phase relations in the binary systems

The Au-Ag binary

No studies were carried out in the Au-Ag binary since the previous work is regarded as adequate.

The Au-Te binary

The present investigation was concerned with the melting point of $AuTe_2$, the extent of solid solution of Te and of Au in $AuTe_2$, if any, and the stability field of Au_2Te_3. The melting point of $AuTe_2$ was confirmed by placing coarsely ground $AuTe_2$ in a sealed, evacuated, silica glass capsule in a horizontal furnace and examining the contents after successive 1°C increments in temperature. The furnace was held at each temperature for at least a half hour. $AuTe_2$ was found to melt at 464 $\pm$ 3°C, in good agreement with the published data (Pellini and Quercigh, 1910b), although Winkler and Bright (1964, p. 7) report 469 $\pm$ 1°C from several heating and cooling arrests.

Runs with $AuTe_2$ plus excess Te, and with excess Au, were heated at 320°, 350°, and 440°C.* No detectable departure from stoichiometry could be discerned for runs with excess Te and excess Au at 320° and 350°C. This was established by measuring the d_{131} reflection of $AuTe_2$ and by confirming the presence of excess Te or Au with polished sections or the Guinier camera. At 440°C, however, there were indications that a small amount of Te was taken into solid solution (d_{131} = 1.3854), although Au solid solution in $AuTe_2$ could not be detected. The run with the least

---

*All phase relations in this study were determined in sealed silica or pyrex tubes in which the condensed phases coexisted with the vapor in the tube. The vapor pressure is a function of the temperature and composition of the charge.

excess Te (0.6 wt. %) showed Te in polished section as well as on the Guinier film, and it is estimated that 0.3 wt. % Te or less is taken into solid solution at 440°C.

Upon increasing temperature the solid solubility of silver in $AuTe_2$ decreases sharply to zero at 435°C (see figure 4). This is about 30°C below the melting point. This behaviour is the result of a postulated polymorphic inversion in $AuTe_2$ at 435°C.

Several runs were examined with the Rigaku-Denki high-temperature x-ray powder diffraction camera but gave irreproducible results. The first capillary with synthetic $AuTe_2$ was heated to about 400°C and then to a temperature above the melting point giving the calaverite pattern and no pattern, respectively. A week later the same capillary was heated to 388°, 427°, and 444°C. The patterns were all those of calaverite although at 427°C and, to a greater extent, at 444°C the calaverite pattern was "spotty". Six months later this same capillary was heated to 444°C and gave the following pattern, also "spotty", which is quite distinct from the previous calaverite patterns. (see table 3)

TABLE 3

X-ray powder diffraction data for a probable high-temperature form of $AuTe_2$

Line No.*	d obs.	hkl	a
1	3.01	100	3.01
2	2.12	110	2.99
3	1.51	200	3.02
4	1.35	210	3.01
5	1.01	221,300	3.02
6	0.948	310	2.99
$7_{\alpha 1}$	0.867	222	3.00
$8_{\alpha 1}$	0.852	320	3.07
$9_{\alpha 1}$	0.815	321	3.05
$10_{\alpha 2}$	0.815		$\bar{a} = 3.02$

*The intensities of the reflections were approximately equal.

This same capillary when x-rayed at room temperature gave a pattern which was unclear. The capillary was then ground and x-rayed with the Guinier camera which showed the patterns of $AuTe_2$ + Te + (Au?). Some phenomena, as yet unclear, produced an effective breakdown of $AuTe_2$ in the capillary. However, the pattern indexed in table 3 shows a close correlation with the work of Luo and Klement (1962). They investigated the Au-Te binary from 5.5 to 60.4 atomic per cent gold by using an extremely rapid cooling technique in air from 650-750°C (described in Klement, 1961). They report a simple cubic, metastable, Au-Te alloy existing between 15.3 and 40.4 atomic per cent gold having a lattice parameter varying from 3.11 to 2.91 $\pm$ 0.01 Å, respectively. Their lattice parameter versus gold composition curve (determined by x-raying at 26°C) indicates a value of a = 2.97 Å for an alloy of $AuTe_2$ bulk composition. This value can be equated with that postulated for the high-temperature polymorph (table 3) which gave a value of a = 3.02 Å when x-rayed at 444°C.

At 388° and 444°C a new capillary of $AuTe_2$ gave a good pattern of $AuTe_2$ and a very spotty, but otherwise normal, pattern of $AuTe_2$, respectively. Upon further heating to ~460°C the charge apparently melted and exposures at that temperature and 392°C yielded very spotty patterns of $AuTe_2$.

Four hour exposures of a third capillary of $AuTe_2$ were taken on successive days at 445°, 447°, 443°, and 436°C. The patterns in all cases could be ascribed to $AuTe_2$ but became progressively more spotty with time, presumably indicating recrystallization.

Therefore there are some indications that the $AuTe_2$ structure breaks down above 435°C, but the process involved is not at present

understood. This transition possibly may be related to the development of "super structure" reflections of the natural and synthetic mineral as discussed in a previous section. This inversion was also suspected by Winkler and Bright (1964, p. 9) from differential thermal analysis endothermic phenomena observed at 435°C.

Attempts to synthesize Au_2Te_3, reported by Peacock and Thompson (1946) as the mineral montbrayite, were unsuccessful. Runs with Au_2Te_3 composition at 320°, 350°, and 440°C all yielded $AuTe_2$ + Au. Runs of Au_2Te_3 composition plus 1% Ag gave $AuTe_2$ + Au + $AuAg_3Te_2$ at 440°C. However, in studying the gold-rich region around $AuAg_3Te_2$, a new phase was detected on the Guinier powder photographs which bears some resemblance to the published pattern of Au_2Te_3. This problem will be discussed in a later section and the x-ray powder data for Au_2Te_3 is compared with that of the new phase in the appendix, table A12. A run of Au_2Te_3 composition (with 1% Ag) was heated to 315° and 385°C in the high-temperature camera but gave only the powder pattern of $AuTe_2$ and Au.

If Au_2Te_3 can in fact be synthesized from the pure elements, its field of stability is probably below 320°C. However, Luo and Klement (1962, p. 1872) note that a metastable gold-tellurium alloy of 37.5 atomic per cent Au (Au_2Te_3 = 40 at. % Au) was relatively more stable than all other metastable alloys studied. This might be related to the mineral montbrayite. There is only one reported occurrence of montbrayite, from the Robb-Montbray Mine, Montbray Township, Abitibi County, Quebec. The rarity of this mineral probably indicates that it was formed under unusual physical-chemical conditions because the assemblages gold-calaverite, and gold-calaverite-petzite are not rare.

The Ag-Te binary

The Ag-Te binary has been investigated by several workers as was discussed earlier. Prior to Dr. F.C. Kracek's death, he had prepared a manuscript for publication (jointly with Ksanda) which gave greater detail (plus some additions) on the data reported by Kracek and Rowland (1955). However, in a report by Kiukkola and Wagner (1957), the presence of a phase intermediate in composition between $Ag_{5-x}Te_3$ and Ag_2Te was indicated. This meant that further work was necessary on the Ag-Te binary. The present writer obtained Kracek and Ksanda's manuscript through the kindness of Dr. R.A. Robie with the intention of clarifying the above point.

Thirteen runs of different compositions (56.75 to 62.38 wt. % Ag) along the binary were synthesized in horizontal furnaces by heating weighed amounts of Ag and Te in sealed evacuated silica glass capsules above 950°C. The charges were subjected to various heat and grinding treatments as tabulated in the appendix, table A2. Portions of most of these runs were ground and transferred into silica glass capillaries which were evacuated and sealed for use in the high-temperature camera.

Most of the runs were performed by letting the camera equilibriate to the first temperature over a period of eight hours. After exposure for five to seven hours at 35 kilovolts and 20 milliamps with filtered Cu radiation, the specimen was progressively heated to higher temperatures, but only half an hour to three hours were allowed to attain equilibrium at each new temperature.

Figure 3 represents a detailed section of the Ag-Te binary system showing the phase relations as deduced from data obtained with the

Rigaku-Denki high-temperature powder diffraction camera and from quenched runs in evacuated silica and pyrex glass capsules. The diagram is essentially in agreement with the data of Kracek and Ksanda (unpublished) together with Kiukkola and Wagner (1957) if data in the former are reinterpreted. The estimated error in temperatures delimiting the stability fields of the phases is based upon both Kracek and Ksanda's (unpublished) data and the present work.

Several anomalous results were ignored in drawing up the phase diagram. It was established, for example, that reliable data could not be obtained if a capillary was used more than once. Heating the same capillary several times is thought to produce inhomogeneity in the charge. Even with capillaries used only once, several runs gave anomalous results, (e.g. the incongruent melting temperature of $Ag_{5-x}Te_3$ varied in some runs up to 445°C, the low to high transition in Ag-rich $Ag_{5-x}Te_3$ occurred as high as 293°C in one run, and the gamma-phase melted incongruently as low as 437°C in some runs). The temperatures and compositional limits as drawn in the phase diagram were derived partly from Kracek and Ksanda's and Kiukkola and Wagner's work and partly from the present investigation and were generally in good agreement.

The phase diagram indicates the presence of three phases: $Ag_{5-x}Te_3$, the gamma-phase, and Ag_2Te. $Ag_{5-x}Te_3$ melts incongruently above 420 ± 5°C to gamma-phase plus liquid. The compositional range of $Ag_{5-x}Te_3$ is from 57.95 to 58.39 wt. % Ag at 300°C according to Kiukkola and Wagner (1957). The low to high polymorphic inversion in $Ag_{5-x}Te_3$ occurs above 265 ± 10°C on the Ag-rich side and above 295 ± 10°C on the Te-rich side. Delineation of the two phase field ($Ag_{5-x}Te_3$ (low) and $Ag_{5-x}Te_3$ (high)) is uncertain

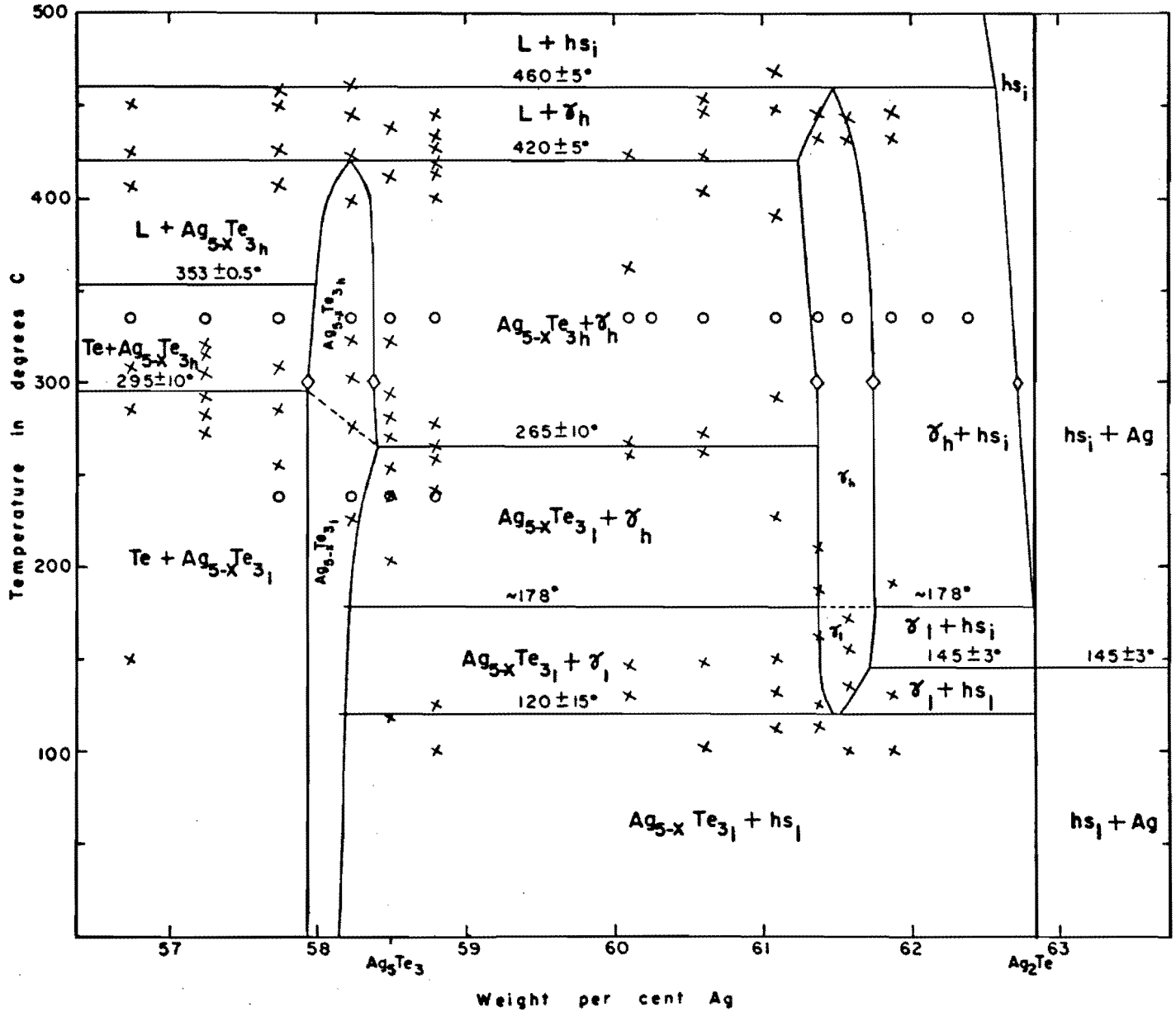

Figure 3.

Phase relations along part of the Ag-Te binary in equilibrium with vapor. Crosses represent high-temperature camera data, circles represent quenched runs x-rayed with the Guinier camera, and diamonds are the solid solution limits from Kiukkola & Wagner (1957). The inversion in Ag_2Te and the temperature of the eutectic are those of Kracek & Ksanda (unpublished).

and is shown in figure 3 only as a dashed line. The high form of $Ag_{5-x}Te_3$ could not be quenched for x-ray at room temperature. There is very little difference in the high-temperature x-ray patterns of the high and low forms (table 4), yet they can be identified in a series of photographs taken with small (10 to 20°C) increments of temperature between exposures.

There has been much confusion in the notation used for polymorphs of Ag_2Te and $Ag_{5-x}Te_3$. Both Roman numerals and Greek letters have been employed. Throughout this text, the terms low, intermediate, and high and their abbreviations l, i, and h in the diagrams are used (this also applies to other minerals such as petzite, etc.).

The phase intermediate in composition between $Ag_{5-x}Te_3$ and Ag_2Te, termed the gamma-phase by Kiukkola and Wagner (1957), is stable between the temperature limits 120 ± 15°C and 460 ± 5°C, above which it melts to Ag_2Te plus liquid. The compositional range of the gamma-phase at 300°C is from 61.38 to 61.75 wt. % Ag according to Kiukkola and Wagner (1957). The low to high polymorphic inversion, heretofore unreported, occurs at about 178°C. No detail was obtained for the narrow field containing both the low and high polymorphs, and this field is indicated in figure 3 as a dashed line. The evidence for this transition is given in table 4 where the high-temperature x-ray patterns for the two polymorphs are compared.

TABLE 4

High-temperature x-ray diffraction patterns for gamma-phase and $Ag_{5-x}Te_3$.

Run No. 258 (61.08 wt. % Ag)				Run No. 378 (58.23 wt. % Ag)			
γ-low @ 150°C		γ-high @ 227°C		$Ag_{5-x}Te_3$ (low) @ 275°C		$Ag_{5-x}Te_3$ (high) @ 302°C	
I	d meas.	I	d meas.	I	d meas.	I	d meas.
				w*	3.55	w	3.57
				w	3.11	w	3.14
				w	3.03	w	3.02
				w	2.62	vw	2.63
				m	2.57	vw	2.57
vw	2.25	m	2.22	w	2.24	w	2.25
s	2.18	s	2.18	s	2.17	s	2.18
vw	2.11			m	2.13	m	2.15
				w	2.04	w	2.04
				w	1.95	w	1.95
				vw	1.88	w	1.88
				w	1.35	w	1.36

* w = weak
vw = very weak
m = medium
s = strong

The transitions in Ag_2Te and the temperature of the eutectic are those of Kracek and Ksanda (unpublished). The intermediate and high forms of Ag_2Te could not be quenched for x-ray at room temperature.

The existence of the gamma-phase was confirmed with the high-temperature camera, the Guinier camera, and polished sections. Table 4 shows the x-ray diffraction pattern obtained with the high-temperature camera compared with the patterns of $Ag_{5-x}Te_3$. The similarity of the patterns, especially of the strongest reflections, made interpretation of the films difficult. However, the change from patterns showing $Ag_{5-x}Te_3 + Ag_2Te$ in runs of about 61.5 wt. % Ag to gamma-phase above 120°C is quite distinct. The Guinier x-ray powder diffraction pattern of the gamma-phase (see appendix, table A3) indicates that the pattern is distinct from those of $Ag_{5-x}Te_3$ and Ag_2Te. The gamma-phase could only be preserved for x-ray by rapid cooling in ice-water and x-raying as soon as possible with the laboratory cooled to 18°C. For the gold free gamma-phase a noticeable breakdown to $Ag_{5-x}Te_3$ and Ag_2Te could be observed after 24 hours at 18°C. As will be discussed in a later section, the gamma-phase can take more than 10 wt. % Au in solid solution, and this apparently stabilizes the structure for a longer period at room temperature. Polished sections of the gamma-phase were made and described in the section entitled "Tie lines within the area bounded by calaverite, sylvanite, $Ag_{5-x}Te_3$, hessite, and petzite."

Kracek and Ksanda's unpublished data can easily be reinterpreted to substantiate the presence of the gamma-phase. Table 5 gives data from their differential thermal analysis.

TABLE 5

Selected differential thermal analysis data from Kracek and Ksanda (unpublished).

Composition range wt. % Ag	Heating arrest	Cooling arrest
58.488 to 61.655	122-138°C	70-85°C
61.655 to 62.295	147°	143°
	131-132°	121-123°
		85-110°

Note: Ag_2Te = 62.836 wt. % Ag

Ag_5Te_3 = 58.49 wt. % Ag

Their interpretation is shown by figure A3 in the appendix. The above data can be reinterpreted on the basis of the present work as follows.

(1) 58.488 to 61.655 wt. % Ag composition range.

The heating arrest represents the formation of the gamma-phase. The cooling arrest represents the breakdown of gamma to $Ag_{5-x}Te_3 + Ag_2Te$. The larger divergence between the cooling arrest temperature and that obtained with the high-temperature camera is not unexpected since the gamma-phase can be preserved at room temperature with very rapid cooling.

(2) 61.655 to 62.295 wt. % Ag composition range.

The highest heating and cooling arrests correspond very well with the Ag_2Te polymorphic inversion (low to intermediate), indicating negligible solid solution in Ag_2Te as 145 ± 3°C is the transition temperature on the Ag-rich side as well. The heating arrest at 131-132°C represents the

formation of the gamma-phase from $Ag_{5-x}Te_3 + Ag_2Te$. The two cooling arrests can be interpreted in two ways. They could be attributed to a partial, followed by a complete breakdown to $Ag_{5-x}Te_3 + Ag_2Te$. Alternatively the highest cooling arrest may be due to a supercooled transition in gamma (found at 178° in the present investigation), with the lowest temperature representing the final breakdown to $Ag_{5-x}Te_3 + Ag_2Te$.

Kracek (1963) and Umino (1926) report the possibility of a solid state transition in tellurium. Von Hippel (1948), on theoretical grounds, wrote that the hexagonal Te structure could be easily distorted to a simple cubic lattice. A capillary with tellurium was x-rayed in the high-temperature camera from room temperature to $434^{\circ}C$ (at intervals of approximately $75^{\circ}C$). The pattern remained essentially the same except for a progressive enlargement of the lattice and gradual convergence of two doublets with increasing temperature. Apparently no transition occurs in this temperature range and at pressures less than one atmosphere.

Attempts to synthesize the phase AgTe, reported as occurring in natural ores, originally by Bradley (1914, 1915) and recently confirmed by Honea (1964), were unsuccessful as shown in table 6.

TABLE 6

Selected runs heated at 194° and 170°C relating to the Ag-Te binary.

Run No.	wt. % Ag	wt. % Te	Thermal history	Products identified on Guinier powder photographs
264	45.81	54.19	M; 90 days @ 194°C, G & P after 6, 25, and 60 days, G after 78 days	$Ag_{5-x}Te_3$ + Te
265	45.83	54.17	90 days @ 194°C, G & P after 6, 25, and 60 days, G after 78 days	$Ag_{5-x}Te_3$ + Te
264A	45.81	54.19	after heating at 194°C above, G & P, 86 days @ 174°C, G & P after 42 days, G after 85 days	$Ag_{5-x}Te_3$ + Te
265A	45.83	54.17	after heating at 194°C above, G & P, 86 days @ 174°C, G & P after 42 days, G after 85 days	$Ag_{5-x}Te_3$ + Te + TeO_2*
331	45.80	54.20	86 days @ 170°C, G & P after 42 days, G after 85 days	$Ag_{5-x}Te_3$ + Te

*TeO_2 was detected in run 265A because the charge was left open to the atmosphere for several weeks after heating at 194°C.

These attempts to synthesize AgTe were made at temperatures well below the upper stability limit of natural AgTe deduced by Honea from differential thermal analysis as 210°C. Binary compositions equivalent to $Ag_{5-x}Te_3$ (58.23 wt. % Ag) and more silver-rich compositions all gave the $Ag_{5-x}Te_3$ pattern with about six extra reflections. The three largest d-values of these extra reflections cannot be indexed according to published patterns of $Ag_{5-x}Te_3$ (see appendix, table A4). These extra reflections, which do not accompany the normal $Ag_{5-x}Te_3$ x-ray pattern cannot be attributed to any known polymorphs of hessite, gamma-phase, or $Ag_{5-x}Te_3$. It is noteworthy that these reflections correpond fairly closely to some of the strongest reflections in the pattern for natural AgTe as reported by Honea. By a further coincidence, most, if not all of the remaining reflections in Honea's AgTe pattern correspond to reflections in $Ag_{5-x}Te_3$ (see appendix, table A4). The reason for these relations is not understood at present. It might be noted that the pattern for synthetic $Ag_{5-x}Te_3$, which contains many more reflections than were observed by either Berry and Thompson (1962) or by Honea (1964), is in much closer agreement to the cell dimensions and indexing of Berry and Thompson.

Luo and Klement (1962), using an extremely rapid quenching technique in air, report the presence of a simple cubic, metastable, Ag-Te alloy existing between 20.5 and 30.5 atomic per cent Ag. Between the compositions 33.5 and 50.5 atomic per cent Ag, the x-ray patterns of this cubic phase became progressively weaker and the pattern of an unidentified phase (or phases) became progressively stronger. (A 114.6 mm. Debeye-Scherrer x-ray film of the 50 at. % Ag-Te alloy, kindly provided by H.L. Luo, was examined and identified as $Ag_{5-x}Te_3$ + cubic Ag-Te alloy.)

In view of the uncertainties remaining in the Ag-Te binary system cited above, the writer considers that not enough is known about the phase AgTe to include it in the Ag-Te phase diagram at this time.

Phase relations along the join $AuTe_2$-"$AgTe_2$"

The phase diagram, figure 4, shows the phase relations along a portion of the join $AuTe_2$-"$AgTe_2$". The solvus curves represent a close approach to equilibrium from the solidus down to 320°C. It is considered that equilibrium was not reached below 320°C, except possibly along the silver-rich solvus of sylvanite, and the interpretation made is guided by the apparent reaction rates at the higher temperatures as well as by the products formed. This will be discussed in greater detail in a later section. Symbols used are those proposed by Chase (1956), unless otherwise indicated.

The extents of the solid solution fields were determined by constructing d-value versus composition curves from the measurements of the interplanar spacings of selected reflections at various compositions and temperatures. It was soon apparent that there were few reflections which satisfied all the requirements of this method and the reflections finally used were selected after considerable trial and error. The d-value versus composition curves for calaverite, krennerite, and sylvanite are given in figures 6, 7, and 8,respectively. The maximum weighing error is estimated to be $\pm$ 0.2 wt. %. As the fit on the curves indicates, it is probably considerably less.

The calaverite d-value versus silver content curve

The calaverite d_{131} reflection (according to indexing by Tunell 1954 , see appendix, table A14) was measured on the x-ray diffractometer. An appropriate amount of internal standard (LiF, a = 4.0270 Å) was mixed with the sample and the diffractometer was set to oscillate four or six times over the region to be measured. The goniometer rotation was $\frac{1}{2}$°/minute and

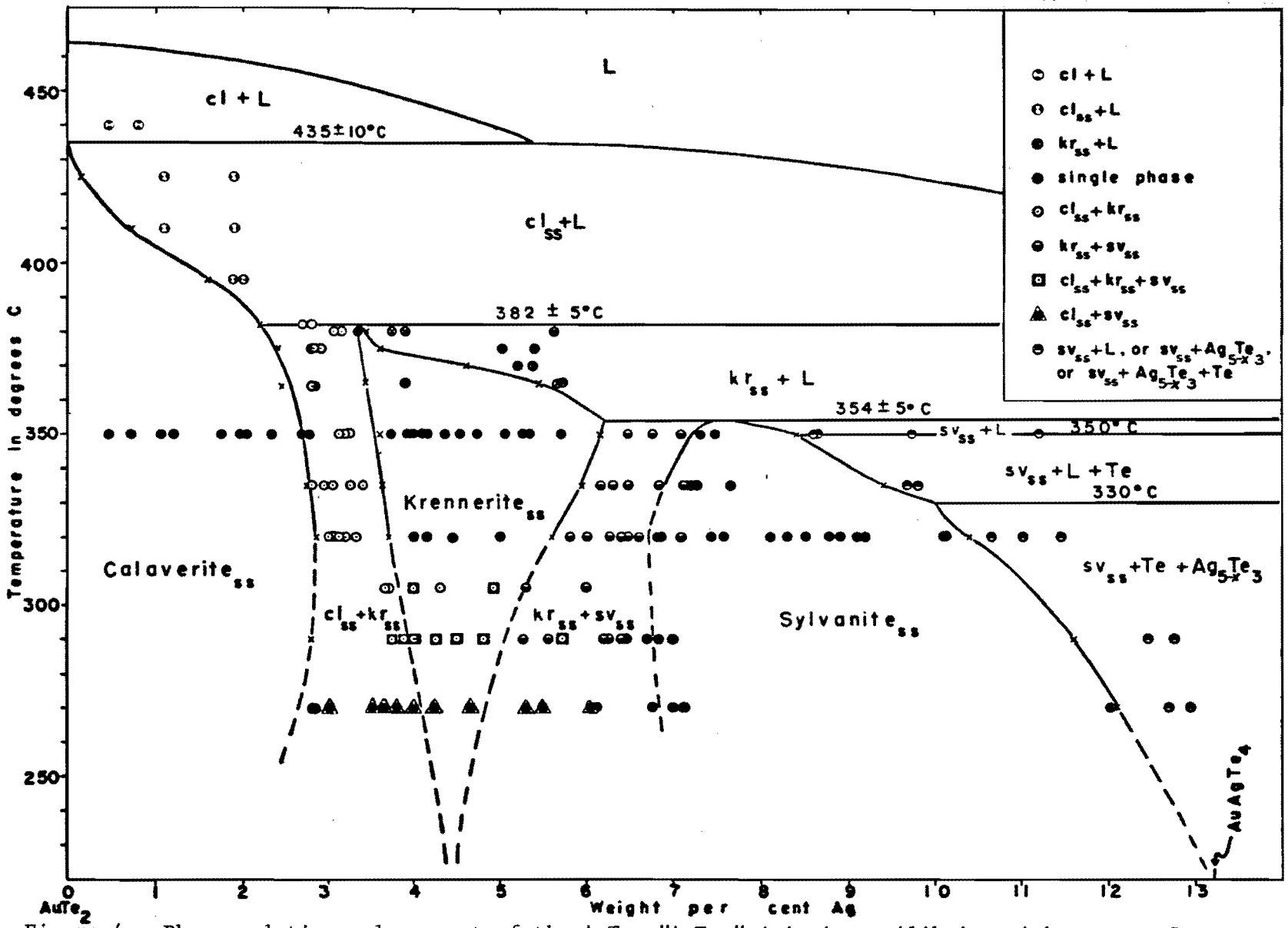

Figure 4. Phase relations along part of the $AuTe_2$-"$AgTe_2$" join in equilibrium with vapor. Crosses represent the limits of solid solution as determined from figures 6, 7, & 8. Note that some runs at 305°C and lower temperatures are not at equilibrium.

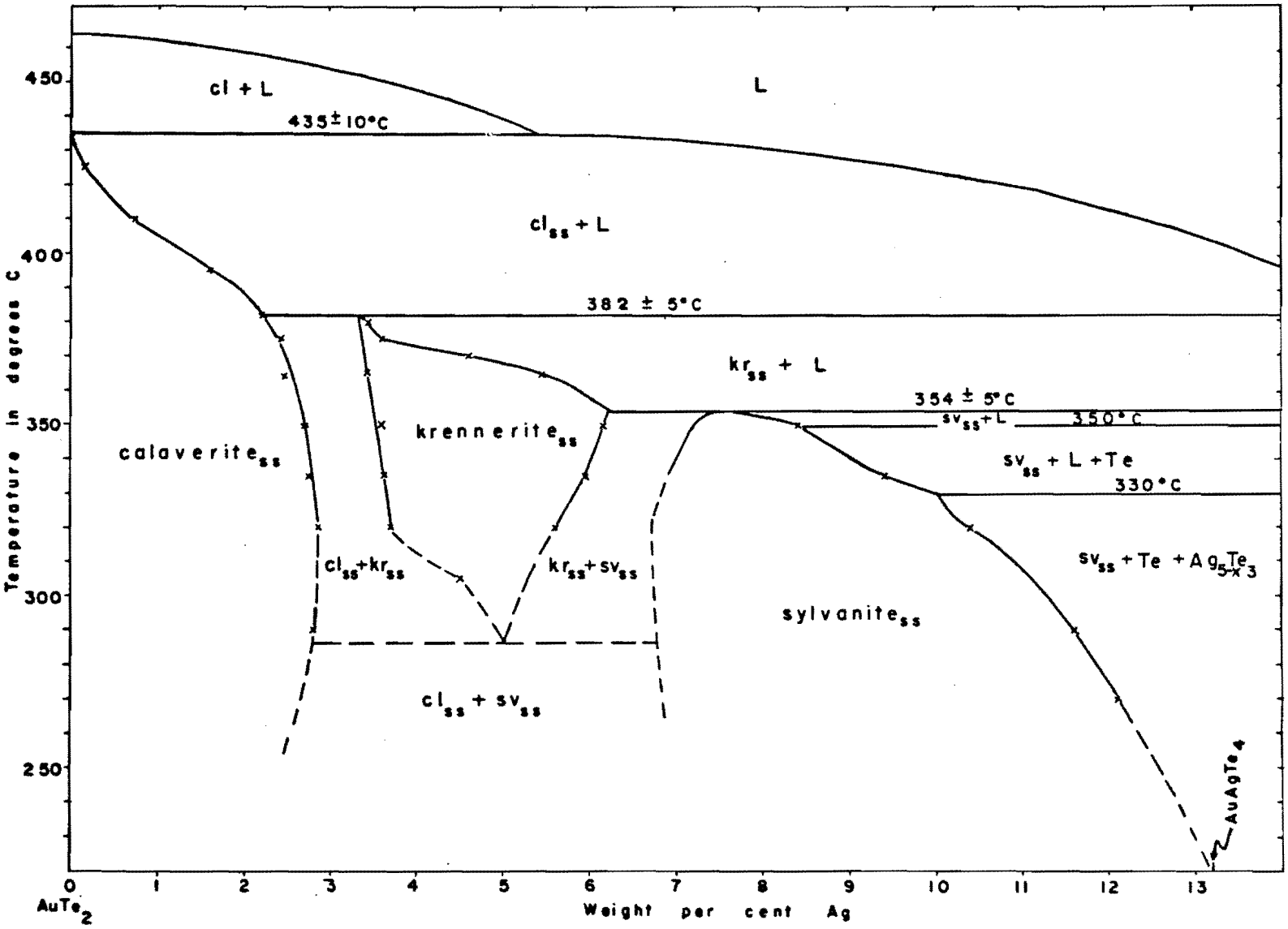

Figure 5. Same as figure 4, but presenting an alternative interpretation of the krennerite stability field.

the chart speed about 1 inch/degree. The standard and unknown reflections were measured with a scale to the nearest 0.01° 2θ at their centers of gravity (visually estimated at 1/3 peak height). A better d-value versus composition curve might be obtained using the Phillips back reflection camera, but this was discovered only after most of the calaverite curve was completed and did not justify doing it again. The runs were x-rayed from two to eleven times each and an examination of those which were x-rayed eleven times gave a standard deviation of 0.0004 Å. The points plotted in figure 6 represent the means of all the d-values obtained for a particular composition. Because a straight line fits the points relatively well, it is estimated that the error for each point is less than $\pm$ 0.0004 Å.

Most of the runs approached equilibrium by being continuously heated at one temperature. Some checks were made, however, by reaching equilibrium on cooling. For example, run 239 (0.46 wt. % Ag) was originally synthesized at 440°C and, after being x-rayed, was ground and heated at 350°C and the resulting product fits the curve very well. Likewise run 86 (1.96 wt. % Au) was synthesized at 382°C and fits the curve which was constructed from runs synthesized at 350°C.

The krennerite d-value versus silver content curve

The Phillips symmetrical back reflection focussing camera was used to establish the curves for both krennerite and sylvanite (figures 7 and 8, respectively). The films were corrected for shrinkage against the fiducial marks. The index of the krennerite reflection measured is not certain; it could be the (0.11.0) or the (2.11.0), or combinations of (0.11.0), (1.11.0), (2.11.0), (12.9.0), (14.8.0), and (16.8.0) (see appendix, figure A4 for typical x-ray pattern). These are all reflections given in Tunell

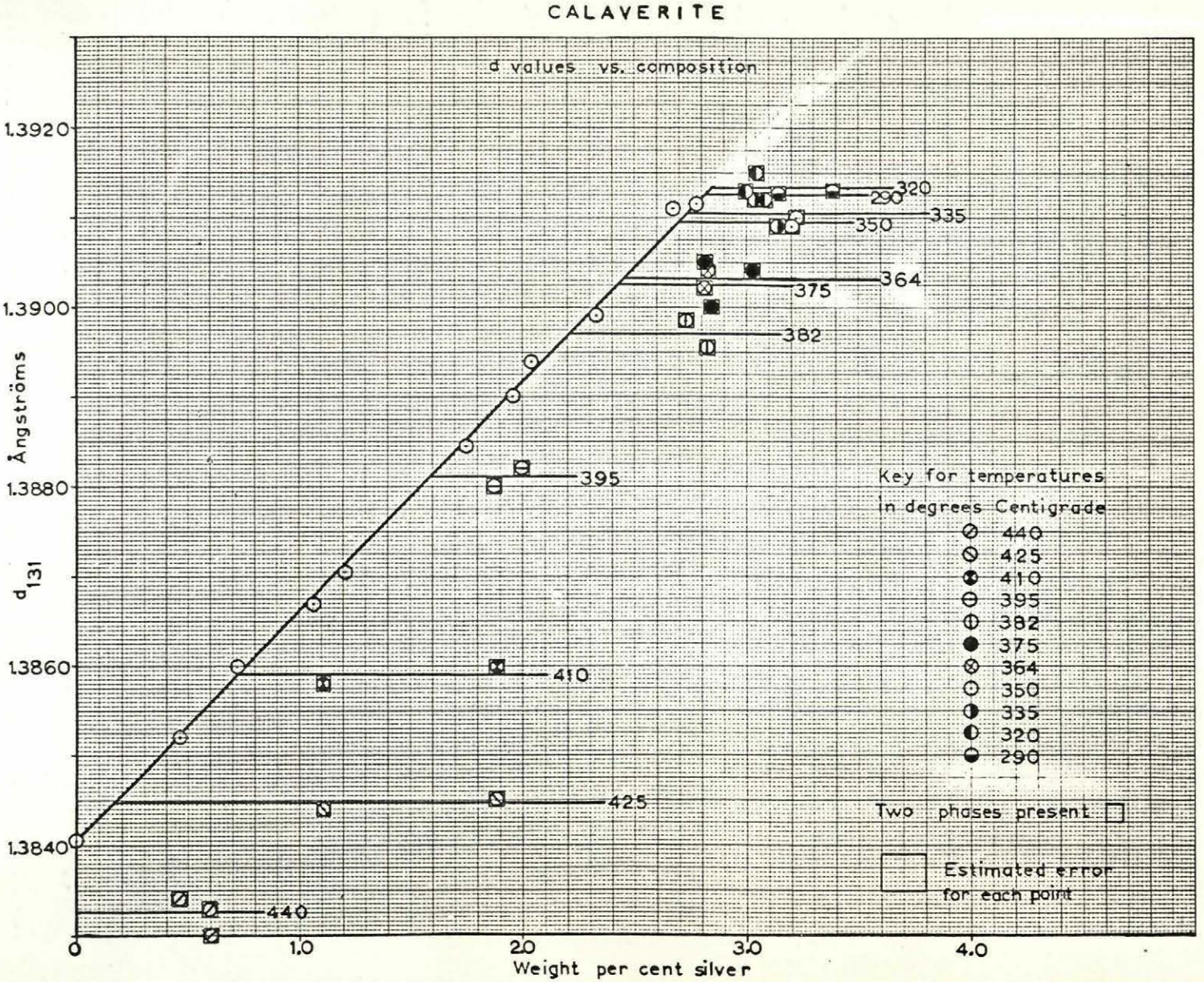

Figure 6. Curve of d-value versus silver content for calaverite.

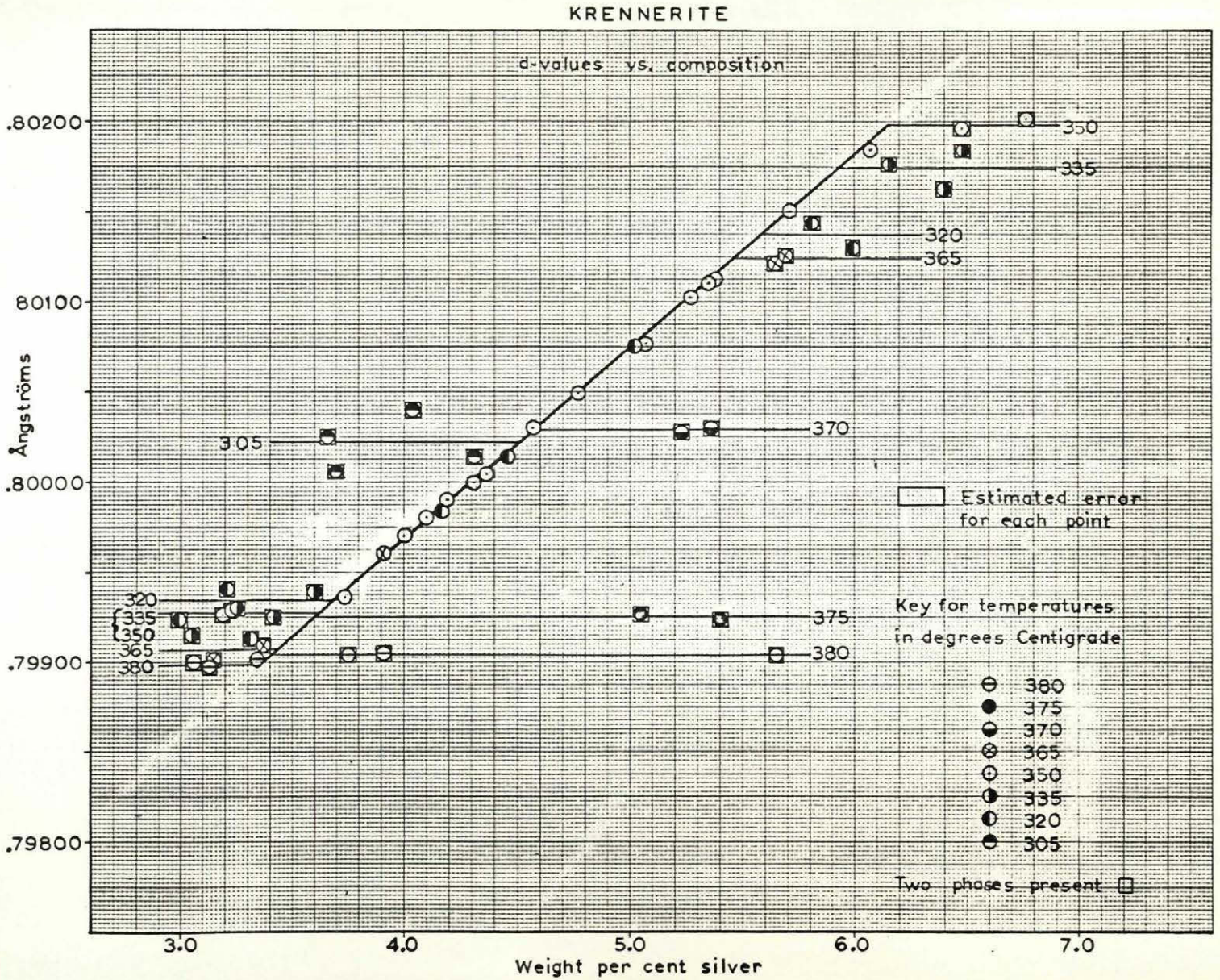

Figure 7. Curve of d-value versus silver content for krennerite.

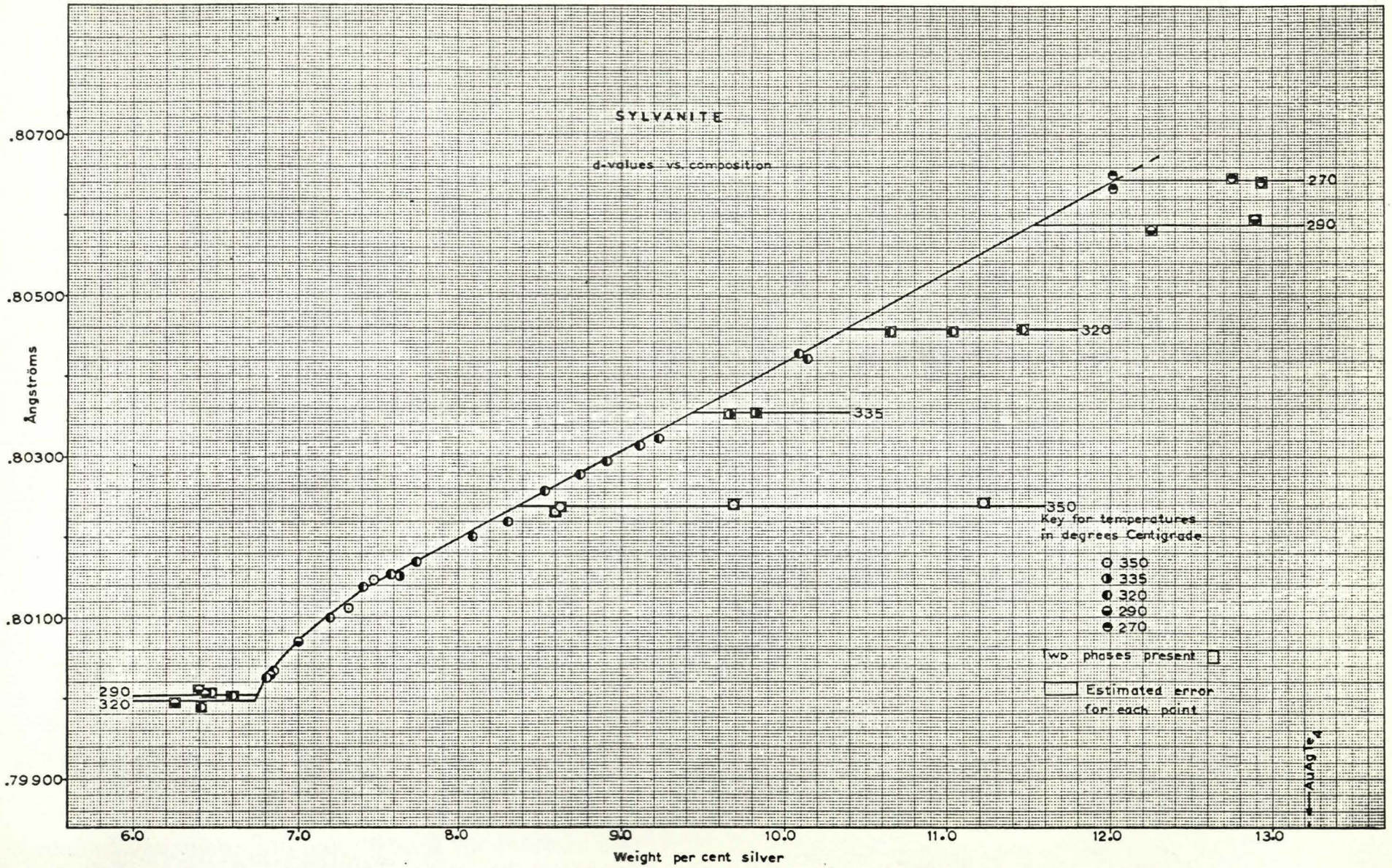

Figure 8. Curve of d-value versus silver content for sylvanite.

and Murata (1950) as having a **d-value** of 0.80 Å and similar intensities. The reflection measured, in the present study, is well resolved into α_1 and α_2 and all readings taken are the mean of measured α_1 and measured α_2. It is estimated that each measurement is in error by no more than $\pm$ 0.0001 Å (based on obtaining a standard deviation of 0.000095 Å for measurements on ten films of the (422) reflection of LiF).

For most of the curve (figure 7) equilibrium was approached in one direction only with runs at 350°C. The close fit of three runs at 320°C and one at 365°C indicates that this curve must represent a close approach to equilibrium. The three runs at 335°C plotted in the krennerite-sylvanite field were synthesized in different ways. The run having the d-value closest to the mean of all three and the run with the largest d-value were brought to equilibrium on cooling. The run having the smallest d-value was only heated at 335°C. However, the run with the value closest to the mean was heated for the longest period (90 days versus 60 and 45 days for the largest and smallest d-values) and probably indicates the closest approach to equilibrium. The runs at 305°C plotted in figure 7 are not at equilibrium, and x-raying after 30 and 120 days did not indicate any change in d-values greater than the probable measuring error. However, there was a stronger krennerite pattern on the Guinier films after 120 days heating. To reach equilibrium at 305°C would be prohibitively long.

The sylvanite d-value versus silver content curve

The sylvanite reflection measured for the d-value versus composition curve (figure 8) is not as well resolved as the reflection for krennerite (see appendix, figure A4 for typical x-ray pattern), and its intensity is weaker. The hkl for sylvanite could be either $(4.5.\bar{8})$ or combinations of

$(4.5.\bar{8})$, $(11.0.\bar{16})$, and $(9.0.\bar{6})$ using the data given in Tunell (1941). The accuracy of the measurements are considered to be less than that of krennerite and are estimated to be $\pm$ 0.00015 Å. Equilibrium was approached from two directions. Most of the curve was constructed from runs synthesized at 320°C. The earlier runs were kept continuously at that temperature, but the later ones were first melted and then heated at 320°C.

Phase relations along the $AuTe_2$-"$AgTe_2$" join

The solvus curves in figures 4 and 5 were constructed with the aid of the d-value versus composition curves (figures 6, 7, and 8) as well as by using appearance or disappearance of phases on Guinier powder photographs. The Guinier focussing camera can indicate the presence of very small quantities of some phases (e.g. 0.5 wt. % Au, 1.25 wt. % krennerite, 0.2 wt. % Te can be detected in $AuTe_2$). The curves are considered correct, within $\pm$ 0.2 wt. % Ag, down to 320°C. Below that temperature equilibrium was not always reached and the curves are tentative.

The incongruent melting points of krennerite, (382 $\pm$ 5°C), and sylvanite, (354 $\pm$ 5°C), were obtained by x-raying synthetic krennerite and sylvanite after 1° and 2°C temperature increments of the charges placed in a horizontal furnace (approximately one hour was allowed for temperature stabilization). The data obtained were checked by the reverse procedure using decreases in temperature.

All the runs below 382°C were designed to contain excess tellurium to facilitate weighing. The composition of the charge, during the weighing procedure, was determined using the lever law on a ternary diagram with 50 cm. sides. The exact composition was later calculated by converting all weights to atomic per cent and keeping the metal tellurium

ratios at 1:2. The excess tellurium varied from 0.1 to 15.0 wt. %. The starting materials for all the runs on this join were $AuTe_2$, Ag, and Te. Reactions are much slower when Au is one of the primary components.

Calaverite solvus curve. All the preliminary work on this solvus curve was done with runs containing excess tellurium. Because of this the silver solid solution field disappears above 405°C. It was then decided to weigh all the runs above 382°C within 0.1 wt. % of the $AuTe_2$-"$AgTe_2$" join because the liquidus field, as shown in figure 2, must affect the composition of runs with excess tellurium at temperatures above 405°C. The results indicate, however, that the silver solid solution field now disappears at about 435°C, still about 30°C below the melting point at 464°C. The work in the Au-Te binary indicates that less than 0.3 wt. % Au or Te goes into solid solution in $AuTe_2$, even at 440°C.

Above 400°C the liquidus field approaches the $AuTe_2$-Te binary and intersects it at 425°C. It is suggested that, as the tie lines from the liquid field to $AuTe_2$ (containing some Ag in solid solution) are unknown, the solvus curve is not well defined above 400°C at present. There is a further complication in that the d-values of the three runs at 440°C are lower than the value given by $AuTe_2$ with no silver. This cannot be explained at present, other than it must be associated with the high-temperature polymorph of $AuTe_2$ discussed previously.

A run to check the spacing curve below 382°C (figure 6) was heated at 375°C with no excess tellurium and the d-value obtained was within the experimental error of runs with excess tellurium. This, together with the fact that good d-value versus composition curves were obtained, even though the amount of excess tellurium varied randomly, indicates that the

curve obtained is generally reliable. The maximum silver to be taken into solid solution by calaverite is estimated to be about 2.8 ± 0.2 wt. % and occurs between 320° and 290°C. The runs in table 7 at 270°C indicate a silver content of about 3.0 wt. %, but it is considered that these runs are not at equilibrium.

TABLE 7*

Selected runs along the $AuTe_2$-"$AgTe_2$" join relating to the reaction rates at 270°C.

Run No.	wt. % Ag	Thermal history	Products	Remarks
185	2.80	M; 86 days, G & P after 43 days, G after 83 days	cl + Te	not heated long enough?
208	2.82	M; 86 days, G & P after 43 days, G after 83 days	cl + Te	not heated long enough?
254	2.85	M; 86 days, G & P after 43 days, G after 83 days	cl	not heated long enough?
298A	3.08	M; 84 days, G & P after 43 days, G after 82 days	cl >> sv + Te	non-equilibrium?
167	3.50	M; 168 days, G & P after 65, 83, and 126 days, G after 166 days	cl > sv + Te	non-equilibrium?
166	3.63	M; 168 days, G & P after 65, 83, and 126 days, G after 166 days	cl > sv + Te	non-equilibrium?

*Key to symbols used in this and subsequent tables:

TABLE 7 (cont'd.)

The first number in the thermal history column refers to total heating period in days (excluding time heated above melting point).

M = initially melted and pelletized before subsequent heating (generally melted @ 700°-970°C for 1-3 days)

G = ground in mortar

P = pelletized in pellet press

cl = calaverite, kr = krennerite, sv = sylvanite,

pet = petzite, hs = hessite, Te = tellurium

"x" = "x" phase, γ = gamma-phase

For all compositions quoted, the second demical place is of only partial significance.

A maximum silver content of 2.8 wt. % corresponds well with the more reliable of the data on natural calaverites given in table 2.

Krennerite solvus curves. The stability field of krennerite is outlined from its incongruent melting point at 382 $\pm$ 5°C to 320°C. The most silver-deficient krennerite (3.35 $\pm$ 0.2 wt. % Ag) is stable at temperatures near the melting point. The solid solution field of this phase broadens rapidly on the silver-rich side with decreasing temperature until the maximum silver content of 6.2 $\pm$ 0.2 wt. % is reached at 350°C. Below 350°C the solvus curves on both the silver-poor and silver-rich limits approach each other and could coalesce at 200°C at an estimated composition of about 4.5 wt. % Ag corresponding approximately to a formula Au_4AgTe_{10} (which would actually have about 4.96 wt. % Ag) (see figure 4). An alternative interpretation of the behaviour of the krennerite solvus below 320°C

is shown in figure 5. Both interpretations are also in fairly good agreement with those reliable analyses of natural krennerite listed in table 2. The two differing interpretations for the krennerite solvus curve below 320°C will be discussed later in the section on 'Reaction rates on the $AuTe_2$-"$AgTe_2$" join.'

Sylvanite solvus curves. The sylvanite solvus curve is rather flat in the region between 350° and the incongruent melting point of this phase at 354 ± 5°C. The exact composition of sylvanite at the melting point is estimated to be at 7.4 ± 0.25 wt. % Ag by projecting the solvus curves from both sides of the solid solution field. The solvus curve on the silver-poor side attains its lowest silver content of 6.7 wt. % Ag at 290°C. The highest silver content obtained for sylvanite (12.0 wt. %) was synthesized at 270°C. On projection to temperatures below 270°C, the solvus curve on the silver-rich side approaches 13.23 wt. % Ag, which is the silver content of stoichiometric $AuAgTe_4$.

The range of silver compositions of natural sylvanites shown in table 2 is from 9.18 to 13.05 wt. %. As noted before, six of the fifteen analyses for sylvanite given by Simpson (1948, 1951, 1952) were regarded by Markham (1960, p. 1169) as representing krennerite, and of these, three have a composition between 6.0 and 6.64 wt. % Ag. It is thus difficult to give too much weight to the reported analyses of sylvanite, but they do indicate that silver-poor sylvanites are relatively rare in natural ores.

Reaction rates on the $AuTe_2$-"$AgTe_2$" join

Examination of the products of runs on the $AuTe_2$-"$AgTe_2$" join indicates that the reaction rates are very dependent on both time and solid diffusion. The Guinier focussing camera was employed to identify

the phases present. Initially, the 114.6 mm. Debeye-Scherrer camera was employed, but it was discovered that a phase in amounts less than 5-10 wt. % could not easily be detected in this way, and that the similar distribution and close spacing of the lines on the powder photograph of the phases made positive identifications difficult. With the Guinier camera, however, less than 0.5 wt. % Te mixed with $AuTe_2$ is detectable.

The greater importance of solid diffusion in runs when the reacting grains are closely packed than when the grains are loosely packed is shown by runs 328a and 328b in table 8. Run 328 was divided into two parts after the first grinding, only one half of which was pelletized. The presence of calaverite in run 328a compared to the development of the single phase krennerite in the pelletized run subjected to the same heat treatment is considered good evidence that solid diffusion across close packed grains is the more important process in these reactions. A similar conclusion is reached by comparing runs 114A and 270 in table 9.

An examination of the data in table 8 shows that, for short heating periods, i.e. 5-9 days at 350°C and with only one grinding operation, one phase more than is allowed by the Phase Rule will be present. This is proof of non-equilibrium conditions (see runs no. 45, 42, 44, and 41).

TABLE 8

Selected runs along the $AuTe_2$-"$AgTe_2$" join relating to the reaction rates at 350°C.

Run No.	wt. % Ag	Thermal history	Products	Remarks
52AA	2.78	50 days,G after 5 and 47 days	cl > kr + Te	equilibrium
45	3.30	5 days,G after 2 days	cl > kr + sv + Te	non-equilibrium
42	4.10	9 days,G after 2 days	cl > kr + sv + Te	non-equilibrium
92	4.12	16 days,G after 3 and 10 days	kr + Te	equilibrium
44	4.36	5 days,G after 2 days	cl > kr + sv + Te	non-equilibrium
72	4.36	15 days,G after 5 and 9 days	kr + Te	equilibrium
328a	4.53	5 days,G after 2	kr ≫ cl + Te	near equilibrium
328b	4.53	5 days,G & P after 2 days	kr + Te	equilibrium
73	4.56	15 days,G after 5 and 9 days	kr + Te	equilibrium
41	4.59	4 days,G after 2 days	sv > kr + cl + Te	non-equilibrium
37	5.04	5 days,G after 2 days	kr + sv + Te	non-equilibrium
111	5.06	13 days,G after 2 and 6 days	kr + Te	equilibrium

TABLE 9

Selected runs along the $AuTe_2$-"$AgTe_2$" join relating to the reaction rates at 320°C.

Run No.	wt. % Ag	Thermal history	Products	Remarks
88	3.52	10 days, G after 2 and 8 days	cl > sv + Te	non-equilibrium
95	4.01	16 days, G after 2 and 10 days	cl > sv + Te	non-equilibrium
250	4.00	M; 29 days, G & P after 6 days; G after 18 days	kr > Te ⋙ cl	very close to equilibrium
143	4.44	14 days, G after 2 and 8 days	cl + sv + Te	non-equilibrium
114A	4.45	32 days, G after 7, 14, and 21 days	cl + sv + Te	non-equilibrium
270	4.46	32 days, G & P after 4 and 15 days, G after 26 days	kr + Te	equilibrium
122	5.10	16 days, G after 6 and 14 days	sv > cl + Te	non-equilibrium
268	5.01	32 days, G & P after 4, 15 days; G after 26 days	kr + Te	equilibrium
75	5.21	15 days, G after 5 and 9 days	sv > kr + Te	non-equilibrium
76	6.00	15 days, G after 5 and 9 days	sv > kr + Te	non-equilibrium
273	5.96	32 days, G & P after 4, 15 days; G after 26 days	kr > sv + Te	equilibrium

Tables 9 and 10 show similar reaction rates, except that it is further evident that the first two phases to form are calaverite and sylvanite (neglecting tellurium). For example, runs 88 and 95 are definitely in the calaverite + krennerite and the krennerite fields, respectively, and yet both contain calaverite + sylvanite. Thus sylvanite has a tendency to form more readily than krennerite under these experimental conditions.

Further proof that sylvanite forms relatively readily at low temperatures is given by a run with 12.02 wt. % Ag heated at 270°C for 51 days, ground after 7 days and then ground and pelletized after 36 days. The d-value of the product was 0.80633 ± 0.00015 Å which gave a close fit on the d-spacing versus composition curve (figure 8). The remainder of the run was melted at 500°C for 6 hours, then ground, pelletized and heated at 270°C for 11 days. The resulting d-value was 0.80650 ± 0.00015 Å which is close to the first value obtained but does not fit on the curve as well. Only sylvanite and tellurium could be detected in both cases.

TABLE 10

Selected runs along the $AuTe_2$-"$AgTe_2$" join relating to the reaction rates at 290°C.

Run No.	wt. % Ag	Thermal history	Products	Remarks
308	4.04	M; 35 days, G & P after 7 & 19 days; G after 28 days	cl + sv + Te	non-equilibrium
308	4.04	M; 35 days as above then G & P, 100 days, G & P after 19 & 50 days, G after 98 days	cl + kr > sv + Te	non-equilibrium
91A	4.12	73 days, G after 3, 45, 60 & 70 days	cl + kr + sv + Te	non-equilibrium
299	4.25	M; 41 days, G & P after 15 & 25 days; G after 34 days	cl + sv > kr + Te	non-equilibrium

TABLE 10 (cont'd.)

299	4.25	M; 41 days as above then G & P, 100 days, G & P after 19 & 50 days, G after 98 days	cl + sv > kr + Te	non-equilibrium
115p	4.51	56 days, G after 6, 14 & 20 days, P after 42 days	cl + sv + Te	non-equilibrium
304	4.48	M; 35 days, G & P after 7 & 19 days; G after 28 days	cl > sv > kr + Te	non-equilibrium
304	4.48	M; 35 days as above then G & P, 100 days, G & P after 19 & 50 days, G after 98 days	cl > kr > sv + Te	non-equilibrium
116	4.86	22 days, G after 7 & 14 days	cl + sv + Te	non-equilibrium
310	4.83	M; 35 days, G & P after 7 & 19 days; G after 28 days	cl + sv > kr + Te	non-equilibrium
310	4.83	M; 35 days as above then G & P, 100 days, G & P after 19 & 50 days, G after 98 days	kr + sv > cl + Te	non-equilibrium

Three-phase assemblages of calaverite, krennerite, and sylvanite indicating non-equilibrium were observed in some runs at 305°C and in most of the runs at 290°C over the composition range 3½-6 wt. % Ag. The longest heating periods at these temperatures (including several grindings and pelletizing)

were 120 days and 140 days, respectively, while the longest heating period at 270°C for runs in that composition range was 160 days. Calaverite and sylvanite were the only two phases present at 270°C. These data can probably be interpreted in two ways.

Since it was established from runs at 350° and 320°C that the first two phases to form in this composition range are calaverite and sylvanite and, further, that krennerite takes progressively longer to form at lower temperatures, it is possible that krennerite would form at 270°C and lower temperatures after a much longer heating period. The rarity of the assemblage calaverite-sylvanite in nature (if it is really present at all!), as was discussed in a previous section, would support such a suggestion. This is the interpretation shown in figure 4.

On the other hand, although the runs at 305°C are not quite at equilibrium, the position of the silver-poor krennerite solvus obtained from the d-spacing versus composition curve, figure 7, curves sharply from about 3.7 wt. % Ag at 320° to 4.5 wt. % Ag at 305°C. If these data are acceptable, then it is conceivable that the krennerite field may contract abruptly, terminating just below 290°C as shown in figure 5. This would indicate that krennerite is always metastable at room temperature and will not form below 270°C. The rarity of the assemblage calaverite-sylvanite, especially when compared to the relatively abundant presence of krennerite in nature, gives greater support to the phase relations as indicated in figure 4. However, this problem is still open for further work, and further detailed examination of natural assemblages of these minerals is badly needed.

Much of the above data conflicts with Markham's (1957, 1960) findings. He determined the maximum solubility of silver in calaverite to be

3 ± 1 wt. % at 300°C, by noting the first appearance of sylvanite on powder photographs using 57.54 mm. and 114.83 mm. Debeye-Scherrer type powder cameras. He reports no krennerite at that temperature and estimated the one phase sylvanite field to extend from about 10.3 to 12.35 wt. % Ag. It should be noted, however, that these runs were heated at 300°C for only 11 or 15 days and that the only grinding was done directly after weighing of the three elements. (It is unclear how gold and silver could be ground.) Markham's unsuccessful attempts to synthesize krennerite at 430°, 400°, 300°, 250°, and 150°C from runs in the krennerite range of compositions (2.0-8.0 wt. % Ag) and the behaviour of natural krennerite and calaverite at some of these temperatures can be reinterpreted in the light of the present investigation, making it unlikely that krennerite is the low-temperature, low-pressure polymorph of calaverite. At 430° and 400°C all Markham's runs produced calaverite (to be expected as krennerite melts incongruently at 382°C to form calaverite plus liquid). At 300°, 250°, and 150°C natural krennerite remained unchanged (to be expected as krennerite is stable at those temperatures according to figure 4). Likewise runs of krennerite composition at 150°C began to form calaverite (also to be expected as these were only heated for 7 days, and the sylvanite was probably not identified on the powder photographs).

The effect of other elements on the stability and solid solution field of krennerite has not been studied.

Phase relations along the join $AuAg_3Te_2$-Ag_2Te

The phase diagram, figure 9, was constructed from data obtained using a Rigaku-Denki high-temperature x-ray powder diffraction camera. Fifteen runs of different compositions along this join were synthesized in horizontal furnaces by heating weighed amounts of $AuAg_3Te_2$ and Ag_2Te in sealed, evacuated, silica glass capsules above 950°C; grinding and pelletizing the charges and then heating them at 440°C for 10 to 14 days. Polished sections of runs along the join showed petzite and hessite combined in irregular intergrowths with about ½ wt. % of Au (see figure 13). Runs having a composition between $AuAg_3Te_2$ and Ag_2Te, when quenched from 440°C, gave the diffraction patterns of the low temperature polymorphs of hessite and petzite only if x-rayed after several weeks. Extra reflections, representing metastable phases,are observed if x-rayed immediately after quenching. Portions of these fifteen runs were ground and transferred into silica glass capillaries which were evacuated and sealed for use in the high-temperature camera.

Most of the runs were performed by letting the camera equilibrate to the first temperature over a period of eight hours. After exposure for three to five hours at 35 kilovolts and 20 milliamps with filtered Cu radiation, the specimen furnace was progressively heated to higher temperatures, but only half an hour to three hours were allowed to attain equilibrium at each new temperature. The phase diagram is considered to be only an approximation because some inversion temperatures were found to be lower by more than 10°C when the camera furnace was progressively cooled. The temperatures indicated on figure 9 are considered to be correct within ± 15°C. The lowering of the hessite low to intermediate inversion is schematic only.

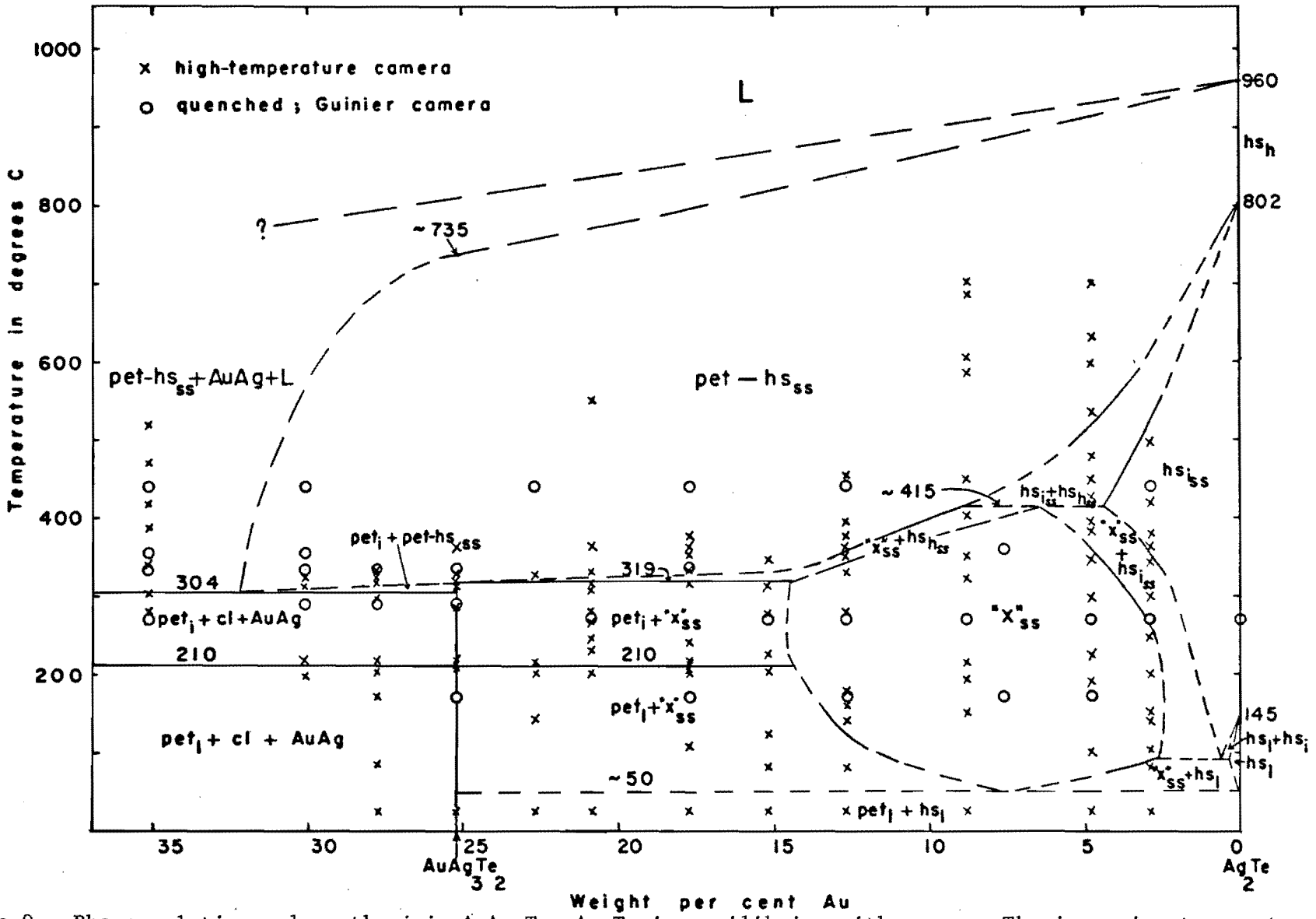

Figure 9. Phase relations along the join $AuAg_3Te_2$-Ag_2Te in equilibrium with vapor. The inversion temperatures for hessite are taken from Kracek & Ksanda (unpublished) and the extent of hessite low and intermediate solid solution is partly schematic.

The phase diagram indicates continuous solid solution between the highest form of $AuAg_3Te_2$ (stable from 319°C to the beginning of melting at approximately 735°C) and the highest form of Ag_2Te (stable from 802° to its melting point at 960°C). This solid solution field, termed pet-hs_{ss} in figure 9, extends beyond $AuAg_3Te_2$ to about 32 wt. % Au at 304°C as indicated on the diagram. A new phase, designated "x", is stable along this join from 2.5 to 14.5 wt. % Au within the approximate temperature limits 50° to 415°C. The solid solution fields of $AuAg_3Te_2$ (low and intermediate) on the gold-rich side are interpreted as being less than one weight per cent, based on observing some gold and calaverite in polished sections quenched from 290° and 170°C (more Au than cl). Similarly, on the silver-rich side of $AuAg_3Te_2$, the solid solution fields of the low and intermediate forms are interpreted as being less than one weight per cent. No "x" phase could be detected in run 199 (see table 15) quenched from 270°C, but this is thought to be due to the similarity of the petzite intermediate and "x" phase x-ray patterns, but "x" phase and some hessite were observed in a run having 22.8 wt. % Au quenched from 440°C. The constant temperatures for the petzite low to intermediate inversion, as determined with the high-temperature camera, are taken to indicate negligible solid solution. Difficulty was also experienced in interpreting patterns for the two-phase assemblage; intermediate $AuAg_3Te_2$ plus "x" phase on high-temperature camera films, as their diffraction patterns are similar. These two were the only two high-temperature forms along this join which could be quenched and x-rayed at room temperature.

The temperature ranges of the stability fields of $AuAg_3Te_2$ (petzite) and Ag_2Te (hessite) polymorphs are tabulated in table 11.

TABLE 11

Temperature ranges of the stability fields of petzite and hessite polymorphs.

Polymorph	$AuAg_3Te_2$ Temp. stability field	$AgTe_2$ * Temp. stability field
low	25° to 210°C	25° to 145°C
intermediate	210° to 319°C	145° to 802°C
high	319° to 735°C	802° to 960°C

* Data from Kracek and Ksanda (unpublished) for Ag_2Te-Ag

Frueh (1959b, p. 701) reported that natural petzite transformed to a higher form between 150° and 250°C and further recorded a personal communication from Drs. F.C. Kracek and C.J. Ksanda indicating that this transition had been determined by differential thermal analysis as 210° ± 10°C (confirmed by the present study). The x-ray powder data obtained for intermediate petzite is compared to that obtained by Frueh (see appendix, table A5) and is similar. The pattern was not indexed; however, a much better pattern was obtained with the Guinier camera after rapid quenching in ice and is given in the appendix, table A6.

The diffraction patterns of the high temperature forms of petzite and hessite are very similar, except that more reflections are visible with increasing gold content. This is probably due to the better scattering effect of gold and/or to the fact that this form occurs at lower temperatures on the gold-rich side of the join so that the larger angle reflections could be missing because of thermal agitation. Frueh (1961, p. 658) reports the reflections observed for natural Ag_2Te using a

Unicam high-temperature camera at 825°C. These are compared below with patterns obtained for $AuAg_3Te_2$ and $Au_{0.472}Ag_{3.528}Te_2$. The patterns correspond quite closely except that more reflections were obtained for the gold-bearing solid solutions.

TABLE 12

X-ray powder diffraction data for the high-temperature solid solution $AuAg_3Te_2$-Ag_2Te.

Frueh @ 825°C Ag_2Te		@ 363°C $Au_{0.472}Ag_{3.528}Te_2$		@ 363°C $AuAg_3Te_2$
hkl	d	d	I	d
110	3.74	3.68	3	3.66
200	2.65	2.61	2	2.61
211	2.16	2.14	10	2.14
220		1.85	3	1.85
310		1.65	1	1.65
321		1.40	½	1.40
330,411		1.23	½	
	a=5.29 Å	a=5.22 Å		a=5.20 Å

The beginning of melting of $AuAg_3Te_2$ (in the form of pet-hs solid solution) was established at 735° ± 10°C by observing the first sign of melting in coarsely ground $AuAg_3Te_2$ in an evacuated silica capsule placed in a horizontal furnace. No change was observed at 730°C but at 740°C all the fragments became rounded, and no further change could be observed at 755°C.

The extension of the pet-hs_{ss} field to about 32 wt. % Au is based on high-temperature camera data at three compositions more gold-rich than $AuAg_3Te_2$ (see figure 9), as well as two other more gold-rich compositions. This interpretation was guided by the data obtained from Guinier patterns and polished sections for quenched runs. This will be discussed in more detail in the section entitled "Tie lines within the area bounded by calaverite, sylvanite, $Ag_{5-x}Te_3$, hessite, and petzite."

The intermediate polymorph of Ag_2Te was indexed by Rahlfs (1935, p. 178), and his indexing compares closely with the present observations (table 13).

TABLE 13

High-temperature x-ray powder diffraction data for intermediate polymorph of Ag_2Te.

Rahlfs* @ 250°C Ag_2Te		Present study Ag_2Te @ 302°C		Ag_2Te (with 2.86 wt. % Au) @ 363°C
d	hkl	d	I	d
	111	3.77	2	3.76
2.32	220	2.32	10	2.32
1.98	311	1.98	4	1.98
1.64	400	1.64	1	1.65
1.52	331	1.51	½	
1.34	422	1.34	2	1.34
1.26	511,333			
1.23				
a=6.57 Å		a=6.55 Å		a=6.56 Å

* Corrected using Ag as internal standard, Kx units which are equivalent to Å when only using two decimal places.

A large section of this join consists of a new phase stable between 50 $\pm$ 20°C and its incongruent breakdown above 415 $\pm$ 20°C to petzite-hessite solid solution and intermediate Ag_2Te. The gold content of this phase, termed the "x" phase, extends from about 2.5 to 14.5 wt. % on the join. The "x" phase gave a high temperature powder pattern which could be indexed as face-centered cubic with a = 14.97 Å, or orthorhombic with a = 7.5 Å, b = 6.8 Å, c = 6.0 Å. The latter tentative indexing is tabulated in table A7 in the appendix. This phase, however, was quenched in ice and the Guinier powder photograph shows a very large number of reflections. Although the strongest reflections fit the high-temperature indexing, this pattern could not be indexed as easily. This pattern is compared to the intermediate temperature form of $AuAg_3Te_2$ in the appendix, table A6.

Table 14 summarizes data for all phases on the join Ag_2Te-$AuAg_3Te_2$. It is noted that the calculated specific gravities decrease with an increase in temperature or an increase in the Ag:Au ratio. The symmetry of most phases increases with increasing temperature. The substitution of Au for Ag, or vice versa, and the ease of movement of the Au or Ag atoms within Te frameworks are consistent with the data obtained and with the difficulty of quenching most of the high temperature phases.

TABLE 14

Selected data for all phases present on the $AuAg_3Te_2$-Ag_2Te join.

		Cell constants Å	Cell volume Å^3	Calc. S.G.	Symmetry	No. of formula wts./cell
Ag_2Te	(1) low form room temp.	a=8.09 b=4.48 c=8.69 β=123°20'	271.4	8.21	P2/c.	4
Ag_2Te	intermediate form @ 302°C	6.55	281.01	8.11	f.c.c.	4
Ag_2Te	(2) high form @ 825°C	5.29	148.04	7.70	b.c.c.	2
$Au_{0.1}Ag_{3.9}Te_2$	intermediate form @ 363°C	6.56	282.30	8.18	f.c.c.	2
$Au_{0.28}Ag_{3.72}Te_2$	"x" phase	a=7.5 b=6.8 c=6.0	306	7.72	ortho-rhombic	2
$Au_{0.472}Ag_{3.528}Te_2$	high form	5.22	142.2	8.51	b.c.c.	1
$AuAg_3Te_2$	high form @ 363°C	5.2	140.6	9.16	b.c.c.	1
	intermediate form	?	?	?	?	?
	(3) low form @ 25°C	10.38	1118.38	9.20	b.c.c.	8

(1) Frueh (1959a) natural material

(2) Frueh (1961) natural material

(3) Frueh (1959b) natural material

The only high temperature phases on this join which could be preserved long enough to give an x-ray powder pattern at room temperature were the petzite intermediate polymorph and the "x" phase. The technique

used was to drop the capsule containing the powdered material in ice water as rapidly as possible using heated tongs and then to mount it on the Guinier sample holder and x-ray it immediately. The x-ray laboratory was kept cool at 18°C during the 10 hour exposures. It was observed, for example, that the "x" phase would begin to break down giving low hessite after thirteen hours at room temperature. Also the slightest pressure on grinding the material would speed the breakdown to low petzite plus low hessite. The data obtained from such runs quenched from 270° and 170°C are summarized in tables 15 and 16.

TABLE 15

Runs quenched in ice from 270°C and x-rayed immediately (10 hour exposure).

Run No.	Formula	wt. % Au	wt. % Ag	wt. % Te	Products identified on Guinier powder photographs
346		35.73	33.26	31.01	pet (low) > cl (low) + Au + pet (int)
182	$AuAg_3Te_2$	25.39	41.71	32.89	pet (low) ≫ pet (int)
199		20.97	45.38	33.64	pet (low) ≫ pet (int)
340		15.37	50.05	34.58	pet (low) > pet (int) + "x" phase
279		12.73	52.23	35.02	"x" phase + pet (low)
280		7.75	56.38	35.86	"x" phase ≫ pet (low)
281		4.81	58.83	36.36	"x" phase > hs (low) + trace? pet (low)
282		2.86	60.45	36.68	hs (low) ≫ pet (low)
155	Ag_2Te	-	62.83	37.16	hs (low)

TABLE 16

Runs quenched in ice from 170°C and x-rayed immediately (10 hour exposure).

Run No.	wt. % Au	wt. % Ag	wt. % Te	Products identified on Guinier powder photographs
278	17.80	48.00	34.20	pet (low) > "x" phase + hs (low)
279	12.73	52.33	35.02	pet (low) > "x" phase + hs (low)
339	7.54	56.55	35.90	"x" phase > pet (low) + hs (low)
281	4.81	58.83	36.36	"x" phase + hs (low) + trace? pet (low)

Tie lines within the area bounded by calaverite, sylvanite, $Ag_{5-x}Te_3$, hessite, and petzite

Markham (1960, p. 1161) states that the hessite-sylvanite join (present at 300°C) changes to a petzite-$Ag_{5-x}Te_3$ join above 315 ± 10°C. This conclusion was based on the results of two runs at 330°C whose compositions lay within the petzite-hessite-sylvanite field. The compositions of these runs are given by Markham (p. 1155), who is evidently in error, since these compositions lie on either side of the proposed petzite-$Ag_{5-x}Te_3$ join and yet both are reported to contain petzite + sylvanite + $Ag_{5-x}Te_3$.

Runs having bulk compositions approximating to 9.0 wt. % Au, 50.0 wt. % Ag, and 41.0 wt. % Te were weighed and heated at 290°, 320°, 335°, and 350°C for periods of over thirty days (including several grinding operations). Debeye-Scherrer films of these runs were not conclusive; petzite and sylvanite were definitely present together with either or both hessite and $Ag_{5-x}Te_3$. The Guinier photographs (taken months later) showed the four phases: petzite, sylvanite, hessite, and $Ag_{5-x}Te_3$. This was considered to be a non-equilibrium assemblage and indicated that a more thorough study of the tie lines in this part of the ternary system was necessary.

Isothermal sections at 356°, 335°, and 290°C for this part of the ternary system

Isothermal sections of this part of the ternary system at 356°, 335°, and 290°C are shown in figures 10, 11, and 12, respectively. Runs heated at 170°C gave the same data as at 290°C. The exact compositions of the runs shown in the figures, their thermal history, and their products as identified on Guinier x-ray photographs are tabulated

Key to Figure 10

Phases present at 356°C in equilibrium with vapor.

1 pet-hs_{ss} + γ_{ss}

2 pet-hs_{ss} + γ_{ss} + "x"$_{ss}$

3 "x"$_{ss}$ + δ_{ss}

4 "x"$_{ss}$ + δ_{ss} + hs(int)$_{ss}$

5 δ_{ss} + hs(int)$_{ss}$

6 pet-hs_{ss} + Liquid + $AuAg_{ss}$

7 pet-hs_{ss} + $AuAg_{ss}$

8 pet-hs_{ss} + $AuAg_{ss}$ + "x"$_{ss}$

9 "x"$_{ss}$ + $AuAg_{ss}$

10 "x"$_{ss}$ + $AuAg_{ss}$ + hs(int)$_{ss}$

11 hs(int)$_{ss}$ + $AuAg_{ss}$

12 pet-hs_{ss} + cl_{ss}

13 pet-hs_{ss} + cl_{ss} + δ_{ss}

14 cl_{ss} + kr_{ss} + δ_{ss}

15 kr_{ss} + δ_{ss}

16 kr_{ss} + γ_{ss} + $Ag_{5-x}Te_3$

17 kr_{ss} + $Ag_{5-x}Te_3$ + Liquid

18 $Ag_{5-x}Te_3$ + Liquid

19 cl_{ss} + Te

20 cl_{ss} + kr_{ss} + Te

21 kr_{ss} + Te

22 kr_{ss} + Liquid + Te

23 kr_{ss} + Liquid

24 Te + Liquid

25 Liquid

26 $Ag_{5-x}Te_3$ + δ_{ss}

27 cl_{ss} + $AuAg_{ss}$

28 cl_{ss} + Liquid + $AuAg_{ss}$

29 cl_{ss} + Liquid

30 cl_{ss} + pet-hs_{ss} + Liquid

31 Liquid

32 Liquid + pet-hs_{ss}

33 Liquid + $AuAg_{ss}$

Some divariant fields, such as cl + δ, cl + kr, etc., are represented by a single line.

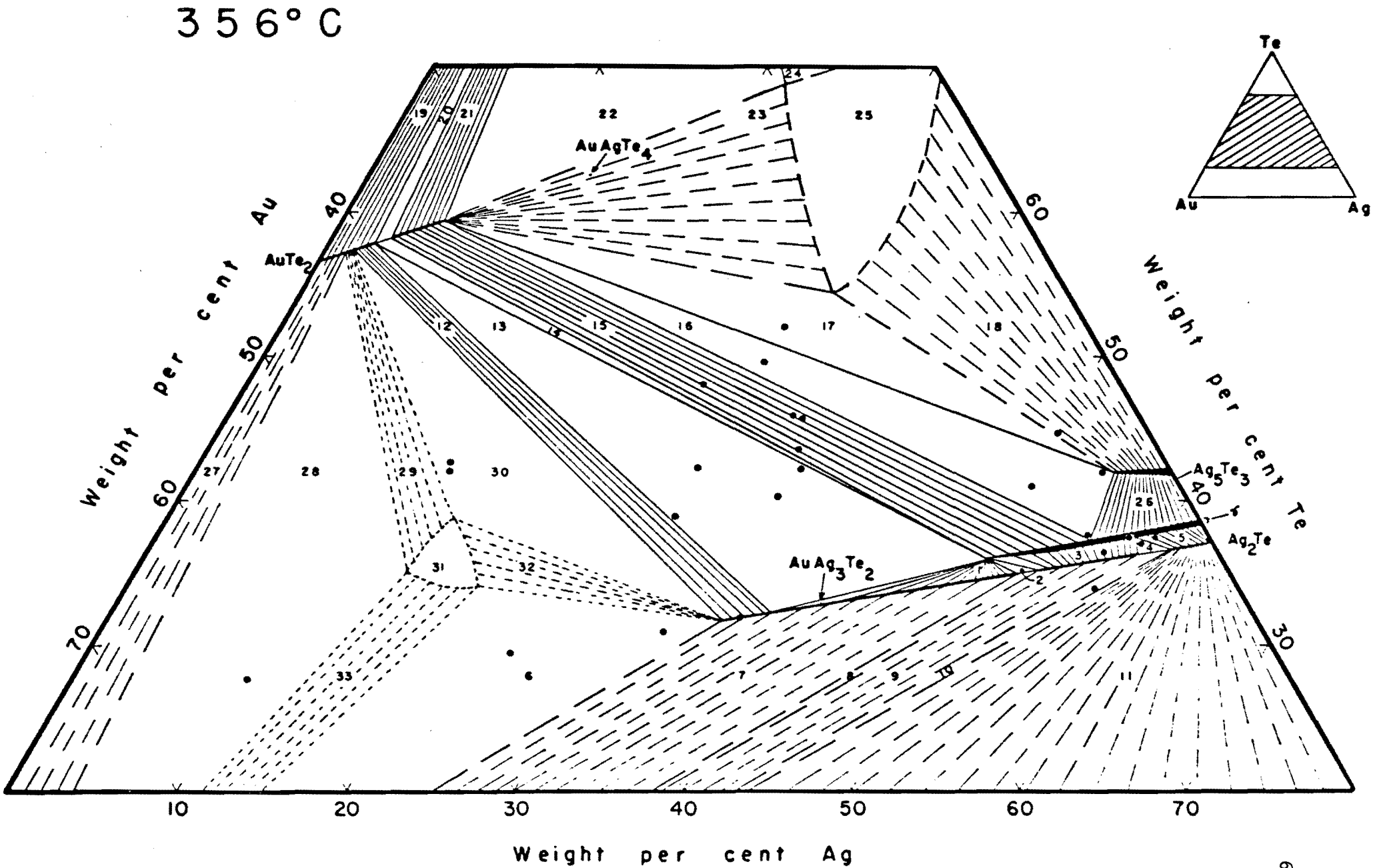

Figure 10. Phase relations in the central portion of the Au-Ag-Te system at 356°C in equilibrium with vapor. Solid circles represent bulk compositions of some runs at 356°C.

Key to Figure 11

Phases present at 335°C in equilibrium with vapor.

1 pet-hs$_{ss}$ + γ_{ss}

2 pet-hs$_{ss}$ + γ_{ss} + "x"$_{ss}$

3 "x"$_{ss}$ + γ_{ss}

4 "x"$_{ss}$ + γ_{ss} + hs(int)$_{ss}$

5 γ_{ss} + hs(int)$_{ss}$

6 pet-hs$_{ss}$ + Liquid + AuAg$_{ss}$

7 pet-hs$_{ss}$ + AuAg$_{ss}$

8 pet-hs$_{ss}$ + AuAg$_{ss}$ + "x"$_{ss}$

9 AuAg$_{ss}$ + "x"$_{ss}$

10 AuAg$_{ss}$ + "x"$_{ss}$ + hs(int)$_{ss}$

11 AuAg$_{ss}$ + hs(int)$_{ss}$

12 pet-hs$_{ss}$ + cl$_{ss}$

13 pet-hs$_{ss}$ + cl$_{ss}$ + γ_{ss}

14 cl$_{ss}$ + kr$_{ss}$ + γ_{ss}

15 kr$_{ss}$ + γ_{ss}

16 kr$_{ss}$ + sv$_{ss}$ + γ_{ss}

17 sv$_{ss}$ + γ_{ss}

18 sv$_{ss}$ + γ_{ss} + $Ag_{5-x}Te_3$

19 sv$_{ss}$ + $Ag_{5-x}Te_3$ + Liquid

20 Liquid + $Ag_{5-x}Te_3$

21 Liquid + Te + $Ag_{5-x}Te_3$

22 $Ag_{5-x}Te_3$ + Te

23 $Ag_{5-x}Te_3$ + γ_{ss}

24 cl$_{ss}$ + Te

25 cl$_{ss}$ + kr$_{ss}$ + Te

26 kr$_{ss}$ + Te

27 kr$_{ss}$ + sv$_{ss}$ + Te

28 sv$_{ss}$ + Te

29 sv$_{ss}$ + Te + Liquid

30 Te + Liquid

31 Liquid

32 sv$_{ss}$ + Liquid

33 AuAg$_{ss}$ + cl$_{ss}$

34 AuAg$_{ss}$ + cl$_{ss}$ + Liquid

35 Liquid

36 Liquid + pet-hs$_{ss}$

37 pet-hs$_{ss}$ + Liquid + cl$_{ss}$

38 cl$_{ss}$ + Liquid

39 AuAg$_{ss}$ + Liquid

Some divariant fields, such as cl + γ, cl + kr, etc., are represented by a single line.

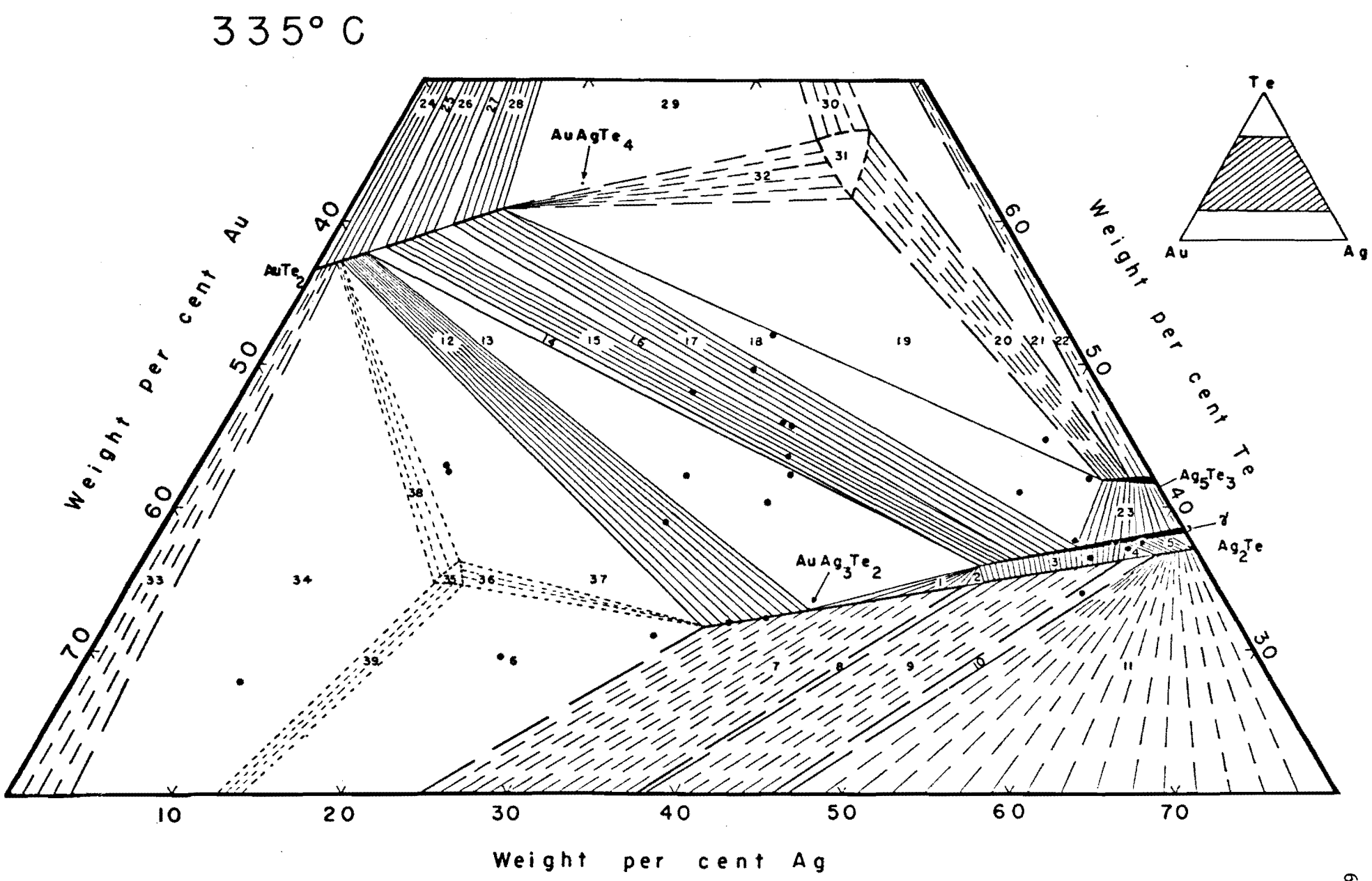

Figure 11. Phase relations in the central portion of the Au-Ag-Te system at 335°C in equilibrium with vapor. Solid circles represent bulk compositions of some runs at 335°C.

Key to Figure 12

Phases present at 290°C in equilibrium with vapor.

1	pet(int) + γ_{ss}	15	cl_{ss} + kr_{ss} + γ_{ss}
2	———	16	kr_{ss} + γ_{ss}
3	"x"$_{ss}$ + γ_{ss}	17	kr_{ss} + sv_{ss} + γ_{ss}
4	"x"$_{ss}$ + γ_{ss} + hs(int)$_{ss}$	18	sv_{ss} + γ_{ss}
5	γ_{ss} + hs(int)$_{ss}$	19	sv_{ss} + γ_{ss} + $Ag_{5-x}Te_3$
6	$AuAg_{ss}$ + pet(int)	20	sv_{ss} + $Ag_{5-x}Te_3$ + Te
7	$AuAg_{ss}$ + pet(int) + "x"$_{ss}$	21	$Ag_{5-x}Te_3$ + Te
8	"x"$_{ss}$ + $AuAg_{ss}$	22	γ_{ss} + $Ag_{5-x}Te_3$
9	"x"$_{ss}$ + $AuAg_{ss}$ + hs(int)$_{ss}$	23	———
10	$AuAg_{ss}$ + hs(int)$_{ss}$	24	cl_{ss} + Te
11	$AuAg_{ss}$ + cl_{ss}	25	cl_{ss} + kr_{ss} + Te
12	$AuAg_{ss}$ + cl_{ss} + pet(int)	26	kr_{ss} + Te
13	cl_{ss} + pet(int)	27	kr_{ss} + sv_{ss} + Te
14	cl_{ss} + pet(int) + γ_{ss}	28	sv_{ss} + Te

Some divariant fields, such as cl + γ, cl + kr, etc., are represented by a single line.

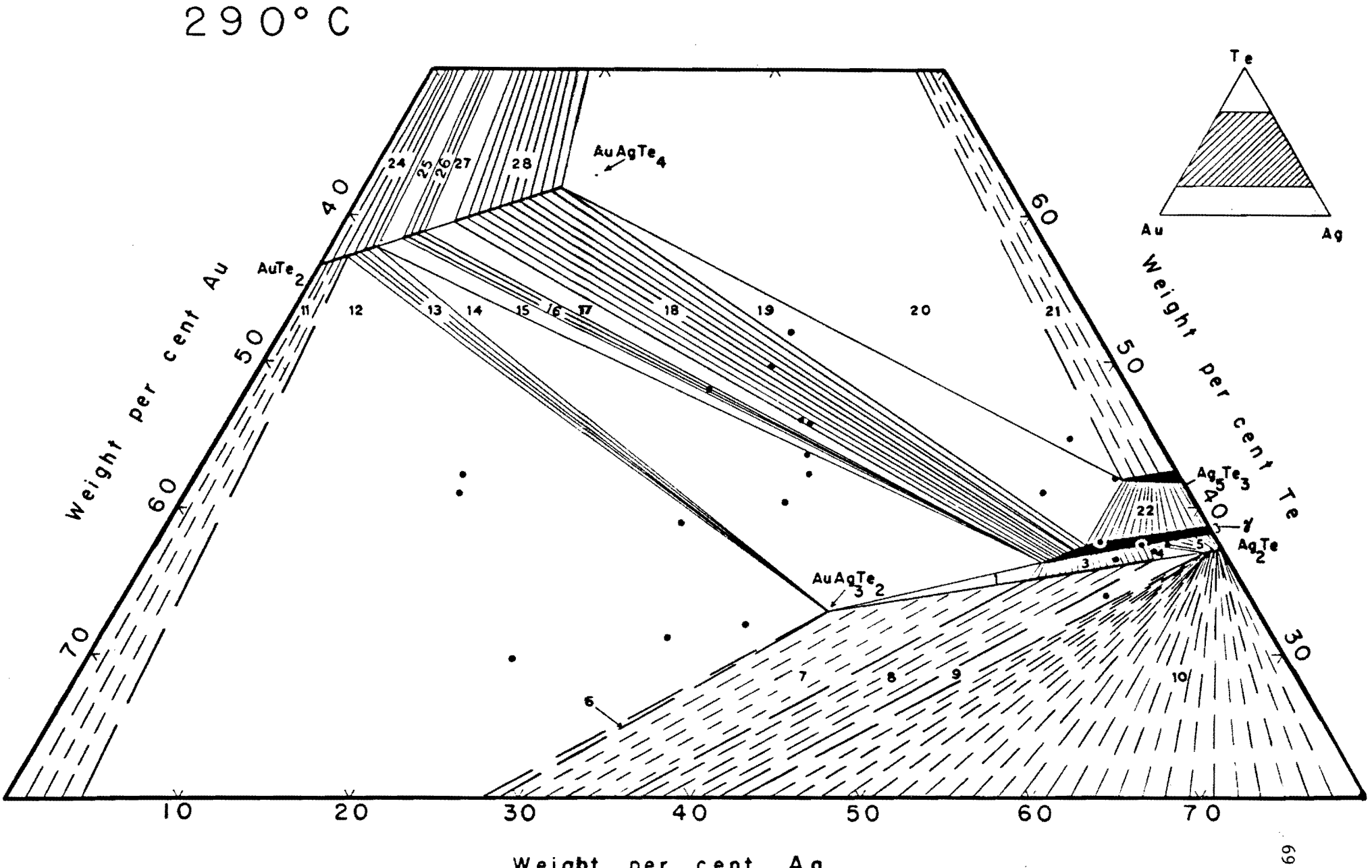

Figure 12. Phase relations in the central portion of the Au-Ag-Te system at 290°C in equilibrium with vapor. Solid circles represent bulk compositions of some runs at 290°C.

in the appendix, tables A8, A9, and A10. All the runs, except where indicated, were rapidly quenched in ice water and x-rayed immediately. The tie lines shown indicate the approximate positions of the two- and three-phase fields. The reactions in this part of the ternary are considered to be faster than those on the $AuTe_2$-"$AgTe_2$" join. The extent of the solid solution fields of calaverite, krennerite, and sylvanite are taken from figure 4. The liquid fields are very approximate and one is taken from figure 2. The tie lines to the AuAg solid solution are guided by the results obtained by Markham (1960, p. 1159).

The gamma-phase

These isothermal sections do not necessarily indicate which assemblages would be expected in natural ores if equilibrated to relatively low temperatures. However, special conditions during crystallization and/or the stabilizing effect of other elements might enable some of the phases which are metastable at 25°C, such as the gamma-phase, to be preserved. Polished sections were made of two runs heated in pellet form at 335°C in which the gamma-phase was preserved.

TABLE 17

Selected runs heated at 335°C containing gamma-phase.

Run No.	wt. % Au	Ag	Te	Products identified on Guinier film	Stable assemblage at 335°C
371C	4.69	57.76	37.55	γ only	γ
375	-	39.40	60.60	$\gamma > Ag_{5-x}Te_3$ + hs (low)	$\gamma + Ag_{5-x}Te_3$

In polished section run 371C consisted mostly of gamma-phase with approximately 10% $Ag_{5-x}Te_3$ and 0.5% Ag_2Te, while run 375 consisted of $Ag_{5-x}Te_3$ and gamma-phase in approximately equal proportions, with less than 0.5% Ag_2Te.

Employing oil immersion objective lenses the gamma-phase appears bluish-grey in polished section (very similar to petzite) and is isotropic. With one exception, reactions to standard etch reagents were very similar to those published for $Ag_{5-x}Te_3$ and hessite. $FeCl_3$ etches the gamma-phase grey-black with iridescent edges, whereas both $Ag_{5-x}Te_3$, hessite and petzite become iridescent only.

TABLE 18

Etch reactions for gamma-phase.

HNO_3	- brown tarnish in 20 sec.
HCl	- iridescent in small circular patches? (60 sec.)
KOH	- negative (60 sec.)
$HgCl_2$	- iridescent (slowly, 60 sec.)
$FeCl_3$	- etches grey-black with iridescent edges (rapidly)
KCN	- slowly iridescent (60 sec.); most of this rubs off easily

---

The reactions with $FeCl_3$ were clearly observed in run 375 where grey-black patches of etched gamma-phase are set within iridescent $Ag_{5-x}Te_3$.

Discovery of a second ternary eutectic

The isothermal sections at 356° and 335°C indicate the development of a new liquid field within the calaverite-petzite-Au field.

All quenched runs within the Au + petzite + calaverite field heated between the temperature limits 440° and 305°C gave the x-ray patterns of Au + calaverite + petzite + an unknown phase. This unknown phase (or phases) gave two patterns, termed for convenience A and B, which sometimes appeared together and sometimes separately. The x-ray data for A and B are given in the appendix, table A12 (compared with the published pattern for Au_2Te_3 [montbrayite]). Though there are some similarities in the patterns, they are significantly different.

Data on the runs in which phases A and B occur and their thermal history are tabulated in the appendix, table A13. Polished sections were made of most of the above runs. The only conclusions that could be drawn from the available data are as follows:

(1) Patterns A and B (and the unknown phase seen in polished sections which is attributed to them) do not occur in runs heated at 290°C or below.

(2) Polished sections indicated at least four phases present in all runs which showed either pattern A or B, or both, on x-ray photographs, indicating a non-equilibrium assemblage.

(3) In polished section the phase corresponding to pattern A is strongly anisotropic and bireflectant and only occurs within petzite grains, while the phase corresponding to pattern B is similar and can only be distinguished in runs where pattern A is absent. By contrast petzite is isotropic (figure 14).

(4) All the above runs which had been heated to 356°C produced a regulus when quenched, indicating the development of a liquid. Examination of polished sections revealed that the liquid probably was mostly of calaverite composition with some Au and petzite (figures 15 and 16).

Figure 13. The assemblage hessite-petzite synthesized at 440°C. Hessite (light coloured, approximately 70% by weight) forms an irregular intergrowth with petzite. Grain boundaries are very indistinct and are practically invisible unless an oil immersion lens is used. Black areas are pits and scratch marks. All photomicrographs, unless otherwise stated, are taken with plane polarized light and oil immersion objective lenses.

Figure 14. Lamellar-like exsolution of phase A in large petzite grain synthesized at 356°C. Two, and possibly three orientations of lamellae are shown. Also present are three grains of gold with a minor amount of calaverite associated with the largest grain. Black areas are pits.

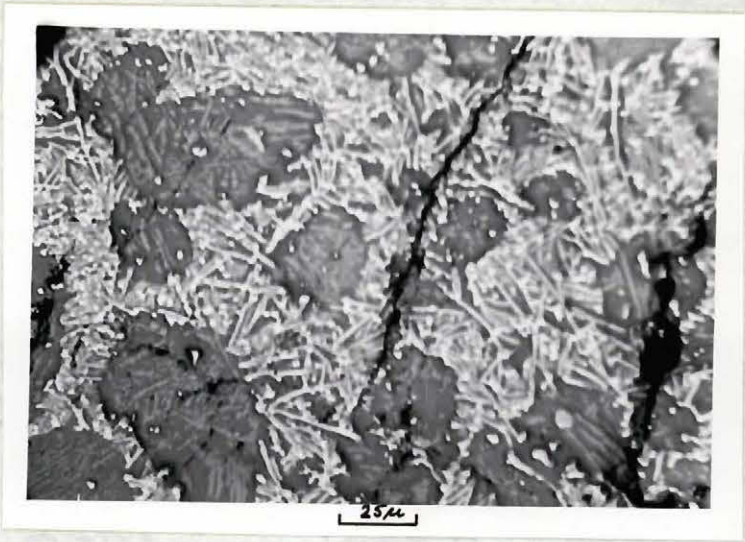

Figure 15. Same polished section as figure 14, but at lower magnification. Rounded grains of petzite contain lamellae of phase A and very small amounts of gold and calaverite. These are surrounded by an intergrowth of calaverite-gold-petzite formed by crystallization from a liquid. The petzite in the crystallized liquid shows no lamellae. Black areas are pits.

Figure 16. Same as figure 15, but greater magnification showing detail of groundmass surrounding large rounded petzite grains. Calaverite forms bladed or acicular crystals in a petzite groundmass while gold occurs in rounded irregular grains. Crossed nicols.

(5) Runs 346 and 376 gave the strongest patterns for A and B.

(6) The composition of phase A in figures 14, 15, and 16 was deduced from an estimation of the volume per cent of A in the petzite grains. This percentage was then applied to the phase relations in figure 9 and an approximate composition arrived at of 42 Au, 28 Ag, and 30 Te, all in weight per cent, by using the lever law.

Heating runs 342, 345, 346, and 376 in the high-temperature camera demonstrated that the pet-hs_{ss} extends to more gold-rich compositions than $AuAg_3Te_2$, and that calaverite disappeared above 304°C. This is in agreement with the above observations and indicates that a liquid field occurs at 335° and 356°C in the approximate areas shown in figures 10 and 11.

The breakdown of the pet-hs_{ss} (of compositions more gold-rich than $AuAg_3Te_2$) on quenching is thought to produce phases A and B which are probably metastable Au-Ag-Te phases of differing compositions. These always occur within petzite and are observed as anisotropic phases in petzite in polished sections (figure 14).

It is interesting to note that two writers have described anisotropic phases in natural petzite. According to Uytenbogaardt (1951, p. 37), "Helke (1934) distinguished between an isotropic, greyish-violet variety (α-petzite) and an anisotropic modification (β-petzite) showing great resemblance to hessite. However, no further details such as transition point, etc., are given." Hawley (1948, p. 111) reported some petzite grains from the Kirkland Lake area as showing anisotropism and a fine grid of twin lamellae at about right angles. The above examples indicate that phases A and B might occur in natural ores. Further work is obviously needed on this problem, and electron microprobe traverses across phases A and B could be very helpful.

The application of the experimental data to natural occurrences of gold-silver tellurides

The phase relations in the pure synthetic Au-Ag-Te system were determined in the presence of vapor. The information presented in figures 3, 4, 5, 9, 10, 11, and 12 is, for this reason, applicable in the strictest sense only when vapor occurs as a phase. Vapor may not always be present during ore deposition, so that the P-T regions in the absence of vapor should be considered as well. The effect of rock pressure and partial pressures ($P_s < P_{total}$) on the phase relations of sulphide systems has been discussed by Kullerud (1959) and Kullerud and Yoder (1959) and similar effects might be expected in telluride systems. Univariant equilibria are commonly shifted 15° to 20°C/1000 atmospheres confining pressure.

The coexisting phases in both natural and artificial systems are determined only by (1) the bulk compositions, (2) the temperatures, and (3) the pressures. Though the range of reaction temperatures extends to lower values in nature than can generally be successfully investigated in the laboratory, the laboratory data may be extrapolated to lower temperatures using P-T projections. However, until many related systems are investigated, the application of experimental data from the Au-Ag-Te system requires certain simplifying assumptions.

The environment of ore deposition is much more complex, chemically, than the three pure components studied in this system. The presence of other components will only affect the phase relations concerned if they enter into the composition of one or several of the minerals formed. Likewise, water, if soluble in a melt, will lower the melting temperature

of that phase. There is virtually no reliable data on trace elements in the gold-silver tellurides. Little is known about the substitution of Se and S for Te in these tellurides, but there are statements reporting relatively high Se contents (e.g. ½% and 0.08% by Simpson, 1912, and 1.13% and 0.20% by Krusch, 1901) from Kalgoorlie tellurides while no Se mineral has, to the writers' knowledge, been positively identified. (Stillwell, 1931, gives evidence on the possibility of aguilarite (Ag_2S,Ag_2Se) in altaite and naumanite (Ag_2Pb)Se in the gold-silver tellurides, but this is not considered to be conclusive.)

The common presence of tellurium in base metal sulphide deposits can be attributed to trace amounts of tellurium within sulphide minerals if no tellurides are observed. Trace amounts of tellurium are reported occurring in galena (Oftedahl, 1959, Hawley et al, 1951, and others), in chalcopyrite (Dr. S. Barabas, personal communication), and in pyrite (Vathrushev, 1940). Sindeeva and Godovikov (1959) report experiments in which up to 2.8 wt. % Te isomorphously replaced S in PbS and also S substituted in PbTe to a similar extent. This only took place when a minimum of 10 at. % PbTe was heated with PbS above fusion. However, Sindeeva (1964) reports that careful optical examination of natural ores has revealed that Te occurs as microscopic segregations in the majority of cases and not within the structure of sulphide minerals. Much remains to be done concerning these problems, and the trace element content of gold-silver tellurides.

Theoretically, the experimental data can be applied in the following manner, assuming no complications due to the presence of foreign elements: (1) for coexisting phases, the limits of solid solution may be

used to make estimates of the temperature of formation, (2) the stability limits determined for some of the assemblages can give a measure of the physical conditions prevailing during deposition, and (3) a natural mineral assemblage containing the same phases as a synthetic mineral assemblage is suggestive of phase-equilibrium.

Limitations in applying the experimental data to gold-silver tellurides

A few specific examples will show the limitations of applying such criteria to the Au-Ag tellurides.

(1) There are few assemblages which may be used for making estimates of the formation temperature, from a practical point of view. Assemblages such as calaverite-krennerite or krennerite-sylvanite which would be useful generally have fields of small compositional extent. The extent of the silver solid solution in sylvanite might prove useful when sylvanite occurs in the presence of a more silver-rich phase. Furthermore, the tellurides must be sufficiently abundant in order to obtain enough material for measuring the relatively weak reflections used for the composition determinative curves or to determine their compositions by other means.

(2) The presence of krennerite gives an upper limit for its formation temperature of $382 \pm 5^{\circ}C$, whereas the upper limit for the formation of sylvanite is $354 \pm 5^{\circ}C$. The presence of an anisotropic phase within petzite (produced by the breakdown of pet-hs_{ss} more Au-rich than petzite)gives a lower limit of $304 \pm 15^{\circ}C$ for its formation. These values must be subject to some small corrections with increasing confining pressure. However, the presence of water or other volatiles, if soluble in the breakdown liquid, would presumably lower the three temperatures noted above.

(3) Most univariant assemblages in the system contain at least one metastable phase which may break down to form two or more phases. This complicates the interpretation of natural assemblages, which appear relatively simpler. The hessite-sylvanite and sylvanite-petzite intergrowths reported to be common at Kalgoorlie (Stillwell, 1931, and Markham, 1960) can be explained in three ways: (a) The minerals formed below approximately 120°C, i.e. below the stability field of gamma-phase, and at these temperatures tie lines probably extend from sylvanite to petzite and to hessite. (b) These intergrowths consist of three and/or four, and not two phases, with some undetected $Ag_{5-x}Te_3$ and/or petzite formed on the breakdown of the gamma-phase. Stillwell (1931, p. 150) states when referring to hessite and petzite, "Well-polished sections are required to detect the faint change in colour at the contact of these two minerals and to reveal the faint bluish tinge of petzite in contrast with hessite. Both minerals appear bluish in contrast with krennerite or sylvanite....." He reported no $Ag_{5-x}Te_3$, but Markham (1960, p. 1171) reports the association $Ag_{5-x}Te_3$ + sylvanite from one specimen. (c) The gamma-phase has been preserved, but not recognized, as it is similar to petzite.

Markham's (1960, p. 1170) explanation that sylvanite-hessite and sylvanite-petzite intergrowths may be interpreted as due to exsolution of an original homogenous phase above 300°C is contradicted by the phase relations determined in the temperature range from 290°C to above the melting point of sylvanite at 356°C.

Natural assemblages of Au-Ag-Te minerals

In order to make some first-hand observations on these minerals, specimens were obtained representative of various telluride deposits.

The specimens commonly contained ore minerals unrelated to the Au-Ag-Te system, which were identified in many cases but were not studied in detail. The samples obtained were of two kinds. Those obtained from the Royal Ontario and Peter Redpath Museums and the Department of Geological Sciences at McGill University were hand picked by the writer from hand specimens in order to obtain material for x-ray only. All other samples obtained consisted of telluride-bearing ore fragments which were polished for optical examination and confirmed by x-ray.

The data on natural calaverites studied are shown in table 19. The calaverite samples were carefully hand picked with the binocular microscope and x-rayed, employing the diffractometer, in the same way as the synthetic runs to obtain the d_{131} value. All hand-picked minerals were checked with the Guinier camera to confirm the identification, as well as to detect other minerals, if present.

TABLE 19

Specimens of natural calaverite examined*.

Sample No.	Locality	d_{131} ± 0.0004 Å	wt. % Ag from curve ± 0.2 wt. % Figure 6	Intimately associated metallic minerals
ROM-M18767	Cripple Creek, Colorado	1.3864	0.92	
McG-2972R2	Cripple Creek, Colorado	1.3866**	1.00	
ROM-M19301	Cresson Mine, Cripple Creek, Colorado	1.3878	1.46	Au
PRM-F716	Independence Mine, Cripple Creek, Colorado	1.3880**	1.54	
PRM-NS716A	Cripple Creek, Colorado	1.3880**	1.54	

TABLE 19 (cont'd.)

ROM-E1924	Cripple Creek, Colorado	1.3890	1.94	
ROM-M22591	Cripple Creek, Colorado	1.3899	2.30	(single crystal)
PRM-F712	Victor, Colorado	1.3898**	2.24	(single crystal)
PRM-F711	Victor, Colorado	1.3898**	2.24	
McG-2972R3	Calaveras County, California	1.3889**	1.90	
L-9	Lamaque Mine, Bourlamaque, Quebec	1.3878	1.46	tellurbismuth, Au, cp, pet
ROM-M21755	Nagyag, Transylvania	1.3884	1.70	
ROM-M13812	Kalgoorlie, Australia	1.3912	2.80	
ROM-E2569	Kalgoorlie, Australia	1.3933***	3.80?	

* Abbreviations used:

ROM - Royal Ontario Museum

USNM - U.S. National Museum

PRM - Peter Redpath Museum, McGill University

McG - Department of Geological Sciences Reference Collection, McGill University

L - Lamaque Gold Mines Ltd.

** d_{131} measured on Guinier film.

*** d_{131} measured on Guinier film and with the diffractometer.

All the above d_{131} values fit the experimental data very well except for sample ROM-E2569 from Kalgoorlie. This was a conchoidally fractured piece of calaverite (about 180 mg.) which appeared very pure under the

binocular microscope. A portion was ground and x-rayed both with the diffractometer and the Guinier camera. A few extra reflections were observed on the Guinier photograph, none of which could be identified (see appendix, table A14). A polished section was made on about 20 mg. of the material and a few small impurities were observed. The total impurities by volume measured on three grains in the section were 0.13, 0.24, and 0.30%. Assuming a similar specific gravity and allowing for errors in measurement and randomness of the impurities, it is estimated that these do not constitute more than 0.5 wt. % of the sample and probably less. The principal impurity was medium mauve-grey in colour, very soft, and isotropic. Etch tests gave the following results:

1:1 HNO_3 - negative (after two minutes)

$FeCl_3$ - positive - tarnished black (30 sec.)

$HgCl_3$ - negative (after two minutes)

KOH - negative (after two minutes)

KCN - negative (after one minute)

These indicate coloradoite (HgTe). However, the coloradoite pattern could not be recognized among the extra reflections reported previously. The other impurities were too small to do any tests. One was greyish white and anisotropic, and the other dark mauve-grey and isotropic.

X-ray fluorescence and optical emission spectrographic analyses were performed on the sample. The former indicated only Au, Ag, and Te. The latter was performed through the kindness of Dr. S. Barabas at the Noranda Research Center, Pointe Claire, Quebec, and gave indications of Hg, Sb, Cu, and Pb. The Hg would correspond to coloradoite and the Sb, Cu, and Pb could come from one or a combination of tetratredrite

($5Cu_2S.2(Cu,Fe)S.2Sb_2S_3$ with occasional Ag, Zn, Bi, Hg, and Te), altaite (PbTe), seligmanite ($2PbS.Cu_2S.As_2S_3$), and nagyagite ($Au(Pb,Sb,Fe)_8(S,Te)_{11}$). All four minerals were reported by Stillwell (1931) and Markham (1960) in Kalgoorlie ores. An analysis was performed on the remainder of the sample by Dr. Barabas and associates at the Noranda Research Center with the following results:

	wet analysis	fire assay
Au	37.1%	37.2 %
Ag		3.06
Te	55.9	
Se	not detected (<0.03)	

The check on the gold is very good. Because of the small size of sample and the small amount of Ag present an error of 10% might be assumed giving a Ag content of $3.06 \pm 0.3\%$. Analysis for selenium was performed because of Simpson's (1912, p. 171) statement that all the tellurides at Kalgoorlie contain about ½% Se as well as two analyses reported by Krusch (1901, p. 200) where he reports 1.13 and 0.20% Se in calaverite and sylvanite, respectively. Selenium would not have been detected by the spectrograph or by x-ray fluorescence. No selenium was detected by the chemical analysis, which will not detect quantities below 0.03%.

Since the analyzed quantities do not total 100%, the results were recalculated below, based on two different sets of assumptions.

	(1)	(2)
Au	37.33%	38.65%
Ag	3.07	3.18
Te	59.60	58.17
	100.00	100.00

In case (1) above, it was assumed that there was 0.5% impurity, and that all the remaining loss was Te. (The assumption that all the loss was Te was suggested by Dr. Barabas because of the unusual composition of the sample.) In case (2) above, it was assumed that all three elements were correct and that there were 3.89% impurities (which is much larger than the writer's estimate from polished sections). When plotted on the ternary diagram only case (2) is reasonably close to the $AuTe_2$-"$AgTe_2$" join. It is considered that neither calculation need be correct, and so it is still not established whether calaverite can contain more than 3% Ag. Likewise, it is not known what the effect of impurities such as Hg, Pb, Sb, and Cu may have on the 131 reflection.

The association calaverite-krennerite was observed in two samples, USNM-C703 and 84511 from Offenbanya, Transylvania, and Lafayette Mine, Cripple Creek, Colorado, respectively. It was extremely difficult to distinguish between the two minerals in polished section as grain boundaries are not easily visible under plane polarized light, but there may be small differences in bireflectance. Under crossed nicols, however, interlocking grains could be observed. These were confirmed by x-rays, but unfortunately not enough material was available to measure the 131 reflection of calaverite or the reflection used for the krennerite d-value versus composition curve.

The data in tables 20 and 21 show good correspondence with the experimental results. Unfortunately, several krennerites and sylvanites examined had reflections which were too poor to measure. One of these contained the assemblage krennerite-sylvanite from Nagyag (PRM-NS717A). Another sample (PRM-F713) from the Stanislaus Mine, California, labeled

calaverite, contained the assemblage petzite + krennerite + unknown mineral. A sample from Boulder County, Colorado (ROM-M4041), labeled sylvanite, actually contained tellurium + unknown mineral. One krennerite sample (McG-2972R1) from Cripple Creek, Colorado, gave an anomalous d-value which would indicate less than 3 wt. % Ag if applied to the d-value versus composition curve (figure 7). An optical emission spectrographic analysis of the sample indicated several impurities (Cu, Mg, Si) and many more which could not be identified. Polished sections, however, showed less than one per cent gangue and metallic mineral inclusions. It is hoped to study this sample in greater detail at some future date and to obtain a chemical analysis.

TABLE 20

Specimens of natural krennerites examined.

Sample No.	Locality	d_{hkl}* ± 0.0001 Å	wt. % Ag from curve (figure 7)
McG-2973R3	Cripple Creek, Colorado	0.79906	3.43
PRM-F717	Nagyag, Transylvania	0.80012	4.21
ROM-M23798	Kalgoorlie, Australia	0.80029	4.56
ROM-E2793	Cripple Creek, Colorado	0.80066	4.90
ROM-M15783	Nagyag, Transylvania	0.80125	5.46

* Measured with the Phillips symmetrical back reflection camera.

TABLE 21

Specimens of natural sylvanites examined.

Sample No.	Locality	d_{hkl}* ± 0.00015 Å	wt. % Ag from curve (figure 8)
PRM-F709	Offenbanya, Transylvania	0.80617	11.83
PRM-F708	Offenbanya, Transylvania	0.80619	11.85

* Measured with the Phillips symmetrical back reflection camera.

The assemblage sylvanite-petzite was also observed in samples from Nagyag, Transylvania (USNM-R919). The petzite consisted of a few irregular, and sometimes lens-like grains within the sylvanite. The experimentally determined phase relations do not permit this assemblage, at least not at temperatures above 170°C. It is very likely that tie line changes occur below that temperature, but it is also possible that the gamma-phase or $Ag_{5-x}Te_3$ and hessite were present in small quantities and not detected.

Five telluride hand specimens were obtained from the 21-34N stope, Horne Mine, Noranda, where telluride mineralization was found associated with a syenite porphyry dike in massive sulphides (mostly pyrite with some chalcopyrite). Eighteen polished sections were prepared and the following minerals observed: chalcopyrite, pyrite, altaite, petzite, gold, hessite, sphalerite, and tellurbismuth. The sulphides and gangue are partly replaced by the tellurides. Petzite and altaite occur in greater quantities than gold and hessite. The association petzite-gold is common (figure 17) and hessite is observed in the

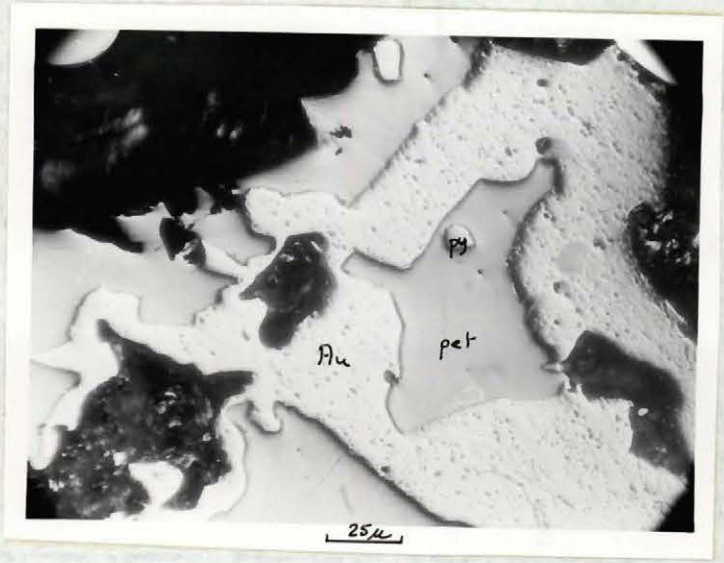

Figure 17. The natural assemblage gold-petzite from the Horne Mine, Noranda, Quebec, with minor pyrite.

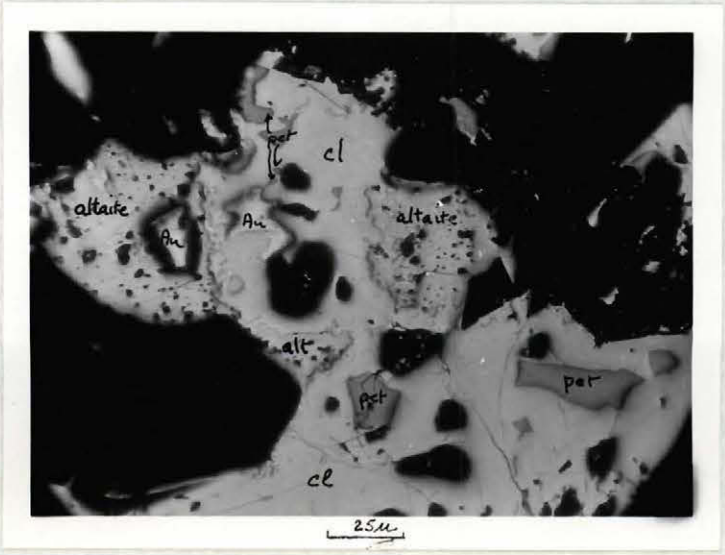

Figure 18. The natural assemblage gold-calaverite-petzite-altaite (USNM-C703) from Offenbanya, Transylvania.

assemblages hessite-petzite-gold and hessite-altaite. Nothing could be determined about telluride paragenesis from the observed textures.

Specimens from the Sigma Mines Quebec Ltd., Bourlamaque, Quebec, contain the associations gold-petzite-tellurbismuth and tellurbismuth-altaite.

Specimens obtained from the Lamaque Gold Mining Co. Ltd., Bourlamaque, Quebec, contain the associations tellurbismuth-petzite-gold-pyrrhotite and pyrite-calaverite-petzite-tellurbismuth. The d_{131} value for calaverite given in table 19 indicates a silver content of about 1.46 wt. %.

Polished section examination of fragments of telluride-bearing ore from Offenbanya, Transylvania (USNM-C703) revealed the following assemblages: gold-calaverite-petzite-altaite (figure 18) and calaverite-krennerite-petzite-altaite. The native gold only occurs in the polished section containing no krennerite, but since the fragments used in both polished sections came from the same sample envelope, it appeared possible that the association gold-krennerite might occur. This assemblage has only been authoritatively reported in a specimen from Kalgoorlie (Markham, 1960, p. 1174) where weissite containing filaments of free gold penetrated along cleavage directions of krennerite and partly replaced it. This is not considered to be an equilibrium assemblage.

To test the possibility of a krennerite-gold assemblage, a series of runs were prepared with the following approximate bulk composition (in wt. %): 42.5 Au, 15.0 Ag, 42.5 Te, and were heated at 356°, 335°, 320°, 305°, 290°, 270°, and 238°C. To insure that equilibrium was

attained, or to determine which were the equilibrium assemblages, two runs were prepared at each temperature employing different starting materials. In one case the starting materials were calaverite + gold + petzite, and in the other they were krennerite + gold + petzite. Runs quenched from 356° to 305°C showed calaverite + petzite + gold + an unknown phase/or phases (phases A and B, believed to be metastable compounds formed from the breakdown of petzite-hessite solid solution), while the runs at 290° and 270°C showed only calaverite + petzite + gold. At 238°C the run with calaverite as starting material remained unchanged, but where krennerite was the starting material, approximately half the krennerite had broken down to calaverite after 53 days, indicating conclusively that the assemblage krennerite + gold is unstable at temperatures from 356° to 238°C. It seems unlikely that the krennerite-gold assemblage would become the stable assemblage at temperatures below 238°C.

This information further points to the possibility that tellurium-rich telluride suites such as that of Vatukoula (coupled with the rarity of native gold) and the native gold-rich telluride suites such as that of Kalgoorlie (coupled with the extreme rarity of native tellurium) are a function of the bulk composition of the ore-bearing fluids and not, necessarily, of temperature. Markham concluded that temperature was the major factor when he proposed krennerite as the low temperature polymorph of calaverite in his isothermal section constructed from assemblages observed at Vatukoula. Similarly, the natural occurrence of three-phase assemblages such as calaverite + gold + petzite and calaverite + krennerite + petzite observed in this study from Transylvania, as well

as the common occurrence of the assemblage sylvanite + petzite + hessite reported by Markham from Kalgoorlie and the $Ag_{5-x}Te_3$ + hessite + petzite and hessite-$Ag_{5-x}Te_3$ assemblages reported by Honea (1964) from Colorado, all show that Korzhinskii's modification of the mineralogical phase rule as discussed by Markham (1960, p. 1461-1463) and Cloke (1963) does not necessarily apply to the gold-silver-tellurium ternary system. The assumption that tellurium behaves as a "perfectly mobile" component is not borne out by the natural occurrence of the four different "prohibited" assemblages (Cloke, 1963, p. 1166) reported above. A glance at the isothermal sections in figures 10, 11, and 12 shows that several of the three-phase assemblages which do not include tellurium (these would be prohibited if tellurium behaved as a "perfectly mobile" component) have a rather small compositional extent so they would be expected to be relatively rare in natural ores.

One specimen (USNM-87511) from the Lafayette Mine, Cripple Creek, Colorado, showed a twinned crystal of krennerite in polished section (figures 19 and 20). This specimen was originally labeled krennerite and calaverite, but all x-ray diffraction photographs showed only krennerite. The twinned crystal shows two types of twinning, a simple type consisting of two large individuals, and a lamellar twinning in one of them. The lamellae are all in optic orientation. Half of the large twin containing the lamellae was removed and a 114.6 mm. Debeye-Scherrer photograph showed only the krennerite pattern. The remainder of the crystal was removed (as deeply as possible) and a Guinier photograph was taken which showed only krennerite present. This is taken to indicate that krennerite can be twinned and observed in polished sections, and that

this might explain misidentifications in published accounts where any twinned material was called sylvanite without x-ray confirmation. Twinned krennerite has only been reported once before, from the La Plata district, Colorado (Galbraith, 1940), but his identifications were solely by microchemical and etch tests.

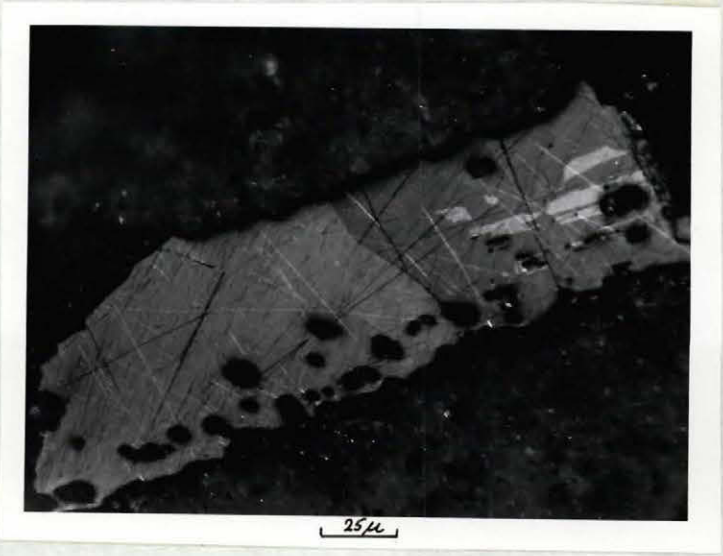

Figure 19. Twinned krennerite crystal (USNM-87511) from the Lafayette Mine, Cripple Creek district, Colorado. Two types of twinning shown. Black areas are pits and air bubbles. Crossed nicols.

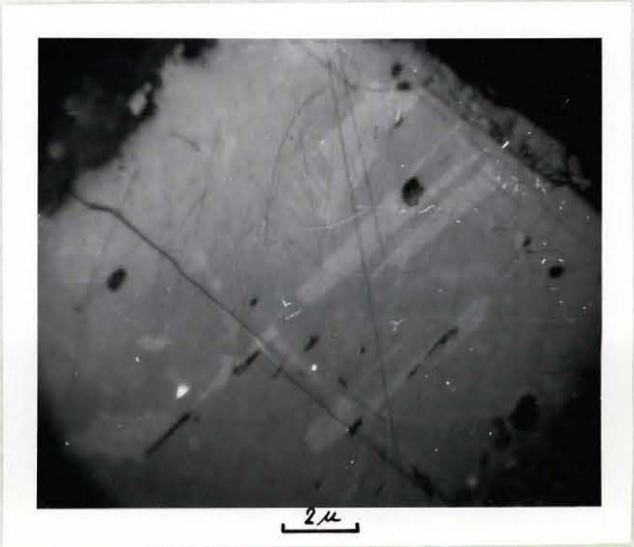

Figure 20. Same as figure 19, but greater magnification showing detail of the lamellar twinning. Crossed nicols.

Note on the x-ray powder diffraction patterns of calaverite, krennerite, and sylvanite

Guinier powder patterns comparing synthetic calaverites and natural calaverites with Tunell's (1954) pattern are tabulated in the appendix, table A14. Tunell lists only four extra reflections (down to an interplanar spacing of 1.30 Å) observed on a 114.6 mm. Debeye-Scherrer powder photograph of natural calaverite and called these "superstructure" lines. There are considerably more extra reflections observed on the Guinier powder photographs of both synthetic and natural calaverites. Most of these extra reflections correspond to extinction positions required by the space group proposed by Tunell. Most of the extra reflections observed in the present study, however, could be accounted for by changing the space group to $P2_1$ or $P2_{1/m}$. Some of these extra reflections correspond to a calculated zero relative intensity according to Tunell's structure. Another possibility is that some, or all of these extra reflections are additional "superstructure" reflections.

It is evident that both the space group and structure of calaverite need further study and that Tunell's data probably represents a pseudocell. The basic cell probably has a space group based upon a primitive lattice.

The x-ray powder data from Guinier photographs of synthetic krennerite (4.53 wt. % Ag synthesized at 350°C) and natural krennerite from Kalgoorlie (ROM-23798) are compared with the pattern for krennerite given by Tunell and Murata (1950) in the appendix, table A15. The patterns compare favourably, especially considering the relatively broad solid solution field of krennerite. It should be noted, however, that

thirteen reflections were observed which had been given a calculated relative intensity of zero by Tunell and Murata. As these reflections are not simply contradictions of the extinction position requirements of the space group, it is suggested that small refinements in the structure are required to account for these extra reflections. The x-ray powder pattern taken by Tunell and Murata with filtered Co radiation detected two of the thirteen reflections mentioned above.

X-ray powder data from Guinier photographs of synthetic sylvanite (10.09 wt. % Ag synthesized at 320°C) and natural sylvanite from Offenbanya, Transylvania (PRM-F708) are compared with the pattern for sylvanite given by Tunell (1941) in the appendix, table A16. The three patterns agree very well, though the interplanar spacings for the natural sylvanite are generally slightly larger than those of the synthetic sylvanite. This is consistent with a greater silver content for the natural sylvanite (approximately 1.76% Ag) as was indicated previously by the interplanar spacing versus composition curve. However, synthetic sylvanites sometimes show two weak reflections which do not fit the indexing (6.12 & 5.99 Å). One of these reflections (6.12 Å) also appears in some patterns of natural sylvanite.

Features in the Au-Ag-Te system that merit further investigation

Although phase relations in the Au-Ag-Te system have now been studied in greater detail than in the past, the present investigation indicates that there are still areas within the system that merit further research. These may be summarized as follows:

(1) Further data on the nature of the $AuTe_2$ inversion (at about 435°C) and on the stability field of Au_2Te_3 would complete our knowledge of the Au-Te binary.

(2) The stability field of AgTe and an explanation for the "extra reflections" in x-ray powder patterns of silver-rich $Ag_{5-x}Te_3$ would be useful points for further study. More detailed work on the Ag-Te system to determine more closely the composition limits of all phases is necessary. Equipment unavailable to the writer, such as that used by Kiukkola and Wagner (1957) would be helpful.

(3) The discovery of a new ternary eutectic indicates that considerable more detailed work is necessary in certain areas of the liquidus diagram.

(4) Considerable study is required to determine the extent of gold solid solution in the gamma-phase, as well as to delineate the gold-rich gamma-phase stability field at lower temperatures.

(5) The effect of pressure on the phase relations, though probably not very pronounced, would provide useful information for more accurate application of the synthetic data to natural assemblages.

(6) A study of the degree of substitution of Se or S for Te and vice versa is also necessary as well as an experimental determination of the effects of trace elements on the determinative curves of the gold-

silver tellurides. This might explain the anomalous d-values obtained on one natural calaverite and one natural krennerite.

(7) Further study on the formation rate and stability of krennerite below 290°C would be useful in determining whether krennerite is stable at room temperature.

(8) There exist crystallographic problems associated with several of the phases present in the Au-Ag-Te system. The elucidation of the "superstructure" of calaverite and possible refinements in the structures of krennerite and sylvanite are one example. Similarly, the indexing of the gamma-phase and the "x" phase would be another.

Conclusions

It is anticipated that many of the findings of this experimental study will be applicable to natural assemblages, permitting a better understanding of the conditions of formation of certain telluride deposits.

The major conclusions of this study may be summarized as follows:

(1) The Au-Te binary. There is no detectable solubility of Au in $AuTe_2$ but limited solubility of Te (~0.3 wt. %) occurs above about 440°C. Above about 435°C no silver is taken into solid solution by $AuTe_2$, reflecting a probable transition at that temperature.

(2) The Ag-Te binary. The "gamma-phase", intermediate in composition between $Ag_{5-x}Te_3$ and Ag_2Te, is stable from 120 ± 15°C to 460 ± 5°C, above which temperature it melts incongruently to Ag_2Te plus liquid. $Ag_{5-x}Te_3$ melts incongruently above about 420 ± 5°C to gamma-phase plus liquid.

(3) The $AuTe_2$-"$AgTe_2$" join. The incongruent melting temperatures of krennerite (382 ± 5°C) and sylvanite (354 ± 5°C) may be taken as maximum formation temperatures for these minerals. The relatively extensive solid solutions of calaverite, krennerite, and sylvanite restrict the divariant regions between them. Krennerite is interpreted as being a single mineral entity with a relatively large solid solution field and an approximate formula Au_4AgTe_{10}. Sylvanite has a very extensive solid solution field extending from stoichiometric $AuAgTe_4$ (13.23 wt. % Ag) to about 6.7 wt. % Ag.

The association calaverite-sylvanite, rarely reported in the literature, is considered to be a non-equilibrium assemblage or may reflect misidentification.

(4) The $AuAg_3Te_2$-Ag_2Te join. Petzite has three polymorphs, with transitions at 210 $\pm$ 10°C and 319 $\pm$ 15°C. The highest polymorph, which forms a complete solid solution field with hessite, extends to compositions about seven wt. % more gold-rich than stoichiometric petzite. The breakdown, on quenching, of the gold-rich petzite-hessite solid solution forms metastable phases of differing compositions, within petzite.

A large section of the join consists of a new phase, the "x" phase, stable between 50 $\pm$ 20°C and its incongruent breakdown above 415 $\pm$ 20°C to high plus intermediate hessite solid solutions. The gold content of the "x" phase varies from about 2.5 to 14.5 wt. % on the join.

(5) The Au-Ag-Te system. Although no attempt was made to study the liquidus, a previously unreported ternary eutectic was discovered occurring at 304 $\pm$ 10°C and the very approximate composition of 50 Au, 15 Ag, 35 Te weight per cent.

(6) Geological applications of the experimental work. Several of the phase relations indicated by the experimental study serve to delimit the temperature conditions of formation of natural Au-Ag-Te minerals. In addition, natural assemblages indicate that there is no justification for assuming that Te behaved as a "perfectly mobile" component in telluride deposits.

Acknowledgements

The entire study was carried out at the Department of Geological Sciences, McGill University, using the laboratory facilities of Drs. L.A. Clark, A.J. Frueh, Jr., and G.R. Webber, to each of whom I am indebted for generous guidance in several phases of the experimental study. I am especially grateful to Dr. L.A. Clark for advisory assistance both in relation to the experimental work and to the manuscript preparation. The extensive laboratory facilities employed were available as a result of National Research Council of Canada grants to the above professors, in particular grant A-1111 to Dr. L.A. Clark plus equipment grants accompanying two Inco Fellowships. Dr. A.H. Clark and Mr. R.G. Roberts also contributed useful suggestions regarding the grammatical composition of some sections of the manuscript. I am also thankful to Dr. R.A. Robie, United States Geological Survey, for sending the unpublished manuscript and laboratory notebooks of the late Dr. F.C. Kracek.

The ore and mineral specimens used in this study were obtained from: The Royal Ontario Museum, Toronto, through the cooperation of Dr. J.A. Mandarino; The Peter Redpath Museum, McGill University, with the cooperation of Mrs. L.S. Stevenson; The Smithsonian Institution, Washington, through the cooperation of Mr. P.E. Desautels; and through the kindness of Dr. J.S. Stevenson, McGill University; Mr. W.L. Bancroft, Noranda Mines Ltd; Mr. R.J. Graham, Lamaque Gold Mines Ltd; and Mr. N.J.S. Hoyles, Sigma Mines (Quebec) Ltd.

I am especially grateful to the National Research Council of Canada for a Studentship (1961-62) and to the International Nickel Company of Canada for two Inco Fellowships (1962-63 and 1963-64).

Claim to original work

Phase relation and associated studies in the Au-Ag-Te system have been made by several workers as indicated in Chapter 2. Markham (1957, 1960) made the first systematic attempt to determine the subsolidus phase relations in a single isothermal section. Three new isothermal sections at 290°, 335°, and 356°C are presented which are different in many respects from Markham's 300°C isothermal section. This is because Markham was unable to synthesize krennerite and to quench and identify the new high-temperature phases present in the ternary system.

The phase relations along the join $AuTe_2$-"$AgTe_2$" are determined in detail for the first time, as well as along the join $AuAg_3Te_2$-Ag_2Te where new phases were discovered. A second ternary eutectic, within the area bounded by calaverite-petzite-AuAg solid solution, was also discovered.

The work on the Ag-Te binary confirmed the occurrence of a previously indicated new phase. Stabilities of phases and assemblages were considerably revised and clarified.

References

Baker, G. (1956) Ore specimens and tailing from Great Boulder Mine, Kalgoorlie, Western Australia. C.S.I.R.O. Melbourne, Australia. Min. Dept. No. 641.

Berry, L.G., and Thompson, R.M. (1962) X-ray powder data for ore minerals: The Peacock Atlas. Mem. 85 Geol. Soc. Am.

Borchert, H. (1935) Neue Beobachtungen an Tellurerzen. Neues Jahrbb. Min. Geol. Pal., Beil. Bd. 69. Abt. A., p. 460-477.

Bradley, W.M. (1914) Empressite, a new silver-tellurium mineral from Colorado. Am. Jour. Sci. 38, p. 163-165.

_____ (1915) On the mineral empressite. Am. Jour. Sci. 39, p. 223.

Chase, F.M. (1956) Abbreviations in field and mine geological mapping. Econ. Geol. 51, p. 712-723.

Chikashige, M., and Saito, I. (1916) Metallographische Untersuchung Ueber das System von Silver und Tellur. Mem. Coll. Sci., Kyoto Univ. v.1, p. 361-368.

Clark, L.A. (1959) Phase relations in the Fe-As-S system. Unpub. Ph.D. dissertation, McGill University.

Cloke, P.L. (1963) Synthetic and natural phases in the system Au-Ag-Te. Discussion in Econ. Geol. 58, p. 1163-1166.

Donnay, G., Kracek, F.C., and Rowland, W.R. (1956) The chemical formula of empressite. Am. Mineralogist 41, p. 722-723.

Eckel, E.B. (1949) Geology and ore deposits of the La Plata district, Colorado. U.S. Geol. Survey Prof. Paper 219.

Eidel, J., and Tunell, G. (1963) Genesis of antimony-mercury deposits. Oral presentation by G. Tunell at Annual Meeting Geol. Soc. Amer., New York.

Frueh, A.J. (1959a) The structure of hessite, Ag_2Te-III. Zeitschrift für Krist. 112, p. 44-52.

_____ (1959b) The crystallography of petzite, Ag_3AuTe_2. Am. Mineralogist 44, p. 693-701.

_____ (1961) Use of the Zone theory in problems of sulphide mineralogy, Part III; Polymorphism of Ag_2Te and Ag_2S. Am. Mineralogist 46, p. 654-660.

Galbraith, F.W. (1940) Identification of the commoner tellurides. Am. Mineralogist 26, p. 368-371.

Genth, F.A. (1868) Contributions to mineralogy. Am. Jour. Sci. xlv ser. 2, p. 305-321.

_____(1874) On American tellurium and bismuth minerals. Am. Phil. Soc. XIV, p. 223-231.

_____(1877) On some tellurium and vanadium minerals. Am. Phil. Soc. XVII, p. 113-123.

Hansen, M., and Anderko, K. (1958) Constitution of binary alloys. 2nd ed., McGraw-Hill Book Co.

Hawley, J.E. (1948) Mineralogy of the Kirkland Lake Ores. Ont. Dept. Mines 57, p. 104-124.

_____, Lewis, C.L., and Wark, W.J. (1951) Spectrographic study of platinum and palladium in common sulphides and arsenides of the Sudbury district, Ontario. Econ. Geol., 46, p. 149-162.

Helke, A. (1934) Die Goldtellurerzlagerstätten von Sacaramb (Nagyag) (in Roumanien). Neues Jahrb. Min. Beil. Bd. 68A, p. 19-85.

Hillebrand, W.F. (1895) Calaverite from Cripple Creek, Colorado. Am. Jour. Sci. (3) L, p. 128-131.

Honea, R.M. (1964) Empressite and stuetzite redefined. Am. Mineralogist 49, p. 325-338.

Jänecke, E. (1911) Metallurgie 8, p. 599-600 (as cited by Hansen & Anderko, 1958).

Kelly, W.C. (1963) Personal communication.

Kiukkola, K., and Wagner, C. (1957) Measurements on galvanic cells involving solid electrolytes. J. Electrochem. Soc. 104, p. 379-387.

Klement, W. (1961) Lattice parameters of the metastable close-packed structures in silver-germanium alloys. J. Inst. Met. 90, p. 27-30.

Koern, V. (1940) Das binare Legierungssystem Ag-Te. Naturwiss. 27, p. 432.

Kracek, F.C. (1941) The melting point of tellurium. J. Am. Chem. Soc. 63, p. 1989-1990.

_____(1963) Melting and transformation temperatures of mineral and allied substances. U.S. Geol. Survey Bull. 1144-D, p. D1-D81.

_____, and Ksanda, C.J. (1940) Ann. Rept. Geophys. Laboratory, Carnegie Inst. Washington Year Book 39, p. 35-36.

_____, and _____ (unpublished).

_____, and Rowland, W.R. (1955) The system silver-tellurium. Ann. Rept. Geophys. Lab., Carnegie Inst. Washington Year Book 54, p. 135-136.

Krusch, P. (1901) Ueber einige Tellurgoldsilberverbindungen von den west-australischen Goldgangen. Centralblatt fur Min. Geol. und Paleont., p. 199-202.

Kullerud, G. (1959) Sulphide systems as geological thermometers. In "Researches in Geochemistry", edited by P.H. Abelson, New York; John Wiley and Sons, Inc. p. 301-335.

_____, and Yoder, H.S., Jr. (1959) Pyrite stability relations in the Fe-S system. Econ. Geol. 54, p. 533-572.

_____, and Yund, R.A. (1960) Cu-S System. Geol. Soc. Amer. Bull. 71, p. 1911-1912.

_____, and _____ (1962) The Ni-S System and related minerals. J. of Petrology, 3, No. 1, p. 126-175.

Lovering, T.S., and Goddard, E.N. (1950) Geology and ore deposits of the Front Range, Colorado. U.S. Geol. Survey Prof. Paper 223 (p. 289-312 for "Cripple Creek district").

Luo, H.L., and Klement, W. (1962) Metastable simple cubic structures in gold-tellurium and silver-tellurium alloys. J. Chem. Phys. 36, No. 7, p. 1870-1874.

Markham, N.L. (1957) Phase relations in the system gold-silver-tellurium. Unpub. Ph.D. dissertation, Harvard University.

_____ (1960) Synthetic and natural phases in the system Au-Ag-Te. Econ. Geol. 55, p. 1148-1178 and 1460-1477.

Oftedal, I. (1959) On the occurrence of tellurium in Norwegian galenas. Norsk Geol. Tids, bd. 39, h. 1, p. 75-79.

Palache, C. (1900) Notes on tellurides from Colorado. Am. Jour. Sci. ser. 4, 10, p. 419-427.

Peacock, M.A., and Thompson, R.M. (1946) Montbrayite, a new gold telluride. Am. Mineralogist 31, p. 515-526.

Pelabon, M.H. (1908) Sur le sulfre, le seleniure, et le tellure d'argent. Comptes Rendus Acad. Sci. 143, p. 294-296.

_____ (1909) Sur la fusibilite des melanges d'or et de tellurure. Comptes Rendus Acad. Sci. 148, p. 1176-1177.

Pellini, G. (1915) I tellururi d'argento e d'oro. Gazz. Chim. Italiana 45, p. 409-484.

_____, and Quercigh, E. (1910a) I tellururi d'argento. R. Accad. Lindei (Roma) (5) 19, p. 415-421.

_____, and _____ (1910b) I tellururi d'oro. Rend. Accad. Lindei (Roma) (5) 19, p. 445-449.

Penfield, S.L. and Ford, W.E. (1901) On calaverite. Am. Jour. Sci. (4) vol. 12, p. 225-246.

Price, P. (1933) The geology and ore deposits of the Horne Mine, Noranda, Quebec. Unpub. Ph.D. dissertation, McGill University.

Rahlfs, P. (1935) Ueber die Kubischen Hochtemperaturmodifikationen der Sulfide, Selenide und Telluride des Silbers und des einwertiben Kupfers. Z. Phys. Chem. Bd. 31, p. 151-194.

Raydt, U. (1912) Z. anorg. Chem. 75, p. 58-62 (as cited by Hansen & Anderko, 1958).

Rose, T.K. (1908) The alloys of gold and tellurium. Inst. Min. Met. London Trans. 17, p. 285-289.

Schneer, C.J., and Whiting, R.W., Jr. (1963) Phase transformation and thermal hysteresis in the system AgI.Am. Mineralogist 48, p. 737-758.

Sharma, S.K. (1963) Transformation of structure in silver-tellurium alloy films. Nature 198, No. 4877, p. 280-281.

Shrauf, A. (1878) Ueber die Tellurerze Siebenburgens. Zeits. Krist. 2, p. 202-252.

Simpson, E.S. (1912) Detailed Mineralogy of Kalgoorlie and Boulder, in W. Aust. Geol. Survey Bull. 42 by Simpson, E.S., and Gibson, C.G., p. 77-151.

_____ (1948, 1951, 1952) Minerals of Western Australia vols. I, II, III. Govt. Printer, Perth, W. Australia.

Sindeeva, N.D. (1964) Mineralogy and types of deposits of selenium and tellurium translated by Geochem. Soc., E. Ingerson, Chairman Translations Committee, Interscience Publishers, John Wiley & Sons, New York, 363 p.

_____, and Godovikov, A.A. (1959) Isomorphism between sulphur and tellurium in galena. Doklady Akad. Nauk SSSR, 127, No. 2, p. 431-434.

Sipőcz, L. (1885) Nehany magyarhoni ritkabb asvanyfaj Összeteteleről. Math. es Term. Tud. Köz. 20, p. 174-176.

Smith, G.F.H. (1902) On the remarkable problem presented by the crystalline development of calaverite. Mineral. Mag. 13, p. 122-150.

Stillwell, F.L. (1931) The occurrence of telluride minerals at Kalgoorlie, Aust. Inst. Min. Met. Proc. No. 84, p. 115-190.

Thompson, R.M. (1948) Pyrosynthesis of telluride minerals. Abs. Am. Mineralogist 33, p. 209-210.

_____ (1949) The telluride minerals and their occurrence in Canada. Am. Mineralogist 34, p. 342-382.

_____, Peacock, M.A., Rowland, J.F., and Berry, L.G. (1951) Empressite and Stuetzite. Am. Mineralogist 36, p. 458-470.

Todd, E.W. (1928) Kirkland Lake gold area (A detailed study of the central zone and vicinity). Ont. Dept. Mines XXXVII, pt. 2, 176 p.

Tunell, G. (1941) The atomic arrangement of sylvanite. Am. Mineralogist 26, p. 457-477.

_____ (1954) The crystal structures of the gold silver tellurides. Office of Naval Research, Res. Project NR-081-105.

_____, and Ksanda, C.J. (1936) The strange morphology of calaverite in relation to its internal properties. Jour. Washington Acad. Sci. 26, p. 509-528.

_____, and Murata, K.J. (1950) The atomic arrangement and chemical composition of krennerite. Am. Mineralogist 35, p. 959-984.

Umino, S. (1926) Kinzoku-no-Kenkyu, 3, p. 498 (as cited by Machol, R.E. & Westrum, E.J. (1958) J. Physc. Chem. 62, p. 361).

Uytenbogaardt, W. (1951) Tables for microscopic identification of ore minerals. Princeton University Press, Princeton, New Jersey.

Vakhrushev, G.V. (1940) Exploration for rare elements in Bashkiriya: Uchenye Zapiski Saratov Univ., 15, No. 1, p. 124-126 (as obs. in Chem. Abs. (1946), 35, p. 6541).

von Hippel, A. (1948) Structure and conductivity in the VI_b Group of the Periodic System. J. Chem. Phys. 16, p. 372-380.

Winkler, E.W., and Bright, N.F.H. (1964) The gold-bismuth-tellurium system. Canada Dept. of Mines and Tech. Surveys, Mines Branch, Mineral Sciences Division, Report MS-64-33.

Yund, R.A. (1963) Personal communication.

APPENDIX

1. Methods of Synthesis

The majority of the runs were performed using 3 mm. internal diameter simple sealed, evacuated tubes of transparent silica glass. For larger charges various diameters up to seven mm. were employed.

A loading technique was developed to minimize the adherence of reagents to the walls of the glass tubes due to electrostatic charges. This was particularly bad during the winter months and a water vaporizer was employed to increase the relative humidity while weighing. The glass tubes were cleaned the night before with a pipe cleaner moistened with a drop of acetone. Pyrex glass funnels of several different lengths were employed so that the charge was dropped as close to the sealed end of the tube as possible. The tube was then weighed after the addition of each reagent. In some cases, the second and third reagents were weighed separately on a watch glass and then swept with a camel's hair brush into the funnel. It was also found that a very rich piece of pitchblende placed next to the tube while loading produced enough gamma radiation to neutralize some of the electrostatic charges within the tube. A three eighth inch long silica glass rod was placed tightly against the charge.

The majority of the runs were quenched in cold water after a few days heating in a furnace, ground in an agate mortar, and reloaded. This grinding procedure was generally repeated at least twice, and the runs below 350°C were generally also pelletized in a small hydraulic press with a 5 mm. bore. Acetone was used to lubricate the cylinder of the press and a pressure of about 21,000 lbs/in^2 was sufficient to

produce good pellets. The pistons were made of drill rod, but these generally bent after about twenty compressions.

Some of the low temperature runs were heated for over two months, whereas only four to six days were necessary for runs above 400°C. In some of the low temperature runs, such as at 270° and 290°C, the charge was first melted for 6 to 48 hours and then quenched, ground, pelletized and put in at the lower temperature.

For pelletized runs below 320° pyrex tubing was satisfactory and less costly.

Bulk quantities of minerals were prepared at 800° to 990°C and kept at those temperatures for about four days.

2. Identification of the Products

(1) Reflecting microscope.

A portion of a charge was placed in an 1/8" steel press with some Acrylic Dental plastic. After squeezing in a vise for approximately five minutes, the hardened plastic pellet was extruded from the press and fastened to a glass slide with vynilite. The polishing was first done dry on various grades of emery paper and then wet using a gamma alumina suspension (Fisher, Grade B) on a "Gamal" polishing cloth mounted on a glass plate. As mentioned previously, there are several phases with very similar optical properties. The characteristics which help to distinguish between them optically are not always evident when the grain size is small or when there is only a small percentage of one phase.

In the calaverite-krennerite-sylvanite group, sylvanite exhibits the strongest anisotropism and bireflectance, but its distinguishing feature is the lamellar twinning when present. Krennerite

and calaverite are very similar, but krennerite can show (001) cleavage, whereas calaverite has no cleavage.

Petzite and hessite are sometimes similar in appearance and can be distinguished by their polarization figures; petzite shows an isometric cross whereas hessite gives two separate isogyres. The polarization figure of $Ag_{5-x}Te_3$ is similar to the one of hessite except for distinct bluish dispersion colours on the concave side of the isogyres. This is best seen in white light.

(ii) X-ray diffraction techniques.

Five different x-ray powder diffraction techniques were tested, using Cu radiation, with the following results:

(a) The 114.6 mm. Debeye-Scherrer camera was found to be time consuming and of insufficient resolution and accuracy. Exposures of up to eleven hours were sometimes necessary at 35 kV and 20 mA.

(b) The "Nonius" Guinier focussing camera was found to be rapid, had an acceptable accuracy ($\pm$ 0.0004Å) in the 55° to 70° 2θ range, but was of limited application since the higher diffraction angles are not obtained. However, it was found very useful for qualitative work as it could detect small amounts of some phases (less $\frac{1}{2}$ wt. % in some cases). Exposures of 10 hours at 40 kV and 15 mA were necessary.

(c) The x-ray diffractometer, although slower, yields results comparable in accuracy to the Guinier camera, and has a larger 2θ range. A G-E diffractometer was employed for the preliminary work on the calaverite solvus, while later additional work was done with a Phillips diffractometer. The results could be correlated. Unfortunately at the larger 2θ angles the intensities of the reflections became too

weak, necessitating another method to determine the solvus curves of krennerite and sylvanite.

(d) A Phillips symmetrical, back reflection, focussing camera was employed in the 140° to 150° 2θ range and gave better results at the higher angles than work done at the lower 2θ angles with the diffractometers. As single coated film could not be obtained, the back side of the film was covered with masking tape while in the developer so the calibration notches and reflections were distinct. The exposure times varied from about 2½ hours in the one phase fields up to about 4 hours in the two phase fields at 35kV and 20 mA. Best results were obtained by using no filter at the x-ray source but employing a nickel foil taped to the camera housing so as to fit immediately adjacent to the film. The camera was evacuated during exposure.

(e) A Rigaku-Denki high temperature camera was used to determine transition points, some melting points, and the stability fields of the non-quenchable high temperature forms and phases stable only at high temperatures. A circuit with the furnace winding acting as one arm of a Wheatstone bridge was the principle of the temperature controlling apparatus. A platinum- platinum+ 13% rhodium thermocouple was placed just beneath the sample and below the x-ray beam. The thermocouple temperatures were calibrated against sample temperatures by determining the melting or transition points of Cu_2S, AgI, HgS, NiS, Zn, Te, CuS and Ni_7S_6. Table A1 shows the purity of the reagents used to determine the calibration curve (Figure A1) as well as the references used.

TABLE A1

Reagents used for high-temperature camera calibration curve.

Element	Grade	Compound	Reference
Cu	99.999+% (spec. pure) American Smelting & Refining Co.	Cu_2S	Yund (1963)
		CuS	Kullerud & Yund (1960)
S	99.999+%, American Smelting & Refining Co.		
Ag	99.999+%, Consolidated Mining & Smelting Co., Cominco 59 grade, lot #2706	AgI	Scheer & Whiting (1963)
I	Fisher Certified Reagent (lot #731036, 99.985%)		
Hg	Engelhard, triple distilled, C.P. U.S.P.	HgS	Eidel & Tunell (1963)
Ni	99.977%, International Nickel Co. of Canada (carbonyl) hydrogen reduced	NiS	Kullerud & Yund (1962)
		Ni_7S_6	Kullerud & Yund (1962)
Zn	99.997%, Consolidated Mining & Smelting Co.	Zn	Kracek (1963)
Te	99.999+%, American Smelting & Refining Co.	Te	Kracek (1941, 1963)

The sample was ground and placed in 0.3 mm. I.D. and 0.01 mm. wall thickness silica glass capillaries which were evacuated and sealed. One end of the capillary was then cemented within a hollow ceramic tube holder with Sauereisen No. 8 cement. It required about eight hours for the sample temperature to become steady after which it would maintain the temperature within $\pm$ 2°C for more than two days. Exposures were of three to four hours duration at 35 kV and 20 mA. It was very important that the camera be continuously evacuated. The flow of cooling water to the camera was about 250 cc/min. but relatively large variations did not affect the temperature significantly.

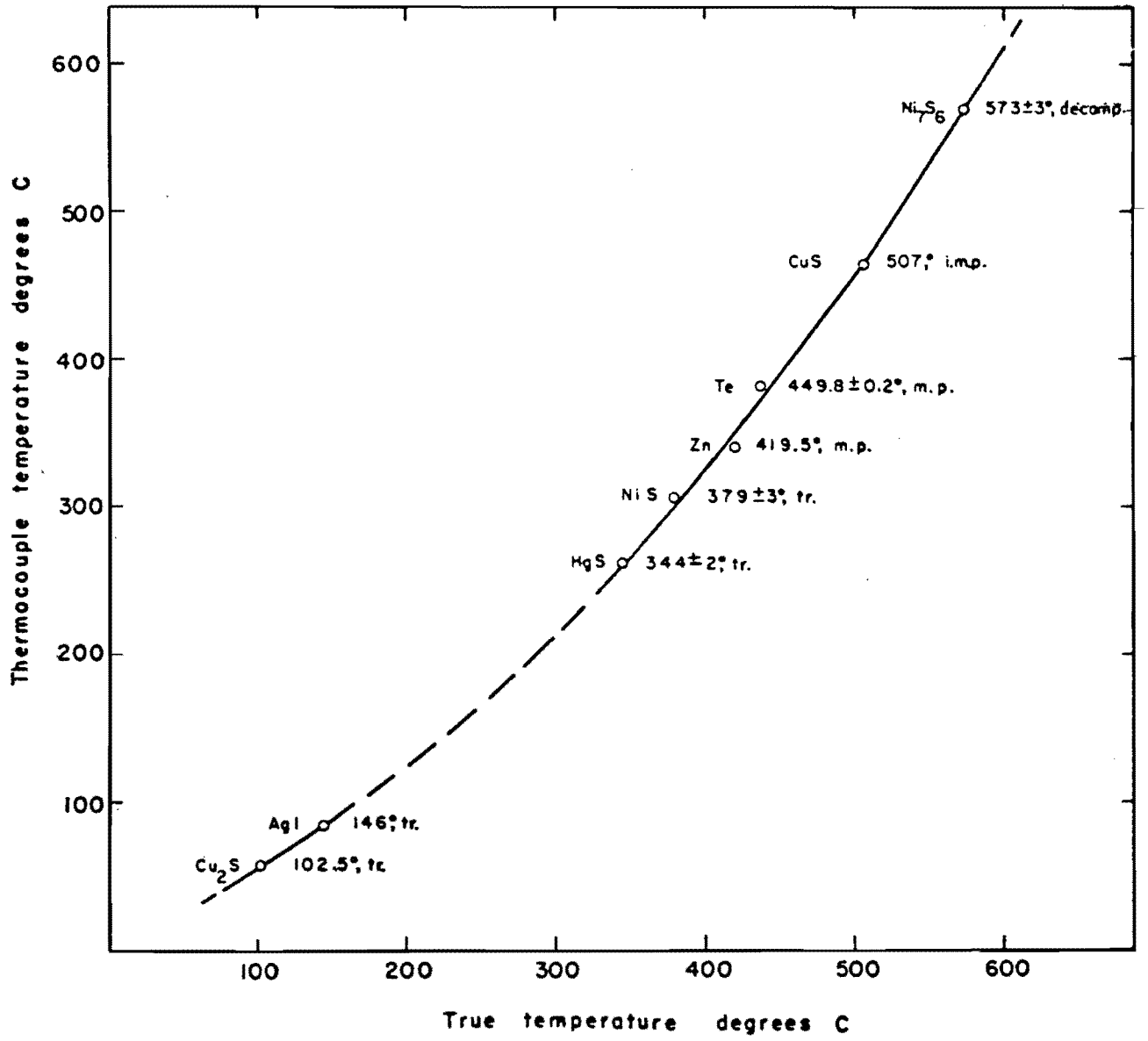

Figure A1. Temperature calibration curve for Rigaku-Denki high-temperature x-ray powder diffraction camera (tr. = transition, m.p. = melting point, i.m.p. = incongruent melting point, decomp. = decomposition).

TABLE A2

Selected runs heated at 335°C relating to the Ag-Te binary (quenched in ice water and x-rayed immediately).

Run No.	wt. % Au	Ag	Te	Ag:Te	Thermal history	Products identified on Guinier powder photographs
301E	3.99	54.00	42.01	1.52	M; 16 days, G after 3 days	$Ag_{5-x}Te_3$
381	-	56.75	43.25	1.55	M; 7 days, G after 6 days	$Ag_{5-x}Te_3$ > Te
380	-	57.25	42.75	1.58	M; 7 days, G after 6 days	$Ag_{5-x}Te_3$ + trace Te
379	-	57.73	42.27	1.61	M; 13 days, G after 4 and 6 days	$Ag_{5-x}Te_3$
378	-	58.23	41.97	1.65	M; 13 days, G after 4 and 6 days	$Ag_{5-x}Te_3$ + trace hs (low)
291	-	58.49	41.51	1.66	M; 1 day @ 440°, 9 days @ 395°, G & P after 3 and 4 days; G, 1 day @ 335°C	$Ag_{5-x}Te_3$ + trace hs (low)
294	-	58.76	41.24	1.68	M; 18 days @ 395°C; G, 1 day @ 335°C	$Ag_{5-x}Te_3$ > hs (low)
257	-	60.09	39.91	1.81	M; 10 days @ 375°C; G, 14 hours @ 335°C	$Ag_{5-x}Te_3$ > γ + hs (low)
371C	4.69	57.76	37.55	1.82	M; 8 days, G after 7 days	γ
258	-	61.08	38.92	1.85	M; 10 days @ 375°C; G, 14 hours @ 335°C	γ > hs (low) + (trace $Ag_{5-x}Te_3$?)
372C	3.05	59.43	37.52	1.87	M; 8 days, G after 7 days	γ > hs (low)
259	-	61.37	38.63	1.88	M; 10 days @ 375°C; G, 14 hours @ 335°C	γ >> hs (low) + (trace $Ag_{5-x}Te_3$?)

TABLE A2 (cont'd.)

260	-	61.57	38.43	1.90	M; 10 days @ 375°C; G, 14 hours @ 335°C	δ + hs (low)
261	-	61.87	38.13	1.92	M; 10 days @ 375°C; G, 14 hours @ 335°C	γ + hs (low)
262	-	62.10	37.90	1.94	M; 10 days @ 375°C; G, 1 day @ 335°C	hs (low) $> \gamma$
263	-	62.38	37.62	1.96	M; 10 days @ 375°C; G, 1 day @ 335°C	hs (low) $\gg \gamma$

TABLE A3

X-ray powder data from Guinier* photographs using CuKα_1 radiation for gamma-phase, d-values in Ångströms. Runs quenched in ice water from 335°C and x-rayed immediately at 18°C. (γ_1 = 61.08 Ag, 38.92 Te wt. %, γ_2 = 4.69 Au, 57.76 Ag, 37.55 Te wt. %)

γ_1 (1)		γ_2 (2)	
I obs.	d meas.	I obs.	d meas.
		½	11.14
½	8.51	2	8.47
		½	8.10
		2	7.65
1	6.93	3	6.86
1	6.68		
		½	5.39
1	5.31	1	5.26
		½	5.13
		½b**	4.43
2b	3.86	2	3.85
1	3.76	3	3.77
3	3.72	3	3.70
2	3.66	3	3.64
2	3.62	2	3.62
3	3.53	3	3.52
2	3.41	3	3.41
2	3.38	1	3.39
2b	3.31	3b	3.30
1b	3.20	1	3.20
3	3.09	4	3.09
		2	3.06
3	3.01	5b	3.02
		1	2.96
		½	2.94
3b	2.91	2	2.91
		3	2.81
		1b	2.83
8	2.69	6	2.69
1	2.67	2	2.66
3	2.63	4	2.63
1	2.61	½	2.61
		1b	2.58
		1b	2.54
		½	2.52
2	2.52	4	2.51
½	2.49	2	2.48

TABLE A3 (cont'd.)

½	2.47		
½	2.46	½	2.46
1	2.43		
½	2.41		
3b	2.38	3	2.37
		½	2.29
		½	2.28
		½	2.26
		7	2.22
10	2.21	10	2.20
1	2.18	2	2.18
6	2.161	2	2.169
		6	2.164
6	2.149	7	2.150
4	2.120	5b	2.126
		½	2.115
		½	2.108
		½	2.099
4	2.095	4	2.091
1	2.070	1	2.071
2	2.059	3	2.056
		½	2.035
		1b	2.022
		½	1.994
		½	1.975
		½	1.968
		½	1.956
		½	1.936
½b	1.930	2	1.923
		1	1.917
½b	1.910	2b	1.906
1	1.878	3	1.883
1b	1.856	3	1.851
		1	1.840
		2	1.822

Reflections with smaller d-values are too broad or too weak or both - not measured.

* Guinier forward reflection focussing camera.

** Signifies broad reflection.

(1) A few reflections of hessite (low) ignored as well as one reflection of $Ag_{5-x}Te_3$.

(2) Only gamma-phase reflections observed on film.

TABLE A4

X-ray powder diffraction data for synthetic and natural $Ag_{5-x}Te_3$ compared to natural AgTe.

Natural AgTe (1) Honea (1964)		Synthetic $Ag_{5-x}Te_3$ (2) Present Study			Natural $Ag_{5-x}Te_3$ (3) (Empressite I) Berry & Thompson (1962)			Natural $Ag_{5-x}Te_3$ (4) (Stuetzite) Honea (1964)			
I	d meas.	I	d meas.	hkl	I	d meas.	d calc.	I	d meas.	d calc.	hkl
		3b*	11.72	100			11.68	5	11.59	11.59	100
4	10.04	1	10.15								
		1	6.86	101			6.86			6.82	101
		½	5.27	111			5.27			5.24	111
		1	4.81	201			4.81	1	4.77	4.78	021
1	4.37	3	4.41	120	½	4.40	4.41	4	4.37	4.38	210
4	4.02	1	3.97	012	½	3.97	3.98			3.97	102
6	3.81	3	3.91	121			3.92	3	3.88	3.89	211
		4	3.58	112	1	3.56	3.59	6	3.56	3.57	112
		5	3.53	031			3.54	6	3.52	3.52	031
				022	½	3.40	3.43			3.41	022
6	3.33	4	3.37	220			3.37	5	3.35	3.35	220
		2	3.23	130	½	3.23	3.24	2	3.21	3.21	310
5	3.18	1	3.17								
		4	3.12	221			3.13	5	3.11	3.11	221
1	3.04	6	3.05	122	2	3.04	3.06	7	3.03	3.04	212
½	2.97	4	3.02	131			3.03			3.00	131
4	2.89	1	2.91	040			2.92			2.90	040
		½	2.86	302			2.87			2.85	302
3	2.85	2	2.82	003	½	2.83	2.83	3	2.82	2.82	003
10	2.70	2	2.80								
		½	2.75	041			2.76			2.74	041
		2	2.67	320			2.68			2.66	320
		6	2.63	222	1	2.64	2.64	7	2.62	2.62	222
2	2.60	1	2.60	113			2.61			2.60	113
		7	2.57	132	5	2.55	2.57	8b	2.55	2.56	132
		6	2.55	231,140			2.55			2.54	321,140
2	2.51	1	2.54	023			2.54			2.53	023
2b	2.43	1	2.43	141			2.44			2.42	141
		3	2.40	042			2.40	½	2.39	2.39	042
		2	2.37	213			2.38	½	2.37	2.37	213
4	2.32	3b	2.33	050			2.33	3	2.32	2.32	500
1	2.29	3	2.28	033			2.29	2	2.27	2.28	033
		3	2.26	232			2.26	4	2.24	2.25	322
		4	2.24	051	1	2.24	2.25			2.24	051
8	2.23	½	2.22	330			2.25			2.23	330
		2	2.20	240			2.21			2.19	240

TABLE A4 (cont'd.)

3	2.18	10	2.18	142			2.18	10b	2.16	2.17	412
		6	2.17	331	10	2.17	2.17			2.16	331
5	2.14	4	2.163	223			2.16			2.15	223
4	2.12	2	2.127	241			2.14	6	2.11	2.12	421
		4	2.118	133	2	2.12	2.13			2.12	133
		1	2.095	004			2.12			2.11	004
		½	2.084	014			2.08			2.08	014
				052			2.05	4	2.03	2.03	052
5	2.04	3	2.044	151	1	2.04	2.04			2.02	511
4	2.01	3	2.032	043			2.03			2.02	043
				114			2.02			2.01	114
		1	1.982	332			1.986			1.972	332
1	1.962	½	1.962	242			1.958			1.944	242
				060			1.947	5	1.931	1.933	323
		4	1.943	233	1	1.933	1.945			1.931	600
3	1.920	1	1.917	340			1.920	3	1.900	1.905	340
		3	1.907	124	½	1.910	1.911			1.903	214
		2	1.888	152			1.881	3	1.865	1.867	512
		3	1.877	341	½	1.873	1.873			1.858	431
½	1.864	2	1.866	250			1.871			1.855	520
		½	1.856	034			1.862				
½	1.833	2	1.823	251			1.827	½	1.816	1.812	521
1	1.796	2	1.796	224			1.795	½	1.790	1.790	053
1	1.771	2	1.770	134			1.774			1.786	224
2b	1.757	2	1.757	333			1.760	½b	1.757	1.765	314
		2	1.708	252			1.711			1.756	062
2	1.699							½	1.699	1.707	044
		4	1.681	513			1.684			1.699	522
								2	1.674	1.674	513

* Signifies broad.

(1) Orthorhombic, Pmmm or Pmn, a = 8.90, b = 20.07, c = 4.62 Å from Empress Josephine mine, Kerber Creek district, Colorado.

(2) 58.23 wt. % Ag. Pattern obtained with a Guinier forward reflection focussing camera using $CuK\alpha_1$ radiation, and LiF as internal standard (a = 4.0270 Å).

(3) Hexagonal, P6/mmm, a = 13.49, c = 8.48 Å from Empress Josephine mine, Kerber Creek district, Colorado.

(4) Hexagonal, C6/mmm, a = 13.38, c = 8.45 Å from May Day mine, La Plata district, Colorado.

TABLE A5

High-temperature x-ray powder diffraction data for intermediate form of petzite.

Frueh (1959b) @ 250°C		Present Study @ 228°C	
I	d meas.	I	d meas.
2	3.802		
6	3.121	½	3.07
3	2.797		
9	2.392	3	2.36
10	2.254	3b*	2.25
2	2.156	3b	2.20
5	2.071	2	2.02
1	1.955		
4	1.495	2	1.33
5	1.247	2b	1.24
2	0.943	2b	0.913
1	0.921		
2	0.839	2	0.835
5	0.791	5	0.787
		$\alpha_1+\alpha_2$	

* signifies broad

TABLE A6

X-ray powder data from Guinier photographs using $CuK\alpha_1$ radiation for intermediate polymorph of petzite and "x" phase quenched in ice from 270°C.

Petzite (intermediate)		"x" phase $Au_{0.28}Ag_{3.72}Te_2$	
I*	d meas.	I**	d meas.
½	8.539***	3	8.036
1	6.950	2	6.577
1b	3.867	1	6.505
½	3.716	1	5.657
1	3.524	1	4.612
1	3.427	1	3.744
1	3.357	4	3.750
1	3.317	2	3.562
2b	3.110	2	3.420
½	3.068	2	3.392
2b	3.027	2	3.246
3b	2.947	1	3.137
½	2.921	1	3.118
½	2.902	4	3.032
2b	2.706	3	3.015
1	2.670	4	3.005
2	2.640	1	2.820
1	2.614	4	2.754
1	2.552	3	2.668
½	2.494	1	2.657
2	2.229	1	2.575
3b	2.211	2	2.530
3b	2.169	3	2.512
3	2.154	3	2.461
1b	2.080	1	2.453
1b	2.061	1	2.399
		1	2.316
		1	2.293
		½	2.264
		1	2.254
		1	2.246
		9	2.224
		9	2.213
		10	2.200
		3b	2.166

* Relative intensity taking strongest low petzite reflection as 10 (petzite (low) reflections not recorded).

** Relative intensity taking strongest "x" phase reflection as 10 (petzite (low) reflections not recorded).

***For measured d-values, the third decimal place is only of partial significance down to d = 2.000, and the fourth decimal down to d = 1.6000.

TABLE A7

High-temperature x-ray powder data for "x" phase ($Au_{0.28}Ag_{3.72}Te_2$) at 261°C. Tentatively indexed as orthorhombic, a = 7.5 Å, b = 6.8 Å, c = 6.0 Å.

I	d meas.	hkl
½	3.75	200
½	3.42	020
1	3.02	002
1	2.54	220
10b*	2.23	221
1	2.18	130
2b	2.11	302
½	2.07	321

* b signifies broad reflection

TABLE A8

Selected runs heated at 356°C relating to the area bounded by cl-sv-$Ag_{5-x}Te_3$-hs-pet (quenched in ice water and x-rayed immediately at 18°C).

Run No.	wt. % Au	Ag	Te	Thermal history	Products identified on Guinier powder photographs
372D	3.05	59.43	37.52	after heating @ 335°C, G, 7 days	γ > hs (low)
374D	4.18	58.72	37.10	after heating @ 335°C, G, 7 days	γ + hs + "x" > pet (low)
371D	4.69	57.76	37.55	after heating @ 335°C, G, 7 days	γ
373D	6.70	56.89	36.41	after heating @ 335°C, G, 7 days	"x" > γ > pet (low)
366D	7.08	55.27	37.65	after heating @ 335°C, G, 7 days	$Ag_{5-x}Te_3$ (low) + γ > pet (low)
370D	8.47	57.51	34.02	after heating @ 335°C, G, 7 days	hs (low) > pet (low) > "x" + Au
362D	24.22	35.44	40.34	after heating @ 335°C, G, 7 days	pet (low) + cl > γ
368D	21.86	35.91	42.23	after heating @ 335°C, G, 7 days	cl > pet (low) + γ
369D	21.36	35.09	43.55	after heating @ 335°C, G, 8 days	kr > pet (low) + γ
364D	20.07	34.22	45.71	after heating @ 335°C, G, 7 days	kr + γ > pet (low)
327AA	20.39	29.98	49.63	M; @ 350°C for 20 days then @ 356°C for 7 days	kr + sv + pet (low) + $Ag_{5-x}Te_3$ (low) + Te > γ
326AA	18.00	29.99	52.01	M; @ 350°C for 20 days then @ 356°C for 7 days	kr + sv + pet (low) + $Ag_{5-x}Te_3$ (low) + Te > γ
*301G	3.99	54.00	42.01	M; G & P, 7 days, G, 6 days	$Ag_{5-x}Te_3$ (low)

TABLE A8 (cont'd.)

365D	5.31	49.99	44.70	after heating @ 335°C, G, 7 days	$Ag_{5-x}Te_3$ (low) > Te >> (sv)
**350	42.48	14.84	42.67	10 days G & P, 5 days	cl + pet (low) + Au + (A + B) ***
****356	42.86	15.07	42.06	10 days G & P, 5 days	cl + pet (low) + Au + (A)
295D	24.86	27.10	48.04	after heating @ 290°C, G, 7 days	kr + pet (low) + γ
176D	30.99	30.09	38.92	after heating @ 290°C, G, 7 days	cl + pet (low) > pet (int) + (A) > γ
174D	31.02	30.07	38.90	after heating @ 335°C, G, 7 days	cl + pet (low) pet (int) + (A) > γ
377D	61.95	11.23	26.82	after heating @ 335°C, G, 5 days	cl + pet (low) + Au > (A)
376D	45.51	24.95	29.54	after heating @ 335°C, G, 5 days	pet (low) + Au + (A) + trace cl
346D	35.73	33.26	31.01	after heating @ 335°C, G, 2 days	(A + B) + pet (low) > Au + trace cl

---

* actually heated @ 350°C

** starting materials were kr + pet + Au

*** see Tables A12 and A13

**** starting materials were cl + pet + Au

TABLE A9

Selected runs heated at 335°C relating to the area bounded by cl-sv-$Ag_{5-x}Te_3$-hs-pet (quenched in ice water and x-rayed immediately at 18°C).

Run No.	wt. % Au	Ag	Te	Thermal history	Products identified on Guinier powder photographs
372C	3.05	59.43	37.52	M; 8 days, G after 7 days	γ > hs (low)
374C	4.18	58.72	37.10	M; 8 days, G after 7 days	hs (low) + γ + "x" > pet (low)
371C	4.69	57.76	37.55	M; 8 days, G after 7 days	γ
373C	6.70	56.89	36.41	M; 8 days, G after 7 days	γ + "x" + pet (low)
366C	7.08	55.27	37.65	M; 11 days, G after 10 days	pet (low) + $Ag_{5-x}Te_3$ (low) + γ
370C	8.47	57.51	34.02	M; 8 days, G after 7 days	hs (low) > pet (low)
362C	24.22	35.44	40.34	M; 11 days, G after 10 days	pet (low) + cl > γ
368C	21.86	35.91	42.23	M; 8 days, G after 7 days	cl > pet (low) + γ
369C	21.36	35.09	43.55	M; 7½ days, G after 7 days	kr > pet (low) + γ
364C	20.07	34.22	45.71	M; 11 days, G after 10 days	pet (low) + γ + kr + sv
367C	20.48	33.64	45.88	M; 8 days, G after 7 days	kr > sv + pet (low) + γ
327B	20.39	29.98	49.63	M; 58 days, G & P after 20 & 36 days, G after 56 days	sv + pet (low) + γ
326B	18.00	29.99	52.01	M; 58 days, G & P after 20 & 36 days, G after 56 days	$Ag_{5-x}Te_3$ (low) + sv + (trace pet (low))
301E	3.99	54.00	42.01	M; 16 days, G after 3 days	$Ag_{5-x}Te_3$ (low)
365C	5.31	49.99	44.70	M; 11 days, G after 10 days	$Ag_{5-x}Te_3$ > Te > sv
174C	31.02	30.07	38.91	M; 12 days, G after 11 days	pet (low) + pet (int) + cl + (B)

TABLE A9 (cont'd.)

*349	42.17	14.91	42.85	21 days, G & P after 6 days, G after 20 days	pet (low) + cl + Au + (B)
**355	42.21	15.30	42.46	21 days, G & P after 6 days, G after 20 days	pet (low) + cl + Au + (B)
346A	35.73	33.26	31.01	M; 11½ days, G after 11 days	pet (low) + Au + (A + B)
***171	8.74	50.23	41.03	40 days, G & P after 10 days	pet (low) + sv + hs (low) + $Ag_{5-x}Te_3$ (low)
***295	24.86	27.10	48.04	M; 43 days, G after 19 days	kr + hs (low) + pet (low)
377	61.95	11.23	26.82	M; 9 days, G after 7 & 8 days	cl + pet (low) + Au > (A + B)
376	45.51	24.95	29.54	M; 9 days, G after 7 & 8 days	(B > A) + pet (low) > Au + cl

---

* starting materials were kr + pet + Au

** starting materials were cl + pet + Au

*** these runs were only x-rayed some weeks after quenching, so that any metastable phases had broken down.

TABLE A10

Selected runs heated at 290°C relating to the area bounded by cl-sv-$Ag_{5-x}Te_3$-hs-pet (quenched in ice water and x-rayed immediately at 18°C).

Run No.	wt. % Au	Ag	Te	Thermal history	Products identified on Guinier powder photographs
372B	3.05	59.43	37.52	M; 14 days, G after 12 days	γ + hs (low)
374B	4.18	58.72	37.10	M; 13 days, G after 11 days	γ + hs (low) > pet (low) + "x"
371B	4.69	57.76	37.55	M; 14 days, G after 12 days	γ
373B	6.70	56.89	36.41	M; 13 days, G after 12 days	"x" > γ + pet (low)
366B	7.08	55.27	37.65	M; 15 days, G after 13 days	γ
370B	8.47	57.51	34.02	M; 14 days, G after 12 days	hs (low) + pet (low) + Au >> "x"
362B	24.22	35.44	40.34	M; 15 days, G after 13 days	cl + pet (low) > γ
368B	21.86	35.91	42.23	M; 14 days, G after 12 days	cl + pet (low) + γ
369B	21.36	35.09	43.55	M; 14 days, G after 12 days	cl + pet (low) + γ
364B	20.07	34.22	45.71	M; 15 days, G after 13 days	sv + γ > pet (low)
367B	20.48	33.64	45.88	M; 14 days, G after 12 days	sv + γ > pet (low)
327E	20.39	29.98	49.63	M; 92 days, G & P after 30 & 71 days, G after 91 days	sv + pet (low) + γ
326E	18.00	29.99	52.01	M; 92 days, G & P after 30 & 71 days, G after 91 days	sv + $Ag_{5-x}Te_3$ (low) + γ
301B	3.99	54.00	42.01	M; 59 days, G & P after 8 & 18 days, G after 52 days	$Ag_{5-x}Te_3$ (low)
365B	5.31	49.99	44.70	M; 15 days, G after 13 days	$Ag_{5-x}Te_3$ (low) > Te > sv
176	30.99	30.09	38.92	(20 days @ 380°C) then G & P, 18 days, G after 12 days	cl + pet (low) > Au

TABLE A10 (cont'd.)

*358	42.15	15.69	40.95	37 days, G & P after 2 days, G after 35 days	cl + pet (low) + Au
**352	42.97	16.09	40.94	37 days, G & P after 2 days, G after 35 days	cl + pet (low) + Au
345A	30.67	37.30	32.03	M; 16 days, G after 14 days	Au + pet (low) + pet (int) > cl
295A	24.86	27.10	48.04	after heating @ 335°C, M; 16 days, G after 14 days	kr > pet (low) +
377B	61.95	11.23	26.82	after heating @ 335°C, G, 7 days	pet (low) + cl + Au
376B	45.51	24.95	29.54	after heating @ 335°C, G, 7 days	pet (low) + cl + Au

* starting materials were cl + pet + Au

** starting materials were kr + pet + Au

TABLE A11

Selected runs heated at 170°C relating to the area bounded by cl-sv-$Ag_{5-x}Te_3$-hs-pet (quenched in ice water and x-rayed immediately at 18°C).

Run No.	wt. % Au	Ag	Te	Thermal history	Products identified on Guinier powder photographs
372A	3.05	59.43	37.52	M; 23 days, G after 21 days	γ> hs (low)
374A	4.18	58.72	37.10	M; 16 days, G after 14 days	γ> hs (low) > "x"
371A	4.69	57.76	37.55	M; 23 days, G after 21 days	γ only
373A	6.70	56.89	36.41	M; 16 days, G after 14 days	γ + pet (low) + "x"
366A	7.08	55.27	37.65	M; 52 days, G after 50 days	$\gamma \gg$ pet (low)
370A	8.47	57.51	34.02	M; 23 days, G after 21 days	hs (low) > pet (low) > "x" + Au
362A	24.22	35.44	40.34	M; 52 days, G after 50 days	cl + pet (low) > γ
363A	28.24	29.64	42.12	M; 52 days, G after 50 days	cl > pet (low) > γ
368A	21.86	35.91	42.23	M; 23 days, G after 21 days	cl + pet (low) + γ
369A	21.36	35.09	43.55	M; 23 days, G after 21 days	cl + pet (low) + γ
364A	20.07	34.22	45.71	M; 52 days, G after 50 days	sv + cl + pet (low) + γ
367A	20.48	33.64	45.88	M; 23 days, G after 21 days	cl + sv + γ + pet (low)
365A	5.31	49.99	44.70	M; 52 days, G after 50 days	$Ag_{5-x}Te_3$ > Te $\gg$ sv
292B	9.03	50.02	40.95	After heating @ 350°, G & P, 53 days, G after 51 days	γ > sv > "x" + pet (low)
175B	31.33	30.06	38.61	After 26 days @ 380°, G & P, 53 days, G after 51 days	pet (low) + Au > cl
295B	24.86	27.10	48.04	After heating @ 335°, G & P, 53 days, G after 51 days	kr > pet (low) + γ
342A	28.26	39.30	32.44	After heating @ 440°, G & P, 53 days, G after 51 days	pet (low) + Au >> cl

TABLE A12

X-ray powder data for unknown phases A and B from Guinier photographs compared with natural Au_2Te_3 (monbrayite).

Run 346* @ 335°C Pattern A & B		Run 355* @ 335°C Pattern A		Run 355* @ 335°C Pattern B		Au_2Te_3 Peacock & Thompson (1962)	
I	d meas.	I	d meas.	I	d meas.	I	d meas.
	masked by a petzite reflection					1	7.50
1	5.28			4	5.28		
4	5.05	masked by a calaverite reflection					
1	4.68			5	4.68		
5	4.38	5	4.37			2	4.48
						½	4.08
3	3.70	masked by a calaverite reflection				½	3.82
1b	3.49			5	3.48	½	3.53
1	3.31			4	3.31	1	3.23
4	3.03	2	3.02			8	2.98
1	2.90			3	2.80	8	2.93
10	2.73	masked by petzite		2	2.73		
5	2.52	5	2.52	5	2.52		
3	2.49			10	2.49	½	2.48
2	2.45	1	2.45	5	2.45	1	2.38
1	2.41						
4	2.29	masked by petzite		3	2.29	1	2.28
5	2.22	4	2.21	9	2.26		
5	2.19	masked by a calaverite reflection					
6	2.15	6	2.15				
2b	2.11			5	2.12	1	2.12
2	2.08					10	2.09
3	2.06					1	2.04
1	2.05						
1	2.04					1	1.98
2	1.95			5	1.95	1	1.91
3	1.85			1	1.86	½	1.86
				2	1.85	½	1.84
4b	1.77					½	1.79
1	1.76						
3b	1.74	masked by a calaverite reflection				2	1.72
3b	1.67	masked by a calaverite reflection				2	1.70
2	1.61						
2	1.60						
3	1.59						
1	1.58						
						2	1.49
						2	1.46

* See Table A13 for compositions and thermal histories.

TABLE A13

Selected runs heated at 440° to 290°C relating to the presence of an unknown phase (or phases) in the area bounded by calaverite-petzite-Au.

Run No.	wt. % Au	Ag	Te	Thermal history	Products identified on Guinier film
*350	42.48	14.84	42.67	10 days @ 356°C; G & P after 5 days	pet + Au + cl + A + B
"	"	"	"	after heating as above, reground and x-rayed	pet + Au + cl + A + B
"	"	"	"	reground; heated for 1 day @ 356°C	pet + Au + cl + A
**356	42.86	15.07	42.06	10 days @ 356°C; G & P after 5 days	pet + Au + cl + A
"	"	"	"	reground; heated for 1 day @ 356°C	pet + Au + cl + A
**355	42.21	15.30	42.46	20 days @ 335°C; G & P after 6 days	pet + Au + cl + A
"	"	"	"	after heating as above, ground, heated 1 day @ 335°C	pet + Au + cl + B
"	"	"	"	after heating as above, reground and x-rayed	pet + Au + cl + B
**348	44.43	14.52	41.03	38 days @ 320°C; G & P after 6 days, G after 31 days	pet + Au + cl + B
"	"	"	"	after heating as above, reground and x-rayed	pet + Au + cl + B
*351	42.47	15.31	42.22	45 days @ 305°C; G & P after 6 days, G after 30 days	pet + Au + cl + trace B
**358	42.15	15.69	40.95	37 days @ 290°C; G & P after 7 days, G after 35 days	pet + Au + cl

TABLE A13 (cont'd.)

342	28.26	39.30	32.44	M; 4 days @ 440°C	pet + A + B > Au
"	"	"	"	after above heating; G, 1 day @ 290°C	pet + Au + trace cl
345	30.67	37.30	32.03	M; 14 days @ 440°C	pet + A > trace (Au + cl)
"	"	"	"	after above heating; G, 2 days @ 356°C	pet + (B > A) > Au + trace cl
"	"	"	"	after above heating; G, 2 days @ 335°C	pet + (A + B) > Au + trace cl
"	"	"	"	after above heating; G & P, 25 days @ 290°C, G after 23 days	pet + cl + Au
346	35.73	33.26	31.01	M; 14 days @ 440°C	pet + A > Au + trace cl
"	"	"	"	after above heating; G & P, 25 days @ 335°C, G after 24 days	pet + (A + B) > Au + trace cl
"	"	"	"	after above heating; G, 2 days @ 356°C	pet + (A + B) > Au + trace cl
376	45.51	24.95	29.54	M; 9 days @ 335°C, G after 7 days	pet + (B > A) > (cl + Au)
"	"	"	"	after above heating; G, @ 356°C for 2 days	pet + A + (Au + cl trace?)
"	"	"	"	after above heating; G, @ 290°C for 7 days	pet + cl + Au
377	61.95	11.23	26.82	M; 9 days @ 335°C, G after 7 days	cl + pet + Au > (A + B)
"	"	"	"	after above heating; G, @ 290°C for 7 days	cl + Au + pet

---

* starting materials were kr + pet + Au

** starting materials were cl + pet + Au

for all other runs shown : starting materials were Au + Ag + Te

TABLE A14

Calaverite patterns from Guinier powder photographs using $CuK\alpha_1$ radiation compared to Tunell's (1954) data. Interplanar spacings (d) given in Ångströms. Films corrected for shrinkage using LiF (a = 4.0270 Å) as internal standard.

No. 70 $AuTe_2$		No. 86 (Au,Ag) Te_2 1.96% Ag		Natural calaverite (Cripple Creek) Tunell (1954)					Natural calaverite (Calaveras,Calif.) McG-2972R3		Natural calaverite (Kalgoorlie) ROM-E2569	
I obs.	d meas.	I obs.	d meas.	I calc.	I obs.	d calc.	d meas.	hkl	I obs.	d meas.	I obs.	d meas.
-	-	-	-	-	-	-	-	-	-	-	½	8.619
½	6.067	½	6.096	-	-	-	-	-	1	6.088	½	6.093
½	5.907	½	5.954	-	-	-	-	-	½	5.898	-	-
-	-	-	-	0.00	-	7.19	-	100	-	-	-	-
7	5.067	7	5.094	1.88	1	5.08	4.98	001	6	5.088	6	5.076
-	-	-	-	-	-	-	-	-	-	-	½	4.627
-	-	-	-	0.00	-	4.40	-	010	-	-	½	4.406
½	4.211	½	4.235	0.00	-	4.15	-	$10\bar{1}$	½	4.211	½	4.206
-	-	-	-	0.00	-	4.14	-	101	-	-	½	4.153
2	3.891	2	3.915	-	½	-	3.83	ss?	3	3.903	2	3.923
3	3.758	3	3.777	0.34	1	3.75	3.74	110	4	3.770	3	3.784
-	-	-	-	0.01	-	3.60	-	200	-	-	-	-
-	-	-	-	0.00	-	3.32	-	011	-	-	-	-
1	3.202	1	3.200	-	½	-	3.30	ss?	2	3.211	2	3.214
-	-	-	-	0.00	-	3.02	-	$11\bar{1}$	-	-	-	-
10	3.016	10	3.032	10.00	10	3.01	2.99	111	10	3.021	10	3.031
9	[2.934	9	[2.945	8.09 0.19	7	[2.94 2.93]	2.91	$20\bar{1}$ 201	9	[2.934	9	[2.948
½	2.674	-	-	-	-	-	-	-	-	-	-	-
1	2.566	1	2.575	0.00	-	2.78	-	210	1	2.569	1	2.571
1	2.538	1	2.536	0.04	-	2.53	-	002	1	2.537	1	2.531
-	-	-	-	0.00	-	2.44	-	$21\bar{1}$	-	-	-	-

TABLE A14 (cont'd.)

-	-	-	-	0.00	-	2.44	-	211	-	-	-	-
1	2.416	1	2.418	0.00	-	2.40	-	300	1	2.418	1	2.421
-	-	-	-	0.00	-	2.39	-	$10\bar{2}$	-	-	-	-
1	2.333	1	2.337	0.00	-	2.39	-	102	½	2.335	1	2.336
1b	2.269	1	2.291	-	½	-	2.31	ss?	1	2.279	1	2.290
5	2.202	5	2.220	5.71	5	2.20	2.19	020	4	2.210	4	2.217
-	-	-	-	0.00	-	2.196	-	012	-	-	-	-
-	-	-	-	0.00	-	2.170	-	$30\bar{1}$	-	-	-	-
2	2.127	2	2.131	0.00	-	2.163	-	301	2	2.133	1	2.138
		7	2.110	4.18		2.105		310	7	2.108	7	2.115
		-	-	0.00		2.104		120	-	-	-	-
9	2.103			3.16	9	2.102	2.09	$11\bar{2}$	7	2.102	8	2.104
		8	2.102	0.45		2.098		112				
				1.89		2.076		$20\bar{2}$			5	2.075
7	2.070	7	2.072	4.80	6	2.068	2.06	202	7	2.070	6	2.071
-	-	2	2.025	0.17	½	2.019	2.01	021	2	2.027	1	2.053
-	-	-	-	-	-	-	-	-	½	1.9540	½	-
				1.12		1.945		$31\bar{1}$				
				0.00		1.944		$12\bar{1}$				
3	1.9443	3	1.9511	0.00	3	1.942	1.94	121	4	1.9482	4	1.9538
				0.04		1.941		311				
-	-	-	-	0.00		1.878		220	-	-	-	-
1	1.8789	1	1.8830	0.00	½	1.878	1.87	$21\bar{2}$	1	1.8823	-	-
-	-	-	-	0.00		1.872		212	-	-	-	-
½	1.8645	-	-	-	-	-	-	-	½	1.8653	-	-
2	1.8549	2	1.8571	-	-	-	-	-	1	1.8573	1	1.8622
2	1.7990	3	1.8026	0.74	½	1.798	1.79	400	2	1.7995	2	1.8057
4	1.7614	4	1.7648	2.73	4	1.761	1.75	$22\bar{1}$	4	1.7658	4	1.7707
½	1.7506	½	1.7531	0.05		1.759		221	½	1.7557	1	1.7606
½	1.7406	1	1.7416	0.00	-	1.745	-	$30\bar{2}$	½	1.7456	1	1.7481
				0.00	-	1.736	-	302				
2	1.7233	2	1.7280	-	½	-	1.72	ss?	2	1.7268	1	1.7299

TABLE A14 (cont'd.)

4	[1.6935	4	[1.6978	0.04 3.12	4	[1.696 1.692	1.69	40$\bar{1}$ 401	4	[1.6953	4	[1.6997
4	1.6899	4	1.6907	2.11		1.690]		003	4	1.6895	3	1.6889
-	-	-	-	0.00	-	1.664	-	410	-	-	-	-
-	-	-	-	0.00	-	1.662	-	022	-	-	½	1.6663
-	-	-	-	0.00	-	1.647	-	10$\bar{3}$	-	-	-	-
-	-	-	-	0.00	-	1.644	-	103	-	-	-	-
1	1.6182	1b	1.6142	0.04	-	1.622	-	31$\bar{2}$	1	1.6230	½	1.6343
-	-	-	-	0.00	-	1.621	-	320	-	-	-	-
-	-	-	-	0.00	-	1.620	-	12$\bar{2}$	-	-	-	-
-	-	-	-	0.00	-	1.618	-	122	-	-	-	-
-	-	-	-	0.02	-	1.616	-	312	-	-	½	1.6241
½	1.5833	1	1.5854	0.00	-	1.583	-	41$\bar{1}$	½	1.5864	½	1.5894
-	-	-	-	0.00	-	1.579	-	411	-	-	-	-
-	-	-	-	0.00	-	1.577	-	013	-	-	-	-
½	1.5540	½	1.5571	0.00	-	1.545	-	32$\bar{1}$	½	1.5521	½	1.5568
-	-	-	-	0.00	-	1.543	-	321	-	-	-	-
4	[1.5417	4	[1.5449	1.16 0.02	1	[1.542 1.540]	1.54	11$\bar{3}$ 113	4	[1.5441	3	[1.5439
2	[1.5298	2	[1.5305	0.03 0.58	-	1.532 1.527	-	20$\bar{3}$ 203	2	[1.5314	1	1.5290
5	[1.5092	5	[1.5138	0.87 1.69	5	1.510 1.507	1.50	22$\bar{2}$ 222	5	[1.5136	4	[1.5150
-	-	-	-	-	-	-	-	-	½	1.4730	1	1.4778
3	1.4699	3	1.4726	1.11		[1.469		40$\bar{2}$	3	1.4699	2	1.4732
-	-	-	-	0.00	1	1.466	1.46	030	-	-	-	-
2	1.4463	2	1.4518	0.07		1.460]		402	2	1.4517	1	1.4564
-	-	-	-	0.00	-	1.445	-	21$\bar{3}$	-	-	-	-
-	-	-	-	0.00	-	1.442	-	213	-	-	-	-
-	-	-	-	0.00	-	1.437	-	500	-	-	-	-
2	1.4399	2	1.4448	0.12	½	1.437	1.44	130	2	1.4448	1	1.4493
1	1.4006	1	1.4052	0.00	-	1.410	-	031	½	1.4048	½	1.4107

TABLE A14 (cont'd.)

-	-	-	-	0.00	-	1.392	-	$41\bar{2}$	-	-	-	-
2	1.3929	2	1.3974	0.31	-	1.391	-	420	2	1.3961	1	1.4009
-	-	-	-	0.00	-	1.388	-	412	-	-	-	-
-	-	-	-	0.00	-	1.384	-	$50\bar{1}$	-	-	-	-
-	-	-	-	0.00	2	1.382	1.38	$13\bar{1}$	-	-	-	-
-	-	-	-	0.00	-	1.382	-	$30\bar{3}$	-	-	-	-
3	1.3840	3	1.3890	1.55	-	1.382	-	131	3	1.3889	2	1.3933
-	-	-	-	0.00	-	1.381	-	501	-	-	-	-
-	-	-	-	0.00	-	1.378	-	303	-	-	-	-
-	-	-	-	0.00	-	1.366	-	$32\bar{2}$	-	-	-	-
-	-	-	-	0.00	-	1.366	-	510	-	-	-	-
-	-	-	-	0.00	-	1.363	-	322	-	-	-	-
-	-	-	-	0.00	-	1.358	-	$23\bar{0}$	-	-	½	1.3573
½	1.3457	2	1.3465	0.02	-	1.343		$42\bar{1}$			3	1.3488
5b	1.3412	3b	1.3432	1.40	4	1.341	1.34	421	5b	1.3445	3	1.3439
				0.95		1.339		$02\bar{3}$				
				1.11		1.320		$51\bar{1}$				
		4b	1.3233	0.64		1.319		$31\bar{3}$	4b	1.3215	3	1.3259
				0.22	5	1.318	1.32	511				
7b	1.3180	-	-	0.00		1.317		$12\bar{3}$	-	-	-	-
		-	-	0.00		1.316		123	-	-	-	-
		4b	1.3194	1.49		1.315		313	3b	1.3183	3	1.3188
-	-	-	-	0.00	-	1.313	-	$23\bar{1}$	-	-	-	-
-	-	-	-	0.00	-	1.312	-	231	-	-	-	-

TABLE A15

Comparison of x-ray powder data from Guinier photographs with Tunell and Murata (1950) for Krennerite. Film corrected for shrinkage using LiF (a = 4.0270 Å) as internal standard, CuK_{α_1} radiation.

Run #328 (4.53 wt. % Ag)		ROM 23798 **		Tunell & Murata (1950)		
I	d meas. Å	I	d meas. Å	I calc.	d calc. Å	hkl
				0.00	16.54	100
1	8.843 ***	1	8.704	0.03	8.82	010
				0.00	8.27	200
2	7.887	2	7.828	0.02	7.79	110
4	6.049	4	6.067	0.61	6.04	210
				0.00	5.51	300
5	4.692	5	4.692	0.68	4.69	310
1	4.482	1	4.477	0.10	4.46	001
				0.00	4.41	020
				0.00	4.31	101
½	4.216	½	4.231	0.01	4.26	120
½	4.153	½	4.144	0.00	4.14	400
2	4.001	2	3.998	0.18	3.98	011
2	3.945	2	3.946	0.00	3.93	201
				0.00	3.89	220
4	3.894	4	3.887	0.55	3.87	111
2	3.761	2	3.751	0.14	3.75	410
2	3.605	1	3.603	0.15	3.59	211
				0.00	3.47	301
				0.00	3.44	320
				0.00	3.31	500
				0.02	3.23	311
2	3.148	2	3.150	0.00	3.14	021
1	3.106	1	3.100	0.09	3.10	510
1	3.096	½	too weak	0.02	3.08	121
10	3.044	9	3.046	10.00	3.03	401
				0.00	3.02	420
9	2.949	10	2.948	3.62	2.94	030
1	2.903	1	2.900	0.03	2.93	221
1	2.880	½	2.877	0.04	2.89	130
				0.02	2.87	411
				0.00	2.76	230
				0.00	2.76	600
2	2.736	1	2.735	0.00	2.73	321
				0.00	2.66	501
½	2.653	½	2.648	0.02	2.65	520
½	2.638	½	2.638	0.00	2.63	610
1	2.602	1	2.600	0.01	2.59	330

TABLE A15 (cont'd.)

1	2.555	1	2.552	0.00	2.54	511
1	2.509	1	2.504	0.00	2.50	421
1	2.465	1	2.461	0.03	2.45	031
1	2.437	1	2.434	0.04	2.43	131
½	2.401	1	2.403	0.00	2.39	430
				0.00	2.36	700
3	2.350	2	2.351	0.00	2.35	231
				0.00	2.35	601
	*		*	0.02	2.34	620
				0.01	2.28	710
				0.01	2.28	521
1	2.271	1	2.271	0.19	2.27	611
				0.07	2.24	331
6	2.240	5	2.241	1.97	2.23	002
				0.00	2.21	102
				0.00	2.20	040
½	2.189	½	2.190	0.02	2.19	530
				0.00	2.18	140
3	2.163	2	2.161	0.00	2.16	012
				0.00	2.15	202
				0.00	2.14	112
1	2.133	1	2.134	0.14	2.13	240
10	2.1173	10	2.1182	5.42	2.11	431
				0.09	2.09	212
				0.00	2.09	701
				0.00	2.08	720
				0.02	2.07	621
8	2.0703	8	2.0724	1.59	2.07	800
				0.00	2.07	302
4	2.0504	4	2.0536	0.39	2.04	340
2	2.0374	2	2.0406	0.21	2.03	711
				0.00	2.01	810
2	2.0214	1	2.0224	0.15	2.01	312
				0.00	2.00	630
				0.00	1.99	022
2	1.9820	2	1.9830	0.23	1.98	041
				0.01	1.98	122
4	1.9688	4	1.9690	0.01	1.97	531
				0.08	1.96	402
2	1.9511	2	1.9502	0.57	1.96	141
				0.21	1.94	440
				0.04	1.93	222
2	1.9239	2	1.9261	0.10	1.92	241
				0.05	1.92	412
½	1.8904	½	1.8897	0.00	1.89	721
1	1.8785	1	1.8807	0.02	1.88	801
				0.00	1.87	322
				0.00	1.87	820
				0.01	1.86	341

TABLE A15 (cont'd.)

				0.00	1.85	502
				0.00	1.84	900
4	1.8380	4	1.8401	0.03	1.84	730
				0.04	1.84	811
				0.00	1.83	631
2	1.8159	1	1.8156	0.24	1.83	540
2	1.7993	2	1.7998	0.04	1.81	512
				0.00	1.80	910
				0.00	1.79	422
				0.00	1.78	441
8	1.7823	5	1.7844	1.52	1.78	032
				0.02	1.77	132
				0.00	1.76	050
				0.00	1.75	150
2b	1.7416	2	1.7429	0.00	1.74	232
				0.00	1.73	602
				0.00	1.73	821
				0.01	1.72	250
1b	1.7157	2	1.7293	0.02	1.72	640
				0.01	1.71	522
				0.01	1.70	731
				0.01	1.70	612
				0.00	1.70	901
				0.00	1.70	541
				0.00	1.70	920
				0.01	1.69	332
8	1.6935	8	1.6957	1.28	1.69	830
				0.01	1.68	350
		½	1.6732	0.02	1.67	911
1	1.6445	½	1.6486	0.00	1.65	10.0.0
1	1.6386	½	1.6406	0.00	1.64	051
½	1.6313	½	1.6320	0.06	1.63	432
				0.02	1.63	151
				0.05	1.63	10.1.0
				0.00	1.62	702
				0.00	1.62	450
				0.02	1.61	622
				0.00	1.61	740
				0.02	1.61	251
1	1.6118	½b	1.6138	0.16	1.61	641
				0.00	1.60	712
				0.01	1.59	921
½	1.5843	½	1.5864	0.01	1.58	831
				0.00	1.57	351
				0.00	1.57	042
1b	1.5733	½	1.5741	0.01	1.57	532
				0.01	1.56	142
				0.00	1.56	930
1	1.5554	½	1.5562	0.01	1.55	550
				0.00	1.55	10.0.1
				0.00	1.55	10.2.0

TABLE A15 (cont'd.)

½	1.5461			0.09	1.54	242
				0.00	1.53	10.1.1
½	1.5272	½	1.5298	0.00	1.52	451
				0.00	1.52	722
7	1.5210	5	1.5219	1.11	1.52	802
				0.34	1.52	741
2	1.5132	1	1.5141	0.28	1.51	342
				0.00	1.51	840
				0.00	1.50	11.0.0
				0.00	1.49	812
				0.00	1.49	632
1	1.4991	½	1.4989	0.03	1.49	003
				0.01	1.48	650
½	1.4857	½	1.4861	0.05	1.48	11.1.0
				0.00	1.48	103
4b	1.4727	4b	1.4741	0.02	1.47	931
				0.01	1.47	551
				0.17	1.47	442
				0.01	1.47	013
				0.11	1.47	10.2.1
				0.19	1.47	060
				0.00	1.46	203
				0.01	1.46	160
				0.04	1.46	113
				0.00	1.45	260
				0.02	1.44	213
				0.00	1.44	10.3.0
				0.00	1.44	303
				0.00	1.43	822
2	1.4325	2	1.4335	0.08	1.43	841
				0.00	1.43	11.0.1
				0.00	1.42	11.2.0
				0.03	1.42	732
				0.00	1.42	360
				0.00	1.42	902
1	1.4220		*	0.17	1.42	542
				0.00	1.42	313
				0.00	1.41	750
½	1.4145	½	1.4155	0.02	1.41	651
				0.00	1.41	940
				0.00	1.41	023
				0.01	1.41	11.1.1
				0.00	1.40	123
				0.00	1.40	912
2	1.4051	2	1.4058	0.83	1.40	403
				0.01	1.40	061
				0.01	1.39	161
½	1.3937	½	1.3961	0.03	1.39	223
				0.00	1.38	052
				0.00	1.38	460

TABLE A15 (cont'd.)

				0.00	1.38	413
				0.00	1.38	12.0.0
½	1.3869	½	1.3889	0.01	1.38	152
				0.00	1.38	261
				0.00	1.37	10.3.1
				0.00	1.37	323
				0.03	1.36	252
				0.02	1.36	642
				0.01	1.36	12.1.0
				0.00	1.36	11.2.1
				0.00	1.36	503
				0.02	1.35	361
				0.00	1.35	922
4b	1.3505	4b	1.3517	1.18	1.35	832
				0.01	1.35	751
				0.13	1.35	941
				0.01	1.34	352
				0.01	1.34	560
				0.00	1.34	850
				0.00	1.34	513
				0.00	1.34	11.3.0
				0.00	1.33	423
				0.00	1.33	10.0.2
1	1.3321	½	1.3344	0.03	1.33	033
4b	1.3252	4b	1.3271	0.34	1.32	461
				0.01	1.32	133
				0.06	1.32	10.4.0
4b	1.3197	4b	1.3212	0.70	1.32	12.0.1
				0.00	1.32	12.2.0
				0.06	1.31	10.1.2
				0.00	1.31	452

* Masked by LiF reflection.

** Sample from Kalgoorlie, Australia.

*** For measured d-values, the third decimal place is only of partial significance down to d = 2.000, and the fourth decimal down to d = 1.6000.

TABLE A16

Comparison of x-ray powder data from Guinier photographs with Tunell (1941) for Sylvanite. Film corrected for shrinkage using LiF (a = 4.0270 Å) as internal standard, $CuK\alpha_1$ radiation.

Run #137(10.09wt%Ag)PRM F.708 **				Tunell (1941)		
I	d meas. Å	I	d meas. Å	I calc.	d calc.*Å	hkl
				0.0	8.398	$10\bar{1}$
				0.0	8.294	001
3	7.360 ***	4	7.372	0.2	7.309	$10\bar{2}$
1	6.125	½	6.125			
½	5.992					
5	5.073	6	5.064	0.7	5.082	100
2	4.496	2	4.507	0.2	4.489	010
				0.0	4.416	$20\bar{3}$
				0.0	4.371	$10\bar{3}$
1	4.189	1	4.184	0.1	4.198	$20\bar{2}$
1	4.156	1	4.160	0.1	4.147	002
				0.0	3.958	$11\bar{1}$
4	3.960	4	3.960	0.7	3.947	011
4	3.835	4	3.843	0.6	3.825	$11\bar{2}$
1	3.673	1	3.676	0.1	3.654	$20\bar{4}$
				0.1	3.364	110
				0.0	3.310	$20\bar{1}$
				0.0	3.291	101
2	3.150	2	3.156	0.1	3.148	$21\bar{3}$
				0.0	3.132	$11\bar{3}$
				0.1	3.066	$21\bar{2}$
10	3.051	10	3.051	9.9	3.046	012
10	2.985	10	2.985	3.9	2.986	$30\bar{4}$
				0.1	2.948	$10\bar{4}$
				0.0	2.833	$21\bar{4}$
				0.0	2.819	$30\bar{5}$
				0.0	2.799	$30\bar{3}$
				0.0	2.799	$20\bar{5}$
				0.0	2.764	003
				0.0	2.664	$21\bar{1}$
2	2.657	2	2.661	0.1	2.654	111
2	2.531	2	2.531	0.1	2.541	200
1	2.485	1	2.485	0.1	2.486	$31\bar{4}$
2	2.474	2	2.475	0.2	2.464	$11\bar{4}$
				0.0	2.436	$30\bar{6}$
				0.0	2.409	$30\bar{2}$
				0.0	2.390	102
2b	2.390	2b	2.394	0.3	2.387	$31\bar{5}$
				0.0	2.375	$21\bar{5}$
				0.1	2.374	$31\bar{3}$

TABLE A16 (cont'd.)

				0.3	2.353	013
4	2.245	4	2.247	2.0	2.244	020
				0.0	2.228	40$\bar{5}$
1	2.205	½b	2.210	0.1	2.211	210
				0.0	2.208	40$\bar{6}$
				0.0	2.199	10$\bar{5}$
				0.0	2.185	20$\bar{6}$
2	2.168	1	2.170	0.1	2.168	12$\bar{1}$
8	2.149	8	2.150	0.7	2.166	021
				0.1	2.145	12$\bar{2}$
8	2.114	9	2.114	4.1	2.141	31$\bar{6}$
				3.5	2.126	31$\bar{2}$
1	2.109			0.5	2.110	112
4	2.088	5	2.090	1.2	2.099	40$\bar{4}$
6	2.077	7	2.076	2.6	2.074	004
2	2.051	2	2.052	0.3	2.053	120
				0.0	2.051	40$\bar{7}$
				0.0	2.040	30$\bar{7}$
				0.0	2.017	30$\bar{1}$
				0.0	2.010	201
				0.0	2.001	22$\bar{3}$
2	2.0003	½	2.0003	0.1	1.997	12$\bar{3}$
				0.0	1.996	41$\bar{5}$
4	1.9809	5b	1.9850	1.7	1.981	41$\bar{6}$
				0.0	1.979	22$\bar{2}$
				0.0	1.974	11$\bar{5}$
		½	1.9779	0.3	1.973	022
				0.0	1.964	21$\bar{6}$
				0.0	1.912	22$\bar{4}$
				0.0	1.901	41$\bar{4}$
				0.0	1.884	40$\bar{3}$
½	1.8913	1	1.8941	0.1	1.882	014
				0.0	1.867	103
1	1.8858	1	1.8849	0.1	1.865	41$\bar{7}$
3	1.8554	3	1.8563	0.2	1.857	22$\bar{1}$
				0.1	1.857	31$\bar{7}$
				0.0	1.854	121
4	1.8346	4	1.8389	0.1	1.839	31$\bar{1}$
				0.0	1.834	211
1	1.8312			0.6	1.827	40$\bar{8}$
4	1.7929	4	1.7937	1.9	1.794	32$\bar{4}$
				0.0	1.788	50$\bar{7}$
				0.1	1.785	12$\bar{4}$
				0.0	1.770	50$\bar{6}$
				0.0	1.767	20$\bar{7}$
				0.2	1.755	32$\bar{5}$
				0.1	1.751	22$\bar{5}$
3	1.7548	2	1.7563	0.5	1.751	32$\bar{3}$
1	1.7478	1b	1.7463	0.1	1.747	10$\bar{6}$
1	1.7440			0.4	1.742	023
				0.1	1.738	41$\bar{3}$

TABLE A16 (cont'd.)

				0.1	1.726	$50\bar{8}$
				0.0	1.724	113
4	1.7206	5	1.7228	1.5	1.712	$30\bar{8}$
1	1.6972	½	1.7015	1.0	1.694	300
3	1.6872	5	1.6858	0.1	1.692	$41\bar{8}$
				0.0	1.682	220
				0.0	1.679	$50\bar{5}$
				0.0	1.659	005
				0.0	1.655	$40\bar{2}$
				0.0	1.651	$51\bar{7}$
1	1.6586			0.1	1.651	$32\bar{6}$
1	1.6539	½b	1.6559	0.1	1.647	$51\bar{6}$
				0.0	1.645	202
				0.0	1.644	$21\bar{7}$
1b	1.6410	2b	1.6417	0.2	1.643	$32\bar{2}$
				0.0	1.636	122
				0.0	1.628	$11\bar{6}$
				0.0	1.611	$51\bar{8}$
				0.0	1.607	$50\bar{9}$
				0.0	1.600	$40\bar{9}$
				0.0	1.600	$31\bar{8}$
				0.1	1.585	310
1	1.5805	2b	1.5793	0.3	1.581	$42\bar{5}$
½	1.5750	1	1.5690	0.1	1.574	$42\bar{6}$
				0.0	1.573	$51\bar{5}$
				0.0	1.571	$12\bar{5}$
				0.0	1.566	$22\bar{6}$
½	1.5589	½	1.5595	0.1	1.556	015
4	1.5466	4	1.5472	1.2	1.553	$41\bar{2}$
				0.1	1.545	212
½	1.5368			0.1	1.545	$50\bar{4}$
3	1.5305	2	1.5316	0.8	1.533	$42\bar{4}$
				0.2	1.529	104
3	1.5260	4	1.5271	1.7	1.523	024
				0.0	1.514	$42\bar{7}$
				0.0	1.513	$51\bar{9}$
1b	1.5160	1b	1.5176	0.4	1.510	$32\bar{7}$
				0.0	1.508	$41\bar{9}$
				0.1	1.500	$32\bar{1}$
				0.0	1.497	221
2	1.4979]	3v.b.	1.4942]	0.2	1.496	030
				0.3	1.493	$60\bar{8}$
				0.0	1.474	$20\bar{8}$
				0.0	1.472	$13\bar{1}$
		½b	1.4752	0.5	1.472	031
				0.0	1.471	$60\bar{9}$
				0.0	1.466	$60\bar{7}$
1	1.4691	½b	1.4691	0.1	1.465	$13\bar{2}$
				0.0	1.461	$5.0.\bar{10}$
				0.0	1.460	$51\bar{4}$

TABLE A16 (cont'd.)

0.0	1.456	$30\bar{9}$
0.0	1.447	114
0.0	1.446	$10\bar{7}$
0.0	1.446	$40\bar{1}$
0.0	1.443	$42\bar{3}$
0.0	1.442	301
0.1	1.435	123
0.0	1.434	130
0.1	1.416	$23\bar{3}$
0.5	1.416	$42\bar{8}$
0.0	1.416	$61\bar{8}$
0.1	1.415	$13\bar{3}$
0.0	1.409	$6.0.\bar{1}0$
0.0	1.409	$23\bar{2}$
0.6	1.407	032
0.0	1.400	$21\bar{8}$
0.1	1.399	$4.0.\bar{1}0$

---

* Tunell's Kx units converted to Å.

** Sample from Offenbanya, Transylvania.

*** For measured d-values, the third decimal place is only of partial significance down to d = 2.000, and the fourth decimal down to d = 1.6000.

Figure A2

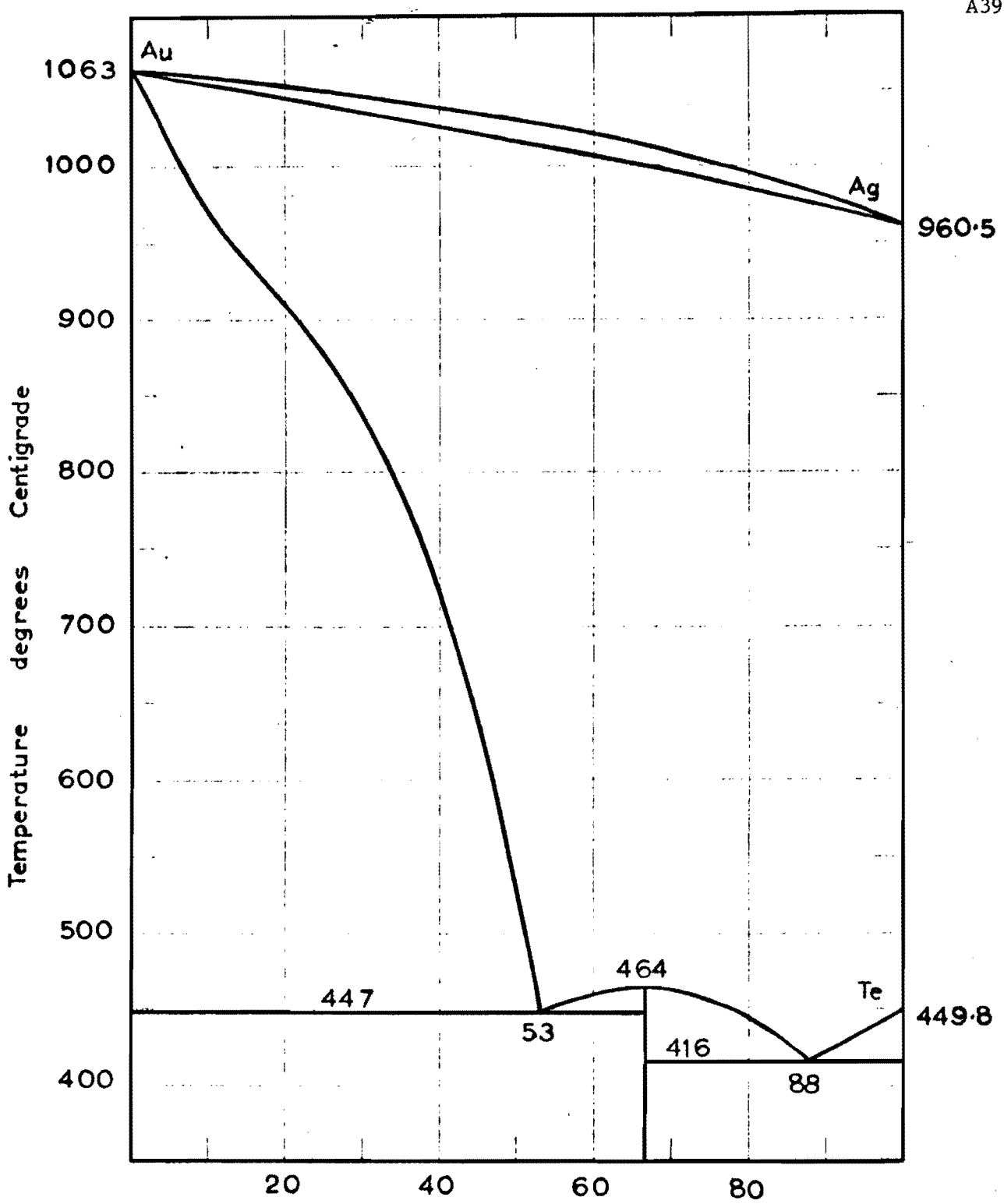

(upper) The binary system gold-silver after Jäneck (1911), Raydt (1912)

(lower) The binary system gold-tellurium after Pellini and Quercigh (1910b), and Kracek (1941)

Compositions in atomic per cent

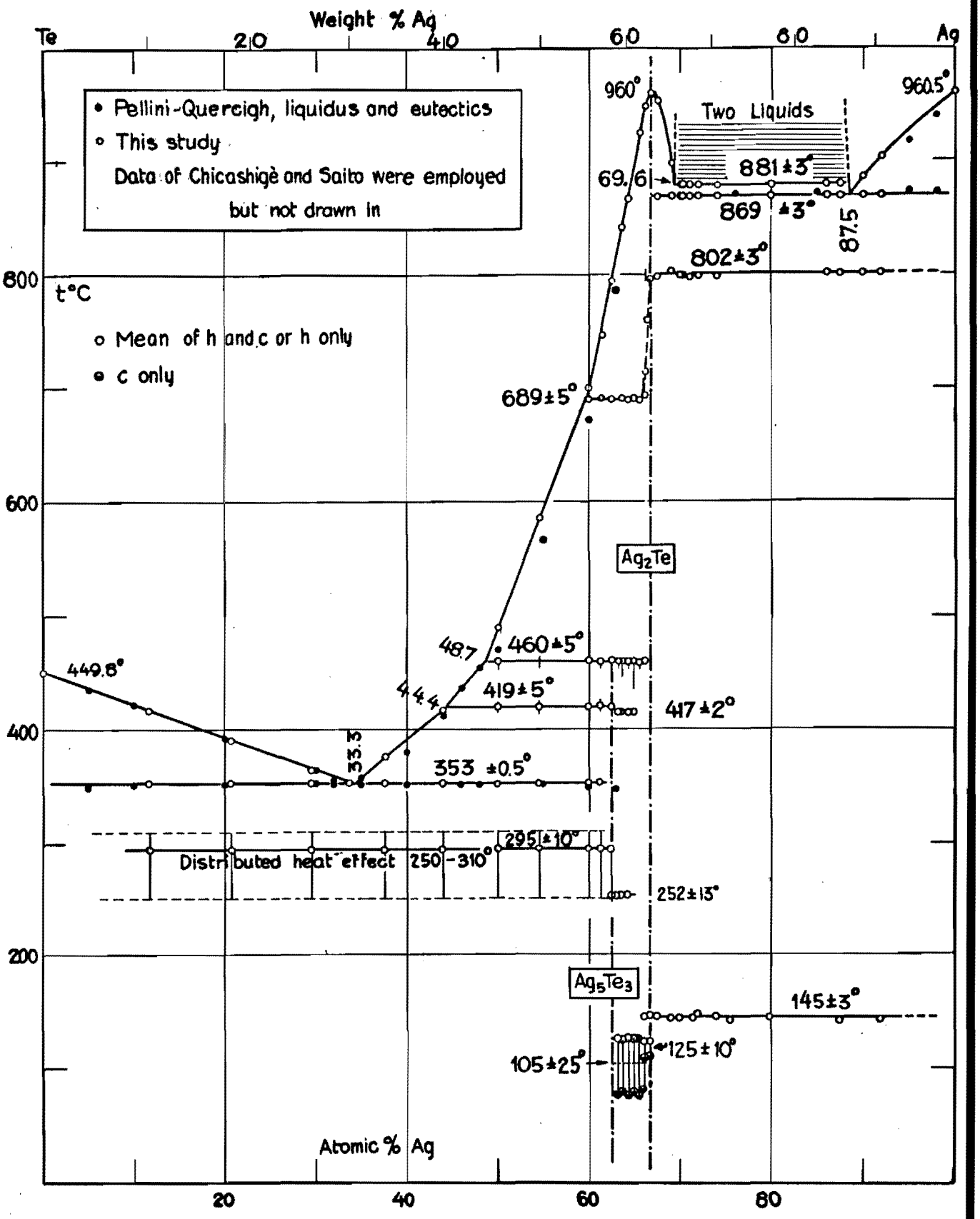

Figure A3. Phase relations in the binary system Ag-Te in equilibrium with vapor by Kracek & Ksanda (unpublished).

Figure A4.

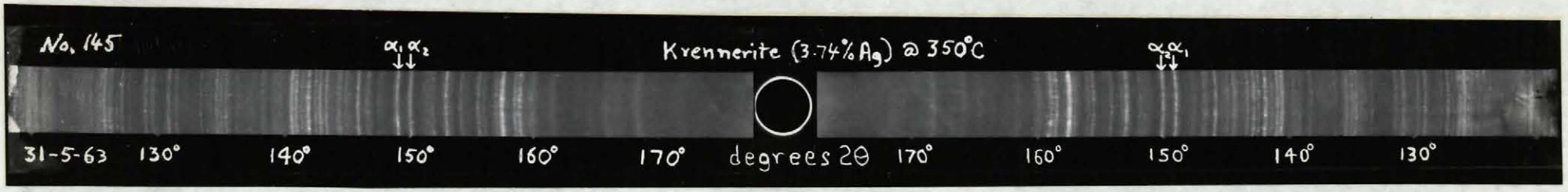

Typical x-ray diffraction photograph for krennerite obtained with the Phillips symmetrical back reflection camera. The α_1 and α_2 reflections measured for the determinative curve (figure 7) are indicated.

Typical x-ray diffraction photograph for sylvanite obtained with the Phillips symmetrical back reflection camera. The α_1 reflection measured for the determinative curve (figure 8) is indicated.